TABLE OF CONTENTS

	Page	
SUMMARY	1	1/A5
INTRODUCTION	3	1/A7
GOVERNING EQUATIONS	6	1/A10
Turbulence Model	8	1/A12
CURVILINEAR COORDINATE SYSTEM	11	1/B1
METHOD OF SOLUTION	15	1/B5
Background	15	1/B5
Computation of Mean Pressure Drop	15	1/B5
Integral Mass Flux Condition	17	1/B7
Solution of the Split Difference Equations	19	1/B9
APPLICATION TO INTERNAL SUBSONIC FLOWS	21	1/B11
Boundary and Initial Conditions	22	1/B12
DISCUSSION OF RESULTS	25	1/C1
RESUME	29	1/C5
APPENDIX - COMPUTER CODE INPUT AND OUTPUT	31	1/C7
REFERENCES	64	1/G13

Stem 830-H-14

NAS1.26:3029

JAN 23 1979

NASA Contractor Report 3029

Development of a Three-Dimensional Turbulent Duct Flow Analysis

P. R. Eiseman, R. Levy, H. McDonald,
and W. R. Briley

COMPLETED
ORIGINAL

CONTRACT NAS3-19856
NOVEMBER 1978

NASA

118

NASA Contractor Report 3029

Development of a Three-Dimensional Turbulent Duct Flow Analysis

P. R. Eiseman, R. Levy, H. McDonald,
and W. R. Briley
United Technologies Research Center
East Hartford, Connecticut

Prepared for
Lewis Research Center
under Contract NAS3-19856

National Aeronautics
and Space Administration

**Scientific and Technical
Information Office**

1978

Blank Page

SUMMARY

A method for computing three-dimensional turbulent subsonic flow in curved ducts has been developed. A set of tube like coordinates is given for a general class of geometries applicable to subsonic diffusers. The geometric formulation is complex and no previous treatment of this class of viscous flow problems is known to the authors. The duct centerline is a space curve specified by piecewise polynominals with continuous third derivatives. A Frenet frame is located on the centerline at each location that a cross section is required. The cross sections are described by superellipses imbedded in the Frenet frame. The duct boundaries are coordinate surfaces, greatly simplifying the boundary conditions. The resulting coordinates are nonorthogonal.

An approximate set of governing equations is given for viscous flows having a primary flow direction. The derivation is coordinate invariant and the resulting equations are expressed in tensor form. These equations are solved by an efficient alternating direction implicit (ADI) method. This numerical method is found to be stable, permitting solution in difficult geometries using the general tensor formulation.

Flow in the entrance region of a circular straight pipe was computed at a Reynolds number of 500. At an inlet Mach number of 0.01 the results compared very favorably with incompressible experimental data. For a pipe of non-circular corss section at a Reynolds number of 500, the inlet Mach number was progressively increased from 0.01 to 0.1, 0.2, and 0.3 and the expected effects of compressibility were observed. For the case with an entrance Mach number of 0.3 the calculation proceeded until the flow choked. This behavior corresponds to that expected from solution of the initial value problem posed.

A series of calculations was performed for flow through a duct which undergoes an S-shaped bend. These cases were run at a Reynolds number of 500 and an inlet Mach number of 0.1. Four different duct cross sections were used: circular, elliptic with shape factor of 1.5, elliptic with shape factor of 0.667, and superelliptic of exponent 10.0. A highly approximate quasi-two-dimensional inviscid pressure formulation was used for the S-bend calculations. The results showed that in the first part of the bend a secondary flow pattern typical of that which is to be expected was produced. A problem was encountered near the end of the first bend where the secondary flows were seen to reverse. This problem is believed to result from the use of the quasi-two-dimensional inviscid pressure model, thus pointing out the need for an accurate three-dimensional inviscid pressure field. Two cases of turbulent flow through an S-shaped bend were computed at a Reynolds number

of 10^5 and an inlet Mach number of 0.1. One case had a circular cross section, the other an elliptic cross section with shape factor 1.1. Flow in an axisymmetric diffuser and in a transition duct are additional cases discussed for completeness.

INTRODUCTION

A continuing problem in the development of the intakes for airbreathing propulsion systems is the design of efficient subsonic diffusers. Not only is the engineer faced with building an efficient diffuser, but frequently he must tailor the diffuser geometry to conform to certain physical constraints imposed by the propulsion engine and airframe. Lacking accurate generalized analytical design methods, the engineer must rely almost exclusively on empirical design methods based on correlations of experimental data. In the case of three-dimensional inlet diffusers, the cross-sectional shape of the ducting must vary in the axial direction, and it is frequently necessary to introduce offset bends (curved duct centerlines). The diffuser geometry is, therefore, complicated, but perhaps more important, the offset bends induce strong secondary flows which have important effects on diffuser performance. Because of the vast number of geometric and flow parameters, comprehensive experimental programs necessary to develop generalized correlations become very costly. Clearly, the availability of better analytical design tools can significantly reduce the time and cost required to arrive at an efficient diffuser design. A generalized subsonic diffuser analysis capable of being used as a design tool must account for several physical phenomena which frequently occur in practical diffusers. First, the analysis must be capable of treating the case when the wall boundary layers are turbulent and possibly of a thickness comparable to the dimensions of the diffuser flow passage. Secondly, the analysis must account for pressure gradients transverse to the direction of flow which can arise because of curvature of the duct centerline. Finally, the analysis should be capable of treating strong interaction problems; i.e., problems in which the viscous flow interacts with the inviscid flow.

Because of their complexity, and particularly the interaction which occurs between primary and secondary flows and viscous and inviscid regions, three-dimensional flows in curved ducts have been extremely difficult to analyze. Rotational inviscid flow theory has provided insight into the behavior of some secondary flows (Hawthorne, Ref. 1), and has now been developed to the point where solutions to the full incompressible, rotational inviscid equations of motion can be computed (Stuart & Hetherington, Ref. 2). Techniques for computing three-dimensional laminar and turbulent boundary layers have also been developed. Some of these are surveyed by Nash & Patel (Ref. 3). However, there are considerable difficulties associated with the synthesis of secondary flow analysis and boundary layer theory into a cohesive method of duct flow analysis. Not the least of these difficulties is the lack of applicability of three-dimensional boundary layer theory in corner regions, and the treatment of interaction between viscous and inviscid flow regions.

In efforts to circumvent these difficulties, Patankar & Spalding (Ref. 4), Caretto, Curr, & Spalding (Ref. 5), and Briley (Ref. 6) devised numerical methods for solving approximate governing equations which are a more or less natural generalization of three-dimensional boundary layer theory. In these studies, solutions were computed for laminar incompressible flow in straight ducts with rectangular cross sections. The governing equations were solved by integrating in a primary flow coordinate direction while retaining viscous stresses in both transverse coordinate directions as opposed to only one direction for three-dimensional boundary layer theory.

In addition to neglecting streamwise diffusion, the pressure is divided into a mean pressure field representing the inviscid pressure and a pressure correction due to viscous effects. This treatment of the pressure gradients permits solution of the governing equations by forward marching integration. Subsequently, this general approach has been used to compute incompressible flow in helical tubes by Patankar, Pratap & Spalding (Refs. 7 & 8). Recently, Ghia, Ghia, and Studerus (Ref. 9) have employed the numerical method of Briley (Ref. 6) to compute flow in a "polar" duct whose cross-sections are annular sectors.

Briley & McDonald (Ref. 10) have also formulated a method for computing three-dimensional turbulent subsonic flow in curved passages, which is also based on a forward marching integration after neglecting streamwise diffusion. Governing equations were derived for flow passages whose bounding walls lie in coordinate planes of an orthogonal coordinate system. The numerical method is an adaptation of the implicit techniques developed by Briley & McDonald (Ref. 11) and McDonald & Briley (Ref. 12) for application to systems of complex nonlinear parabolic and/or hyperbolic equations. In Ref. 10, some preliminary results were given for flow in a curved rectangular duct which is shaped like the flow passage between adjacent blades of a turbine. The preliminary calculations were made using a rather simple turbulence model requiring an a priori specified mixing length. Reference 13 represents a further development of the method of Briley & McDonald (Ref. 10) and an extension to include a more sophisticated turbulence model based on solution of conservation equations for turbulence kinetic energy and turbulence dissipation. The present study represents a further generalization of this method to encompass general coordinates and complex tube-like geometries. Although a derivation of the governing equations, description of the general method and details of the coordinate system can be found in Ref. 14, much of this material is repeated here in updated form for completeness.

A series of cases was run, including the entrance region to a straight pipe at a Reynolds number of 500 and at inlet Mach numbers from 0.01 to 0.3. A variety of cross sections was used, including ellipses of shape factors from 1.0 to 2.0 and superellipses from exponent 2.0 to 10.0. The flow in a duct with an S-shaped bend was calculated at a Reynolds number of 500 and an inlet Mach number of 0.1. A highly approximate inviscid pressure formulation was used for these cases. Four different duct cross sections were used: circular, elliptic with shape factor of 1.5, elliptic with shape factor of 0.667, and superelliptic exponent of 10.0. Two turbulent S bend cases were run with circular and elliptic (shape factor 1.1) cross sections at Reynolds number of 10^5 and inlet Mach number of 0.1. An additional series of diagnostic calculations is also included.

GOVERNING EQUATIONS

Central to the present analysis is the formulation of approximate governing equations which can be solved by forward marching integration in the direction of a "primary flow". The entire flow field can thereby be obtained by a sequence of essentially two-dimensional calculations. This feature of the method results in a substantial saving of computer time and storage compared to that which would be required for solution of the full Navier-Stokes equations. The equations are derived in a coordinate independent manner. A vector field that reasonably approximates the primary flow direction is chosen and then used as the basis for an approximation of the stress tensor. The time-averaged equations are written in general conservation law form, and then the approximate stress tensor is inserted to obtain the approximate equations. Note that this process depends only on the choice of a primary vector field, and not on the particular coordinate system used for the numerical solution. The primary vector field used here consists of the tangent vectors to a certain family of coordinate curves that are roughly aligned with the flow geometry.

The governing equations are derived from the Navier-Stokes equations for compressible flow of a viscous, perfect gas. In conservation law form (Ref. 15) and, in general curvilinear coordinates (y^1, y^2, y^3), these equations are given by

$$\frac{\partial}{\partial t}\left(\rho\sqrt{g}\right) + \frac{\partial}{\partial y^i}\left(\rho v^i \sqrt{g}\right) = 0 \tag{1a}$$

for continuity and

$$\frac{\partial}{\partial t}\left[\rho v^i \frac{\partial x^s}{\partial y^i}\sqrt{g}\right] + \frac{\partial}{\partial y^j}\left[\left(\rho v^i v^j + \tau^{ij}\right)\frac{\partial x^s}{\partial y^i}\sqrt{g}\right] = 0 \tag{1b}$$

for momentum. Constant total temperature is assumed, and thus an energy equation is not required. We have used (x^1, x^2, x^3) for fixed cartesian coordinates, ρ for density, $\vec{v} = v^k \vec{e}_k$ for velocity, $g = \det(g_{ij}) = \left|\det\left(\frac{\partial x^i}{\partial y^j}\right)\right|^2$ for the metrical determinant, and τ^{ij} for the components of the stress tensor in the basis $\vec{e}_i \otimes \vec{e}_j$. In terms of the metric, the components of the stress tensor are given by

$$\tau^{ij} = g^{ij} p + \alpha_k{}^{ij} v^k + \beta_k{}^{ijj} \frac{\partial v^k}{\partial y^j} \tag{2a}$$

where

$$\alpha_k{}^{ij} = \frac{\mu}{Re} \left(\frac{2}{3} g^{ij} \Gamma^{\ell}_{k\ell} + \frac{\partial g^{ij}}{\partial y^k} \right) \tag{2b}$$

and

$$\beta_k{}^{ijj} = \frac{\mu}{Re} \left(\frac{2}{3} g^{ij} \delta^{\ell}_{k} - g^{i\ell} \delta^{j}_{k} - g^{j\ell} \delta^{i}_{k} \right) \tag{2c}$$

for viscosity μ, inverse metric $g^{i\ell}$, Kronecker deltas $\delta^i_j = \delta^{ij} = \delta_{ij}$, and Christoffel symbols

$$\Gamma^k_{ij} = \frac{g^{km}}{2} \left\{ \frac{\partial g_{im}}{\partial y^j} + \frac{\partial g_{jm}}{\partial y^i} - \frac{\partial g_{ij}}{\partial y^m} \right\} \tag{2d}$$

From the ideal gas law and the constant total temperature assumption, the perfect gas relation has the form

$$p = AB_T \cdot \rho + AB_Q \cdot \rho \cdot g_{ij} \cdot v^i v^j \tag{3}$$

where AB_T and AB_Q are constants. In all of the above, the Einstein summation convention is assumed. That is, matching upper and lower indices are to be summed from 1 to 3.

To account for turbulent transport processes, the governing equations are time-averaged in the usual manner for turbulent flows (e.g., Hinze, Ref. 16). This process of averaging produces turbulent correlations which are conventionally termed Reynolds stresses. Certain components of viscous stress

are removed from the time-averaged equations. The process of viscous approximation is based upon the assumption that a primary flow direction exists. The present approach can be regarded as a natural extension of three-dimensional boundary layer theory. Unlike conventional boundary layer theory, however, the approximate equations are to be applicable in the inviscid flow region as well as the viscous region and, thus, no approximations are made for inviscid terms other than those to be used for the pressure field in subsonic flow. A detailed account of the viscous approximation is given in Ref. 14.

For subsonic flow the inviscid flow region is known to be governed by equations which are elliptic; that is, by equations which require downstream boundary conditions for solution. In this circumstance, solution by forward marching integration is not appropriate, at least not without some sort of iterative procedure to satisfy the downstream boundary conditions. To circumvent this problem for subsonic flows, it is therefore assumed that the pressure field appropriate for irrotational inviscid flow through the passage represents a given, reasonable first approximation to the actual pressure field. Thus, inviscid axial pressure gradients computed with appropriate downstream boundary conditions are "imposed" upon the flow, much as in conventional boundary layer theory, so as to permit solution by forward marching integration for subsonic flows. For internal flows, the inviscid pressure gradients are corrected for internal flow losses associated with the well known viscous pressure drop and blockage effects by a process which is consistent with forward marching integration. The imposition of inviscid pressure gradients incorporates a priori the elliptic effects associated with a subsonic pressure field without the necessity of solving elliptic equations other than for an inviscid flow. The inviscid pressure field can be generated from any convenient source and does not necessarily require the solution of compressible or even three-dimensional inviscid flow equations. In the S-shaped bend cases presented, the three-dimensional inviscid pressure field was not available, so a highly approximate method was used to provide the inviscid pressures.

Turbulence Model

The mixing length model used in this analysis employs the eddy-viscosity formulation for the Reynolds stresses, i.e.,

$$\rho \overline{v'_i v'_j} = -\frac{\mu_T}{Re} \frac{\partial v_j}{\partial x_i} \qquad (4)$$

Hence, this formulation still suffers from the physical shortcoming that there is zero Reynolds stress wherever the velocity gradient is zero. In addition, the eddy viscosity formulation is isotropic which may be incorrect in many three-dimensional and swirling flows. However, for practical calculations of turbulent internal flows there are no other available transport models which are as suitable or even as relatively well developed.

The mixing length turbulence model employed in this analysis is based on a mixing length distribution. The mathematical form of the expression for the turbulent viscosity follows from Ref. 17:

$$\frac{\mu_T}{Re} = \rho \ell^2 (2\bar{\bar{e}}:\bar{\bar{e}})^{1/2} \tag{5}$$

where $\bar{\bar{e}}$ is the mean flow rate of strain tensor

$$\bar{\bar{e}} = 1/2 \left[(\nabla \hat{v}) + (\nabla \hat{v})^T \right] \tag{6}$$

The mixing length ℓ is determined from the empirical relationship of McDonald & Camarata (Ref. 18) for equilibrium turbulent boundary layers which can be written

$$\ell(\tilde{y}) = 0.09\, \delta_b \tanh \left[\kappa \tilde{y} / (0.09\, \delta_b) \right] \cdot \mathcal{D} \tag{7a}$$

where δ_b is the local boundary layer thickness, κ is the von Karman constant, taken as 0.43, $\tilde{y}$ is distance from the wall, and $\mathcal{D}$ is a sublayer damping factor defined by

$$\mathcal{D} = P^{1/2} (y^+ - \overline{y^+}) / \sigma \tag{7b}$$

where P is the normal probability function, $y^+ = \tilde{y}(\tau/\rho)^{1/2}/(\mu/\rho)$, τ is local shear stress, $\overline{y^+} = 23$, and $\sigma_1 = 8$.

As a means of simplifying the present preliminary calculations, $\tilde{y}$ is taken as the distance to the nearest wall, and δ_b is simply a rough estimate of the average boundary layer thickness in the duct. The shear stress τ appearing in y^+ was computed assuming a local skin friction coefficient C_f of about 0.0035, the value appropriate for the inlet boundary layers. Here, C_f is based on the local inviscid velocity U_I, i.e., $C_f = \tau/12\rho U_I^2$.

CURVILINEAR COORDINATE SYSTEM

An overview of the nonorthogonal tube-like coordinate system is presented here. A complete description of the construction and component parts of these coordinates can be found in Ref. 14.

Tube-like coordinates have been constructed to provide a natural setting for the study of flows within, between, or outside of a set of prescribed tubes. The prescribed boundary tubes become coordinate surfaces, and, as a result, the specification of fluid dynamic boundary conditions is greatly simplified. Although the equations of motion contain more terms than for a cartesian system, this does not add excessively to the run time of the program. The basic geometry of the bounding tubes then provides the intrinsic constraints upon the coordinate construction. Since the primary goal is the computation of fluid flows within nontrivial geometries and not the development of coordinate systems per se, the coordinates are kept as simple as possible, given the desired generality.

The first step in the construction of tube-like coordinates is to create a suitable family of two-dimensional surfaces which, in some sense, are transverse to a given centerline. If the transverse surfaces are selected to be two-dimensional planes, then the construction of coordinates is greatly simplified. The fluid dynamic computation is only marginally different due to the resulting coordinate nonorthogonality. Consequently the coordinate system that we shall construct will have planar transverse surfaces.

Since each planar transverse surface is a linear subspace of the real three-dimensional Euclidian vector space R^3, any such plane can be completely specified by any two spanning linearly independent vectors in R^3. The specification of the planar family of transverse surfaces is then a result of a construction of two vector fields along a given centerline curve in R^3. The origin of each plane is chosen to coincide with the associated centerline point (Fig. 1). To assure that the planes are always indeed transverse, it will be assumed that they are orthogonal to the centerline at their origins. Tube-like surfaces are generated by loops about the planar origins which deform in some way as we move along the centerline curve; in general, these tube-like surfaces will not intersect the transverse planes orthogonally. Thus, only the centerline direction determines the transverse nature of the cross sectional planes. Specifically, the centerline tangent vectors form a vector field which, at each point, is orthogonal to the plane of the two transverse vectors, and thus each centerline point carries a triple of linearly independent vectors. By the Gram-Schmidt orghogonalization procedure, each such triple of vectors can be made into an orthogonal set, and hence, an orthonormal set which is simply called a frame. Thus, tube-like coordinate systems

notation, $y^1 = \theta$, $y^2 = r$ and $y^3 = t$ for pseudo-angular, pseudo-radial, and axial variables. In this notation, we have thus far developed (1) a length factor, $L = L(y^1, y^2, y^3)$, which is a generalization of radius, (2) an angular distribution function, $\theta = \theta(y^1, y^3)$ which is a generalization of angle, (3) a rotation function, $\Omega = \Omega(y^3)$, and (4) the Frenet frame, $(\vec{V}_1, \vec{V}_2, \vec{V}_3) = (\vec{V}_1(y^3), \vec{V}_2(y^3), \vec{V}_3(y^3))$ upon which the coordinates are built. That the length factor, L, and the angular distribution function, θ, give us a generalization of polar coordinates is obvious since polar coordinates are easily retrieved by taking $L(y^1, y^2, y^3) = y^2$ and $\theta(y^1, y^3) = y^1$. It is also worth noting that the angular distribution function, θ, was chosen to be independent of pseudo-radius, y^2. Although it is not immediately evident, we have removed a considerable amount of potential computational complexity in the process of obtaining metric information by limiting the number of derivatives which must be computed. Furthermore, there is no real loss of flexibility in the construction of angular distribution functions. Since most commonly used analytic descriptions of loops are, in fact, controlled by a collection of parameters which depend only on axial location, y^3, a knowledge of only these parameters is often sufficient for the construction of the angular distribution function. For example, if the loops were to consist of a family of concentric homogeneous ellipses, then the major and minor axes of the outermost ellipse would form a collection of two such parameters.

With the above functions and the Frenet frame, the class of tube-like coordinates comes directly out of the transformation

$$\vec{x} = \vec{\gamma} + L\left\{\vec{V}_2 \cos\phi + \vec{V}_3 \sin\phi\right\} \tag{8a}$$

which transforms curvilinear coordinates, $\vec{y} = (y^1, y^2, y^3)$ into cartesian coordinates $\vec{x} = (x^1, x^2, x^3)$ where

$$\phi(y^1, y^3) = \theta(y^1, y^3) + \Omega(y^3) \tag{8b}$$

At each transverse location, y^3, the space curve vector, $\vec{\gamma}$, translates the origin to the space curve. At a given pseudo-angle, y^1, a unit vector, $\vec{V}_2 \cos\phi + \vec{V}_3 \sin\phi$, is determined by the sum, $\phi = \theta + \Omega$ of the radial distribution function, θ, and the transverse rotation, Ω. This unit vector sweeps out a full 360 degs in the transverse plane as y^1 passes through all of its values. Hence, we could call this a direction pointer for the transverse plane. When this direction pointer is scaled by the length factor, L, we obtain a point

are constructed from a specified centerline curve and an associated frame field. Now the basic question is whether there is a canonical construction of tube-like coordinate systems from either a given centerline or a given frame field. From the theory of space curves (Ref. 19), it is well known that for positive curvature and specified torsion there is a local one-to-one correspondence between frame fields and space curves which pass through a given point. Thus, for nonzero curvature, the centerline space curve has a canonical frame field which is known as the Frenet frame. Consequently, the coordinates will be derived from the Frenet frame when it exists. At centerline points of zero curvature, the Frenet frame is degenerate and must be treated specially.

Once the Frenet frame of the space curve $\vec{\gamma}$ has been established, the unit normal and binormal vectors $\vec{V}_2$ and $\vec{V}_3$ at each point of $\vec{\gamma}$ determine a transverse plane orthogonal to the unit tangent vector $\vec{V}_1$ (Fig. 2). Relative to any such transverse plane, these vectors are also the standard orthonormal basis. Consequently, we can examine the plane separately from the curve, $\vec{\gamma}$, which will only appear as the point at the origin. In two dimensional functional terminology, the unit normal direction can be considered as the abscissa and the unit binormal as the ordinate; or more simply, as x and y axes, respectively. Since the tube-like coordinates are to be generated from some family of tubes encasing the space curve, $\vec{\gamma}$, a cross-sectional cut by a transverse plane produces within the plane a family of loops about the origin. We shall assume that each loop is representable by a strictly monotone radial function of angle. In this regard, a polar type of description is the most suitable. But, of course, the loops are usually more complicated than circles, and thus, we must replace the radius by a function L of both radial and angular variables r and θ. Furthermore, when noncircular loops bound a cross section of fluid, there are regions of varying wall curvature. In a numerical solution, it is desirable to put proportionately more mesh points in regions of higher curvature than in regions of less curvature. Consequently, an angular distribution function, Θ, is a good replacement for the simple angular specification θ, of simple polar coordinates. The net result is a generalization where polar coordinates are replaced by a pseudo-radius, r, and pseudo-angle, θ. Since the loops generally vary from transverse plane to transverse plane, the pseudo-radii and angles must also be functions of axial location, t, on the centerline space curve, $\vec{\gamma}(t)$. Since the normal and binormal directions are usually functions only of the centerline curve, $\vec{\gamma}(t)$, our loops may have symmetries that do not reflect about either of these Frenet directions. Since the use of known symmetries is a great simplification in most problems, we need an option which allows one to define axes that can be aligned in an optimal way. This option is easily established from the specification of a function, $\Omega(t)$, which is a rigid rotation relative to the normal-binormal directions. To bring this development of tube-like coordinates within the framework of the preceding tensor derivations, we shall use the

of our transformation. Since the length factor depends on all three variables, any set of tube-like surfaces can be obtained provided, of course, that loops are representable by a strictly monotone radial function of angle and also that no two transverse cross sections are allowed to intersect.

In a geometric setting, the transformation is really an embedding of tube-like coordinate systems into three dimensional Euclidian space. An illustration is provided in Fig. 3. From the transformation, it is also easy to see that the surfaces of constant y^3 are the transverse planes, the surfaces of constant pseudo-angle, y^1, are ruled surfaces generated from the centerline curve, $\vec{\gamma}$, and the surfaces of constant pseudo-radius, y^2, are just the concentric tubes about the space curve, $\vec{\gamma}$. Separate illustrations of these various coordinate surfaces are given in Figs. 4a, 4b, and 4c, respectively.

METHOD OF SOLUTION

Background

The governing equations can be solved (after modeling the Reynolds stresses) following the general approach developed by McDonald & Briley (Ref. 12) for laminar supersonic flow in rectangular jets. A detailed discussion of the calculation procedure is not included here, as such a discussion would be lengthy, and discussions of the general approach are available elsewhere (Briley & McDonald, Ref. 11; McDonald & Briley, Ref. 12). The method used is based on an implicit scheme which is potentially stable for large step sizes. Thus, as a practical matter, stability restrictions which limit the axial step size relative to the transverse mesh spacing and which become prohibitive for even locally refined meshes (e.g., in laminar sublayers) are not a factor in making the calculations. The general approach is to employ an implicit difference formulation and to linearize the implicit equations by expansion about the solution at the most recent axial location. Terms in the difference equations are then grouped by coordinate direction and one of the available alternating-direction implicity (ADI) or splitting techniques is used to reduce the multidimensional difference equations to a sequence of one-dimensional equations. These linear one-dimensional difference equations can be written in block-tridiagonal or a closely related matrix form and solved efficiently and without iteration by standard block elimination techniques. The general solution procedure is quite flexible in matters of detail such as the type and order accuracy of the difference approximations and the particular scheme for splitting multidimensional difference approximations. Based on previous experience of the authors, however, it is believed that the consistent use of a formal linearization procedure, which incidentally requires the solution of coupled difference equations in most instances, is a major factor in realizing the potential favorable stability properties generally attributed to implicit difference schemes.

Computation of Mean Pressure Drop

To compute the mean pressure drop, the streamwise pressure gradient term in the momentum equations is replaced by $(dp_m/dx)^n$ plus a function of two parameters having the form

$$\pi_1(x,z),\ \pi_2(x,y) \tag{9}$$

where π_1 and π_2 are introduced as a computational device to allow an implicit splitting of the change in the pressure drop term across a step. The dependence of π_1 on z and π_2 on y is removed (to order Δx) as part of the solution procedure. During a step of the solution procedure, the mean pressure drop term is replaced by

$$(dp_m/dx)^n/2 + \pi_1^*(x,z) - \pi_2^n(x,y) \tag{10a}$$

during the first ADI sweep and by

$$(dp_m/dx)^n/2 - \pi_1^n(x,z) + \pi_2^{**}(x,y) \tag{10b}$$

during the second ADI sweep. The variables π^* and π^{**} are parameters computed as part of the implicit solution procedure so as to satisfy an integral mass flux condition. The parameters π_1 and π_2 contain information concerning the mean pressure drop for a given step. To extract this information, it is necessary to define mean values $\tilde{\pi}_1$ and $\tilde{\pi}_2$, averaged in the transverse directions such that

$$\tilde{\pi}_1(x) \equiv \int_{z_1}^{z_2} \pi_1(x,z)\, dz/(z_2 - z_1) \tag{11a}$$

$$\tilde{\pi}_2(x) \equiv \int_{y_1}^{y_2} \pi_2(x,y)\, dy/(y_2 - y_1) \tag{11b}$$

It will be seen that, at the beginning of a step, π_1^n and π_2^n are adjusted to have zero mean for the step about to be taken, i.e., $\tilde{\pi}_1^n = \tilde{\pi}_2^n = 0$. After a step is complete, the updated mean pressure drop is obtained from the area averaged parameters as

$$(dp_m/dx)^{n+1} = (dp_m/dx)^n + \tilde{\pi}_1^* + \tilde{\pi}_2^{**} \tag{12}$$

and the unaveraged parameters are adjusted for the next step so as to have zero mean as follows:

$$\pi_1^{n+1} \equiv \pi_1^{*} - \tilde{\pi}_1^{*}, \quad \pi_2^{n+1} \equiv \pi_2^{**} - \tilde{\pi}_2^{**} \tag{13}$$

The difference approximation across a complete step consisting of both ADI sweeps is obtained by adding Eqs. (10a & b) and invoking the definitions (13) to obtain

$$\begin{aligned} (dp_m/dx)^{n+1} \approx (dp_m/dx)^{n} + \tilde{\pi}_1^{*} + \tilde{\pi}_2^{**} \\ + \left[\pi_1^{n+1} - \pi_1^{n}\right] + \left[\pi_2^{n+1} - \pi_2^{n}\right] \end{aligned} \tag{14}$$

The last two bracketed terms in Eq. (14) represent error terms of order Δx and have zero mean. Thus, the mean values of the parameters π_1 and π_2 account for the change in mean pressure drop across a step, whereas the transverse variation of π_1 and π_2 from the mean is effectively subtracted out during each step to within the aforementioned error terms which in practice are found to be quite small. The overall technique is designed to permit the implicit computation of mean pressure drop using an ADI method without the necessity of iterating. Calculations which serve to verify the procedure are presented subsequently.

Integral Mass Flux Condition

The value of π_1^{*} and π_2^{**} are determined as part of the splitting process so as to satisfy the integral continuity condition for internal flow with no mass addition

$$\int_{y_1}^{y_2} \int_{z_1}^{z_2} \partial \rho u / \partial x \; dy \, dz = 0 \tag{15}$$

The integral condition (15) cannot be split conveniently for use with an ADI method; however, the presently used split form of the continuity equation is

$$\left[(\rho u)^{*} - (\rho u)^{n}\right]/\Delta x + \partial(\rho v)^{*}/\partial y = 0 \tag{16a}$$

$$\left[(\rho u)^{**} - (\rho u)^{*}\right]/\Delta x + \partial(\rho w)^{**}/\partial z = 0 \tag{16b}$$

Integrating Eqs. (16) with respect to the implicit direction and invoking the condition of zero mass addition yields

$$\int_{y_1}^{y_2} \left[(\rho u)^{*} - (\rho u)^{n}\right] dy = 0 \tag{17a}$$

$$\int_{z_1}^{z_2} \left[(\rho u)^{**} - (\rho u)^{*}\right] dz = 0 \tag{17b}$$

which is the split form used as auxiliary conditions to determine π_1 and π_2. Integrating Eqs. (17) with respect to the explicit direction yields

$$\int_{z_1}^{z_2}\int_{y_1}^{y_2} \left[(\rho u)^{*} - (\rho u)^{n}\right] dy\,dz = 0 \tag{18a}$$

$$\int_{y_1}^{y_2}\int_{z_1}^{z_2} \left[(\rho u)^{**} - (\rho u)^{*}\right] dz\,dy = 0 \tag{18b}$$

and thus the integral continuity condition is satisfied across a complete step.

Solution of the Split Difference Equations

The coupled set of linear implicit difference equations arising along rows of grid points during each step of the ADI solution procedure, together with the prescribed boundary condition, can be written in a form having the following matrix structure

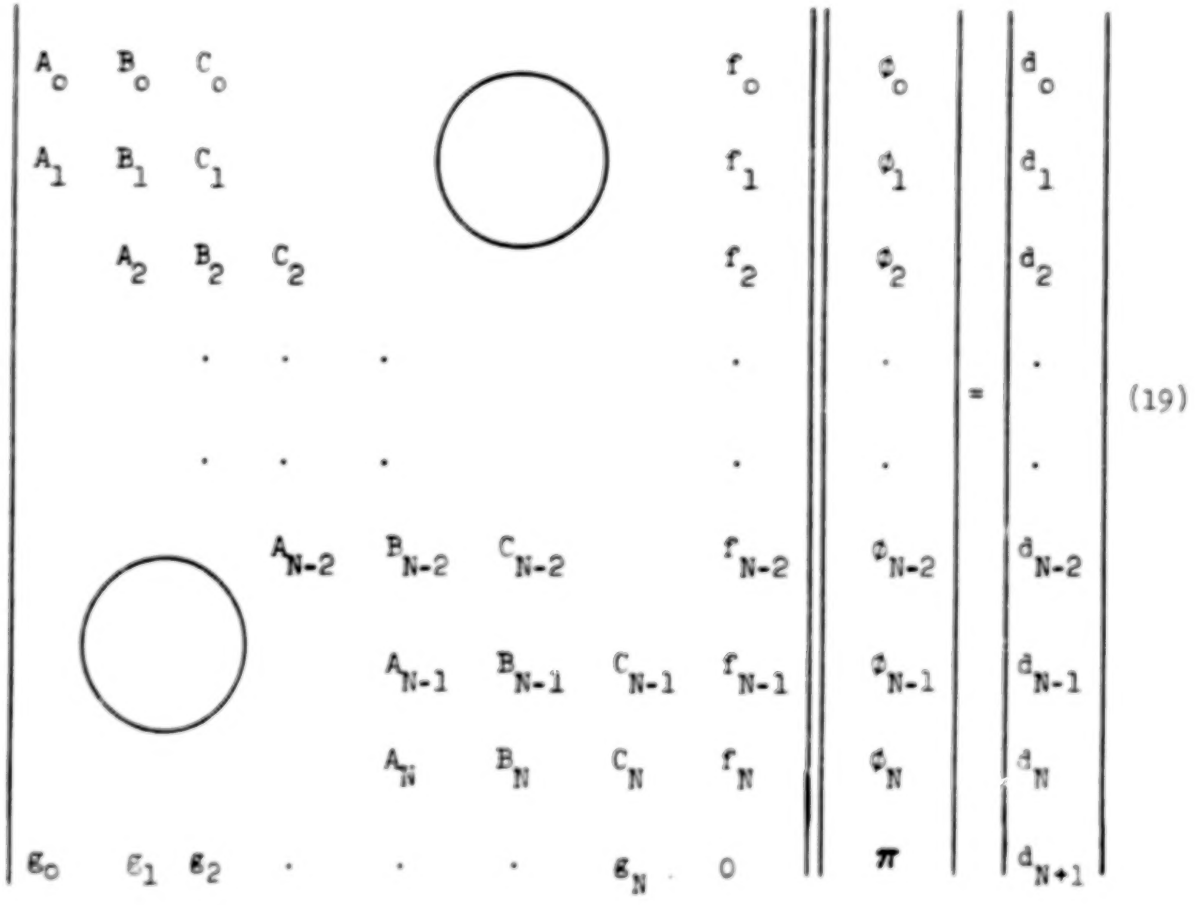

$$
\begin{vmatrix}
A_0 & B_0 & C_0 & & & & & f_0 \\
A_1 & B_1 & C_1 & & & & & f_1 \\
 & A_2 & B_2 & C_2 & & & & f_2 \\
 & & \cdot & \cdot & \cdot & & & \cdot \\
 & & \cdot & \cdot & \cdot & & & \cdot \\
 & & & A_{N-2} & B_{N-2} & C_{N-2} & & f_{N-2} \\
 & & & & A_{N-1} & B_{N-1} & C_{N-1} & f_{N-1} \\
 & & & & A_N & B_N & C_N & f_N \\
\varepsilon_0 & \varepsilon_1 & \varepsilon_2 & \cdot & \cdot & \cdot & \varepsilon_N & 0
\end{vmatrix}
\begin{Vmatrix}
\phi_0 \\ \phi_1 \\ \phi_2 \\ \cdot \\ \cdot \\ \phi_{N-2} \\ \phi_{N-1} \\ \phi_N \\ \pi
\end{Vmatrix}
=
\begin{vmatrix}
d_0 \\ d_1 \\ d_2 \\ \cdot \\ \cdot \\ d_{N-2} \\ d_{N-1} \\ d_N \\ d_{N+1}
\end{vmatrix}
\qquad (19)
$$

For each grid point index i, ϕ_i is a column vector containing the dependent variables ρ, u, v, w. P, a single variable, is the pressure correction p_1 or p_2 depending on the ADI step. A_i, B_i, and C_i are square (4x4) matrices containing the implicit difference coefficients. f_i is a column vector containing the implicit coefficients of P, and d_i is a column vector containing only computationally known quantities. There are N+1 grid points along the row under consideration. Difference approximations for the four governing equations are associated with symbols having subscripts 1 through N-1; the subscripts 0 and N are associated with the boundary conditions, which may involve up to three grid points. Equation (19) represents 4 (N+1) linear equations in 4 (N+1) dependent variables plus the additional parameter variable P. Thus, one additional boundary condition or auxiliary relation is required to close the system, and this additional relation is presumed to be

available when needed. Excluding the elements C_O, A_N, and f_i, the matrix structure of Eq. (19) is block tridiagonal, and direct solution by standard block elimination techniques (cf., Isaacson & Keller, Ref. (20) is both straightforward and efficient. The precise scheme used here consisted of Gaussian elimination for a simple tridiagonal system (sometimes called the Thomas algorithm) but with elements of the tridiagonal matrix treated as square submatrices rather than as simple coefficients. The required inverses of diagonal submatrices were obtained by a Gauss-Jordan reduction. The additional operations necessary to include the non-block-tridiagonal elements C_O, A_N, and f_i are easily incorporated provided the original block tridiagonal coding is carefully organized.

APPLICATION TO INTERNAL SUBSONIC FLOW

The analysis of the previous sections has been applied to the flow in a pipe whose centerline is specified by piecewise polynomial functions with continuous third derivatives. Cross sections of the pipe in planes normal to this centerline are described by the equation of a superellipse (in local cartesian coordinates):

$$b^a |x|^a + |y|^a = m^a \tag{20}$$

where a is the superelliptic exponent constrained to the range $2 \leq a \leq 10$, b is the ratio of major to minor axes (sometimes called the shape factor), and m is the length of the minor axis.

Throughout the remaining discussion, all variables in the governing equations are nondimensional, having been normalized by the following reference quantities: distance, L_r; velocity, U_r; density ρ_r; temperature, T_r; total enthalpy, U_r^2; pressure, $\rho_r U_r^2$; viscosity, μ_r. Here, the subscript r denotes a reference quantity. After the various modifications outlined above are implemented, the governing equations (2a-e) can be written, after neglecting all density fluctuations, as

$$\frac{\partial}{\partial y^i}\left(\bar{\rho}\,\bar{v}^i\sqrt{g}\right)=0 \tag{21a}$$

$$\frac{\partial}{\partial y^j}\left[\left(\bar{\rho}\bar{v}^i\bar{v}^j + g^{ij}\bar{p} + \bar{\omega}^{ij}\right)\frac{\partial x^s}{\partial y^i}\sqrt{g}\right]=0 \tag{21b}$$

where ω^{ij} is the viscous portion of the stress tensor (Eq. 2a) modified by the viscous approximation of Ref. 14, α and β are redefined to include the Reynolds stresses as:

$$\alpha_k^{ij} = \frac{\mu+\mu_T}{Re}\left(\frac{2}{3}g^{ij}\,\Gamma^{\ell}_{k\ell} + \frac{\partial g^{ij}}{\partial y^k}\right) \tag{22a}$$

and

$$\beta^{ijl}_{k} = \frac{\mu + \mu_T}{Re}\left(\frac{2}{3} g^{ij}\delta^{l}_{k} - g^{il}\delta^{j}_{k} - g^{jl}\delta^{i}_{k}\right) \qquad (22b)$$

and the pressure is

$$\bar{p} = \frac{\gamma-1}{\gamma}\bar{\rho}\left[\bar{E} - \frac{1}{2} g_{kl}\ \bar{v}^{k}\bar{v}^{l}\right] \text{ for } j=1,2 \qquad (23a)$$

$$\bar{P} = P_I + P_M \qquad \text{for } j=3 \qquad (23b)$$

where γ is the ratio of specific heats, P_I is the specified inviscid pressure, and P_m is the mean pressure drop computed by the technique outlined above.

Boundary and Initial Conditions

In computing turbulent flow near solid boundaries a problem can arise from the juxtaposition of large and small physical length scales within very small physical distances. One method of solving this problem is to use a coordinate transformation to pack computational points near the wall to resolve the sublayer. Spacing between grid points is increased as the distance from the wall and the length scale increase. A second method is to employ an analytical wall function to model the near wall region, thus avoiding solving the governing equation in this region (Refs. 8 and 21). Both methods are available within the computer code. Because of the economy of grid points, and the resulting reduction in computational cost, only the wall function method has been used to date.

To implement the wall function boundary conditions, the first grid point away from a wall is positioned in a highly turbulent region of the flow. Since the near wall region is not resolved, the usual specification of no-slip conditions is no longer satisfactory. This is shown schematically in Fig. 5 by reference to a typical turbulent boundary layer velocity profile with a superimposed grid point distribution. The line segment CD represents the slope of the velocity profile at the first grid point. If one-sided differencing were used for $\partial V/\partial n$ together with the no-slip condition at the wall, the computed slope would be the line segment AB and substantial error

would occur. To circumvent this difficulty, a fictitious slip velocity 0' is introduced and is determined from the wall function boundary condition such that the finite difference value of $\partial V/\partial n$ at the first grid point is consistent with the assumed analytical form for the turbulent velocity profile.

To derive wall function boundary conditions, it is assumed that the velocity component normal to the wall is zero and that the magnitude of the resultant velocity vector, $\tilde{u}$, obeys a universal log law

$$\tilde{u} = u_\tau \, \ell n(u_\tau n/\nu)/\kappa + c \tag{24}$$

where U_τ is the friction velocity $U_\tau = (\tau_w/\rho)^{1/2}$, $\kappa = 0.41$ is the von Karman constant, and C is a constant taken as 5.0. The boundary condition is obtained by differentiating Eq. (24) with respect to n and neglecting the contribution due to skewing of the resultant velocity $\tilde{u}$, yielding:

$$\frac{\partial \tilde{u}}{\partial n} = u_\tau/\kappa n \tag{25}$$

The wall density is specified from a knowledge of the pressure. At the symmetry planes of θ = constant, symmetry conditions are used.

Since a small tube is placed around the centerline to circumvent the geometric singularity there, careful handling of the boundary conditions is required. Since this area is distant from the walls, gradients of the fluid properties are expected to be small. Consequently the first derivative of the streamwise velocity is set to zero. The pressure gradients are all mild so that the second derivative of the density is also set to zero. The cross flows at the centerline tube must be set to insure that total mass flow is conserved. The transverse velocity at the centerline tube is set as a function boundary condition whose value is equal to the average transverse velocity at the previous computational plane in the neighborhood of the centerline.

To obtain upstream starting conditions, the inviscid velocity distribution in the plane at the initial axial location $x = x_1$ was scaled near the wall by normalized two-dimensional compressible turbulent boundary layer velocity profiles having a prescribed thickness, Reynolds number, and Mach number. The particular profile shape used consisted of a Coles (Ref. 22)

profile modified for compressibility as suggested by Maise and McDonald (Ref. 23) and made continuous through the sublayer region following the suggestion of Waltz (Ref. 24). With the backward difference formulation, starting conditions for $\overline{v}$ and $\overline{w}$ are not required other than in the linearization procedure, and setting $\overline{v} = \overline{w} = 0$ at the starting plane was found to produce a smooth and reasonable starting process for the calculation. Given the velocity, the density can be computed from the inviscid pressure P_I, here assumed constant across the initial value surface.

DISCUSSION OF RESULTS

Results from computed solutions are presented for two flow problems. The first problem is the laminar flow in the entrance region of a straight pipe. This flow has been thoroughly studied both experimentally and analytically providing a good means for testing the validity and accuracy of the overall calculation procedure. The second problem treated is that of flow through an S-shaped bend. Calculations have been performed at a series of Reynolds numbers, both laminar and turbulent, for several cross-sectional duct shapes.

For completeness, some results from a series of diagnostic runs are also included in this report. These cases consist of flow in an axisymmetric diffuser and of flow in transition ducts whose cross sectional shape varies from nearly square to round. The results from these runs are not as yet adequate, pointing out the need for further code development addressed to these problems.

The flow in the entrance region to a circular straight pipe was computed at a Reynolds number of 500 based on pipe radius. The initial Mach number was set to 0.01 to approximate the incompressible solution. The initial boundary layer thickness was set at 0.075 diameter. This test case is considered important as a means for verifying large portions of the code since the entire nonorthogonal geometric package was used to generate coordinates that reduce to cylindrical coordinates for this case. The entire general tensor formulation of the equations was used to generate the familiar "parabolized" Navier-Stokes equations in the cylindrical coordinates. In addition the entire ADI procedure was used to split the equations into radial and circumferential parts for the two part solution procedure even though the problem was axisymmetric. The results of this calculation were compared to the detailed experimental data of Reshotko (Ref. 25). Excellent agreement between the measured and computed velocity profiles was found over the developing region as seen in Fig. 6. In the fully developed limit, the calculations, measurements and classical analytical solution were virtually identical.

This test case was repeated for a variety of cross sectional duct geometries including ellipses up to a shape factor (ratio of major to minor axis) of 2.0. A series of test cases was also run for a series of ducts whose cross sections were superellipses with exponents ranging from 2 to 10. Although no experimental data were found for comparison with these solutions, the results nevertheless appear reasonable. Figure 7 presents the centerline velocity distributions for the series of superelliptic ducts.

An additional set of straight pipe calculations was run to check the computation of the effects of compressibility. Using a straight pipe of superelliptic cross section (exponent 3.0) the initial Mach number was progressively increased from 0.01 (incompressible solution) to 0.1, 0.2 and 0.3. As expected, the compressible solutions did not exhibit the limiting value of centerline velocity. At a given nondimensional distance from the start of the pipe ($\frac{X/R}{Re}$) the nondimensional centerline velocity increased as the effects of compressibility increased as seen in Fig. 8. This behavior is entirely consistent with the well know effect of Mach number on pressure loss due to friction.

A final test of the calculation procedure occurred in the case having an initial Mach number of 0.3. As the flow proceeded downstream, the pressure losses due to friction caused the centerline Mach number to increase past the sonic point into a region where the centerline flow became supersonic. The calculation remained stable in this region. Finally the velocity in the centerline region became sufficiently large that, in the mean, the flow encountered the sonic singularity. This singularity arises from the factor $(1-M^2)^{-1}$ appearing in the one-dimensional pipe flow equations where M is here taken to be a mean Mach number at an axial location. Although this term does not appear directly in the three-dimensional equations being solved, the phenominological correspondence between the computed and the one-dimensional results strongly suggests a valid integration of the finite difference equations. When the flow in the pipe choked the calculation procedure broke down immediately. This behavior corresponds to that expected from solution of the initial value problem posed.

The second set of results being presented is a series of calculations of flow through an S-shaped bend. The baseline configuration is a circular pipe with an offset of 1 diameter in a length of 10 diameters shown in Fig. 9. The first test case was laminar with a Reynolds number of 500 based on radius, and an inlet Mach number of 0.1. The accuracy of the flow predictions obtained for this sequence of calculations is limited by the present lack of an adequate inviscid pressure field as determined by the potential flow through the S-bend geometry. This was not a problem in the previous straight duct calculations since in these geometries the inviscid pressure is known to be constant.

To demonstrate the potential of the present method, a highly approximate method was used to generate an inviscid pressure field. Using the radius of curvature of the pipe centerline at each computational plane, a two-dimensional inviscid free vortex solution in the plane of the pipe centerline and the radius of curvature was assumed. The corresponding pressure at each computational point was computed. Although this simplified model does not produce any

pressure gradients normal to the plane of symmetry and does not account for any cross flows, it does produce a pressure higher at the outside of the bend than on the inside. Using the same procedure at each computational plane, the inviscid pressure gradients were computed from backward differences of these pressures.

Using this quasi-two-dimensional pressure field the flow through the S-duct of Fig. 9 was computed. The results showed that in the first part of the bend a secondary flow pattern typical of that which is to be expected was produced. The low inertia fluid in the boundary layer moves from the high pressure at the outside of the bend along the wall toward the inside of the bend. The flow outside the boundary layer responds to the centrifugal forces caused by the turning of the duct. A series of vector plots of the cross flow velocities is presented in Fig. 10. A problem was encountered near the end of the first bend where the secondary flows were seen to reverse. This problem is believed to result from the use of the quasi-two-dimensional pressure model for this three-dimensional problem, thus pointing out the need for a three-dimensional inviscid pressure field.

Several additional cases for the curved centerline in elliptic ducts of shape factor 0.667 and 1.5 and in a superelliptic duct of exponent 10.0 were run to demonstrate the geometric capability of the code. In figures 10-13, Station No. 5 is the end of a 1 1/4 diameter long straight section. From Station No. 6 through Station No. 13 the radius of curvature decreases until it reaches 15 diameters.

An additional series of cases was run for turbulent flow at a Reynolds number of 10^5 and an inlet Mach number of 0.1. Using the same centerline as the above cases, ducts with circular and mildly elliptic (shape factor 1.1) cross sections were run. The results of these calculations are not available for publication at this time. Each of the S-shaped bend cases was run on a 15 x 15 computational grid at each of 45 streamwise planes. Using the Univac 1110 computer, each case ran approximately one hour.

Several additional calculations were performed in the course of the present investigation. Although these are diagnostic calculations whose results are not as yet adequate, several of these are included for completeness.

The case of flow through an axisymmetric diffuser produced a problem in which the velocity near the centerline decreased rapidly, even at wall angles on the order of 1°. This unrealistic deceleration was confined to the 3 or 4 grid points near the centerline. A detailed examination of this calculation showed that the streamwise velocity and density were changing locally in a compensating manner to maintain the imposed static pressure.

The other set of diagnostic runs is of flow in transition ducts whose cross section varies from nearly square to circular as shown in Fig. 14. The calculations were run both laminar and turbulent, and additional pipes of constant cross section were added both before and after the transition section. When these were being run, the computer program was being coupled to the computer graphics system developed under the direction of Bernhard Anderson at NASA Lewis Research Center. The lines of constant velocity at several cross sections produced by the computerized graphics system are shown in Fig. 15. Again, difficulties were apparent in the region of the centerline. Further investigation is needed to resolve the problem encountered near the centerline in the axisymmetric diffuser and transition duct calculations.

RESUME

A method for computing three-dimensional turbulent subsonic flow in curved ducts has been developed. A set of tube like coordinates is given for a general class of geometries applicable to subsonic diffusers. The geometric formulation is complex and no previous treatment of this class of viscous flow problems is known to the authors. The duct centerline is a space curve specified by piecewise polynominals with continuous third derivatives. A Frenet frame is located on the centerline at each location that a cross section is required. The cross sections are described by superellipses imbedded in the Frenet frame. The duct boundaries are coordinate surfaces, greatly simplifying the boundary conditions. The resulting coordinates are nonorthogonal.

An approximate set of governing equations is given for viscous flows having a primary flow direction. The derivation is coordinate invariant and the resulting equations are expressed in tensor form. These equations are solved by an efficient alternating direction implicit (ADI) method. This numerical method is found to be stable, permitting solution in difficult geometries using the general tensor formulation.

Flow in the entrance region of a circular straight pipe was computed at a Reynolds number of 500. At an inlet Mach number of 0.01 the results compared very favorably with incompressible experimental data. For a pipe of non-circular corss section at a Reynolds number of 500, the inlet Mach number was progressively increased from 0.01 to 0.1, 0.2, and 0.3 and the expected effects of compressibility were observed. For the case with an entrance Mach number of 0.3 the calculation proceded until the flow choked. This behavior corresponds to that expected from solution of the initial value problem posed.

A series of calculations was performed for flow through a duct which undergoes an S-shaped bend. These cases were run at a Reynolds number of 500 and an inlet Mach number of 0.1. Four different duct cross sections were used: circular, elliptic with shape factor of 1.5, elliptic with shape factor of 0.667, and superelliptic of exponent 10.0. A highly approximate quasi-two-dimensional inviscid pressure formulation was used for the S-bend calculations. The results showed that in the first part of the bend a secondary flow pattern typical of that which is to be expected was produced. A problem was encountered near the end of the first bend where the secondary flows were seen to reverse. This problem is believed to result from the use of the quasi-two-dimensional inviscid pressure model, thus pointing out the need for an accurate three-dimensional inviscid pressure field. Two cases of turbulent flow through an S-shaped bend were computed at a Reynolds number

of 10^5 and an inlet Mach number of 0.1. One case had a circular cross section, the other an elliptic cross section with shape factor 1.1. Flow in an axisymmetric diffuser and in a transition duct are additional cases discussed for completeness.

APPENDIX

COMPUTER CODE INPUT AND OUTPUT

The input to the PEPSIG code is provided through three Namelist tables. Although the code is still in the development stage and elegant input has not yet been devised, the Namelist method provides a serviceable means of setting up the cases to be run. The three Namelists are, in order of being read: GEOB, LIST1, and COEFL. The numbers in parenthesis following the explanation of the input variable are the recommended values.

GEOB:

NRAD - Number of grid points in the radial direction (15)

MQ - One less than the number of grid points in the circumferential direction (14)

RTUBE - Radius of the tube put around the centerline to remove the geometric singularity (0.05)

VIS(2) - Fraction of a quadrant to be computed (0.5 for half quadrant symmetry, 2.0 for two quadrants)

P(1,J) - Coefficients of polynominal in x for shape factor - ratio of major to minor axis where:

$$S.F. = P(1,1) + P(1,2)\,x + P(1,3)\,x^2 + P(1,4)\,x^3 \ldots + P(1,11)\,x^{10}$$

P(2,J) - Coefficients of polynominal in x for radius of major axis

P(4,J) - Coefficients of polynominal in x for superelliptic exponent between 2 and 10.

PA(3,1,J) - Coefficients of polynominal in x for traverse cartesian component of centerline curve. Set to zero for straight duct.

NOTE: The P and PA arrays determine the location of the grid points. Since the position vector of the grid points is differentiated three times within the code, the piecewise polynominals describing these locations must be continuous to three derivatives. One must be careful of these derivatives, they have a great effect on the code.

LIST1:

YZERO - Reference length in ft (1.0)

RZERO - Reference density in slugs/ft^3

UZERO - Reference velocity in ft/sec

CMACH - Reference Mach Number

NOTE: Set either CMACH or UZERO and the other will be computed within the code.

IRSTIN - The station number to be read in for restart

If IRSTIN = 0, not a restart case

IRSTOT - The interval for saving restart information

If IRSTOT = 0, no restart information saved

JRSTIN - Logical file name from which restart information is to be read

JRSTOT - Logical file name onto which restart information is to be written

NFILE - The sequence number in JRSTIN of the desired restart information

NSAVED - The number of restart stations saved on JRSTOT; must be initialized in inputs to the number of stations already written (and to be preserved) on JRSTOT. Nominally initialized NSAVED = 0.

NOTE: By setting JRSTOT = JRSTIN and NFILE = NSAVED, one file can be used for both read and write information, without destroying the already saved information.

YSLOT(2) - Initial nondimensionalized boundary layer thickness

NS - Number of the last marching step to be taken

NFIRST - Number of the first marching step whose geometry is to be specified (usually 1)

X(NFIRST) - Nondimensionalized location of first two marching steps
X(NFIRST + 1)

AP - Ratio of consecutive step sizes in the marching direction

$$x(i) = x(i-1) + AP * [x(i-1) - x(i-2)]$$

REY - Reynolds number based on UZERO and YZERO

KTURB - 0 Laminar with no slip boundary conditions
- 1 Turbulent with wall function boundary conditions

IPLOT - 1 Write plot file (Logical Unit 8)
- 0 No plot file

ICOEF(I,J) - Controls dump of terms being loaded into the block tri-diagonal matrix

I=1 J=1,10 Momentum Eqs.
I=2 J=1,3 Continuity Eq.

ICOEF(1,20) - 1 Dumps the stored geometric data at start of equation writing subroutine coefg.

COEFL:

IGDMP - 2 Dumps equations loaded into matrix inverter
- 0 No dump

There are three types of output generated by the PEPSIG code. First is the restart information that is written on a user specified data file. This information is used to permit a problem to be run as a series of short computer runs instead of running it all at once. The restart is exact in that cases run using the restart capability yield exactly the same results as those run all the way through without using the restart.

The second type of output is the printed output delivered on paper or microfiche. This output contains tables of parameters of interest at each calculation plane. A sample printed output has been anotated to explain its salient features and is included below.

In three dimensional flow problems the flow characteristics can become very complicated. To make the results of this calculation procedure readily available to the user, some visualization techniques were required. Bernhard Anderson of NASA Lewis Research Center has headed up the development of a family of advanced graphics packages that can be readily coupled to two

and three dimensional fluid dynamics computer codes. The computer code developed in this investigation has been coupled into this NASA graphics system to automatically provide Calcomp, 16 mm film strip, and even movies of the results. This is the third form of output. These graphics capabilities can be used during code development to help highlight problem areas. The graphics are expecially useful in presenting the results of calculations to help the user understand how the features of his duct design affect the flow of gas within the duct.

Microfilmed From
Best Available Copy

```
@ADD,   PEPSIG.CURVED CENTERLINE TEST CASE  RALPH LEVY
@PRT,S  PEPSIG.RUN.
@PRT,TL PEPSIG.
@ASG,T  9,U                    Scratch File
@ASG,AX GK1.                   Restart File
@USE 11,GK1.
@ASG,AX PEPSIGPLOT(3).         Plot File
@USE 8,PEPSIGPLOT(3)
@XQT PEPSIG.ABSA
 $GEOM
 NRAD=15,MQ=14,
 P(1,1)=1.5,
 P(2,1)=1.0,
 P(3,1)=0.0,
 P(4,1)=2.0,
 VIS=0.35,2.0,1.0,0.0,
 $END
 $LIST1
 NS=5,IRSTIN=0,IRSTOT=5,NFILE=0,
 NFIRST=1,
 X(1)=0.0,
 X(2)=0.4,
 AP=1.3,
 YSLOT=.0,.35,
 REY=5000.,KTURB=0,
 CMACH=.1,
 $END
 $COEFL
 IGDMP=0,
 $END
@XQT PEPSIG.ABSA
 $GEOM
 NRAD=15,MQ=14,
 P(1,1)=1.5,
 P(2,1)=1.0,
 P(3,1)=0.0,
 P(4,1)=2.0,
 PA(3,1,5)=.436E-3,
 PA(3,1,6)=-.48E-4,
 PA(3,1,7)=.144E-5,
 VIS=0.35,2.0,1.0,0.0,
 $END
 $LIST1
 NS=13,IRSTIN=5,IRSTOT=5,NFILE=1,
 NFIRST=5,
 X(5)=0.0,
 X(6)=0.5,
 AP=1.0,
 YSLOT=.0,.35,
 REY=5000.,KTURB=0,
 CMACH=.1,
 $END
 $COEFL
 IGDMP=0,
 $END
```

Microfilmed From
Best Available Copy

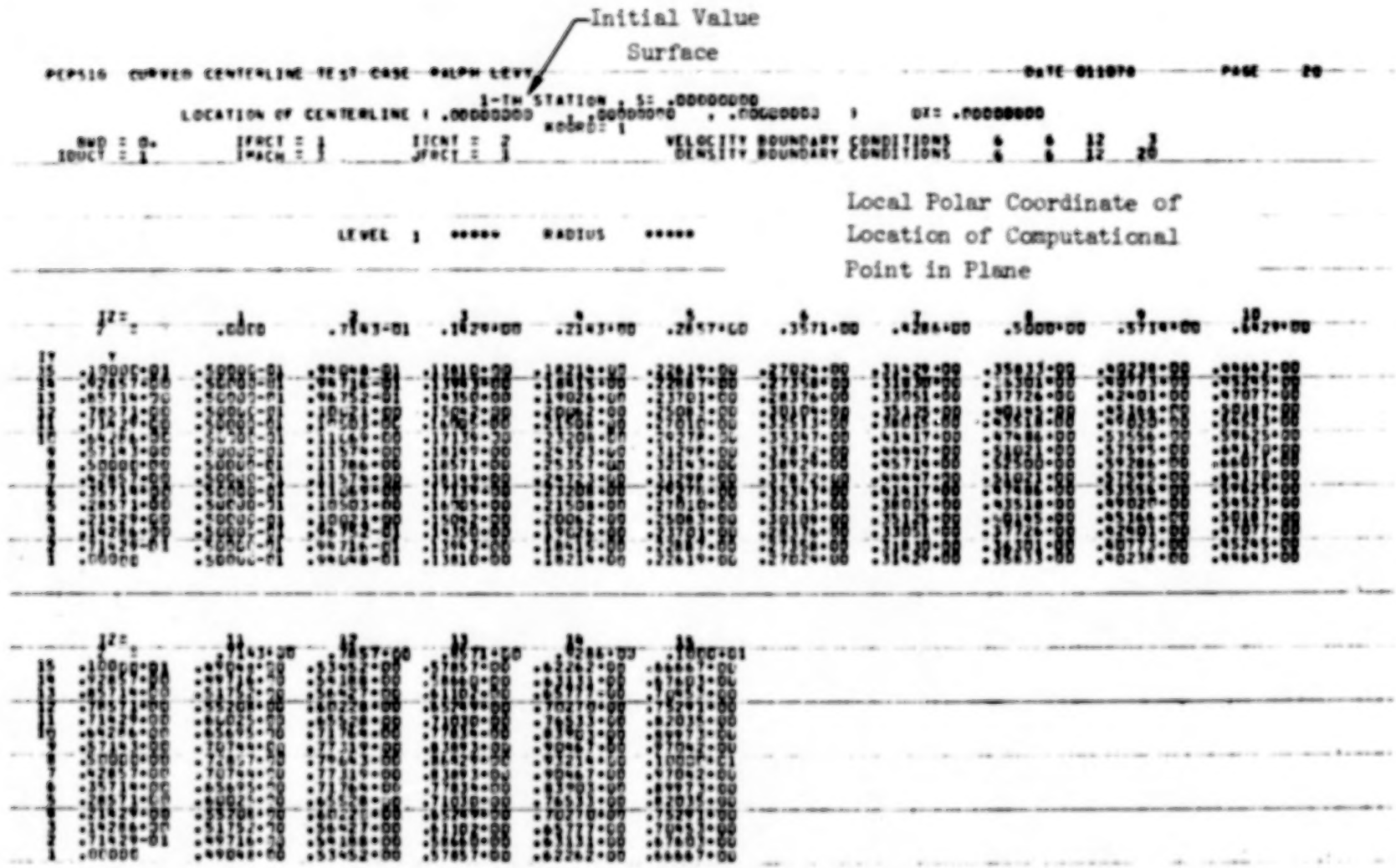

Microfilmed From
Best Available Copy

Second Local Polar Coordinate

LEVEL : ***** THETA *****

IY	Y \ IZ =	1 .0000	2 .7143-01	3 .1429+00	4 .2143+00	5 .2857+00	6 .3571+00	7 .4286+00	8 .5000+00	9 .5714+00	10 .6429+00
15	.10000+01	180.00	180.00	180.00	180.00	180.00	180.00	180.00	180.00	180.00	180.00
14	.92857+00	167.14	167.14	167.14	167.14	167.14	167.14	167.14	167.14	167.14	167.14
13	.85714+00	154.29	154.29	154.29	154.29	154.29	154.29	154.29	154.29	154.29	154.29
12	.78571+00	141.43	141.43	141.43	141.43	141.43	141.43	141.43	141.43	141.43	141.43
11	.71429+00	128.57	128.57	128.57	128.57	128.57	128.57	128.57	128.57	128.57	128.57
10	.64286+00	115.71	115.71	115.71	115.71	115.71	115.71	115.71	115.71	115.71	115.71
9	.57143+00	102.86	102.86	102.86	102.86	102.86	102.86	102.86	102.86	102.86	102.86
8	.50000+00	90.00	90.00	90.00	90.00	90.00	90.00	90.00	90.00	90.00	90.00
7	.42857+00	77.14	77.14	77.14	77.14	77.14	77.14	77.14	77.14	77.14	77.14
6	.35714+00	64.29	64.29	64.29	64.29	64.29	64.29	64.29	64.29	64.29	64.29
5	.28571+00	51.43	51.43	51.43	51.43	51.43	51.43	51.43	51.43	51.43	51.43
4	.21429+00	38.57	38.57	38.57	38.57	38.57	38.57	38.57	38.57	38.57	38.57
3	.14286+00	25.71	25.71	25.71	25.71	25.71	25.71	25.71	25.71	25.71	25.71
2	.71429-01	12.86	12.86	12.86	12.86	12.86	12.86	12.86	12.86	12.86	12.86
1	.00000	.00	.00	.00	.00	.00	.00	.00	.00	.00	.00

IY	Y \ IZ =	11 .7143+00	12 .7857+00	13 .8571+00	14 .9286+00	15 .1000+01
15	.10000+01	180.00	180.00	180.00	180.00	180.00
14	.92857+00	167.14	167.14	167.14	167.14	167.14
13	.85714+00	154.29	154.29	154.29	154.29	154.29
12	.78571+00	141.43	141.43	141.43	141.43	141.43
11	.71429+00	128.57	128.57	128.57	128.57	128.57
10	.64286+00	115.71	115.71	115.71	115.71	115.71
9	.57143+00	102.86	102.86	102.86	102.86	102.86
8	.50000+00	90.00	90.00	90.00	90.00	90.00
7	.42857+00	77.14	77.14	77.14	77.14	77.14
6	.35714+00	64.29	64.29	64.29	64.29	64.29
5	.28571+00	51.43	51.43	51.43	51.43	51.43
4	.21429+00	38.57	38.57	38.57	38.57	38.57
3	.14286+00	25.71	25.71	25.71	25.71	25.71
2	.71429-01	12.86	12.86	12.86	12.86	12.86
1	.00000	.00	.00	.00	.00	.00

Microfilmed From
Best Available Copy

1-TH STATION , S= .00000000
LOCATION OF CENTERLINE (.00000000 , .00000000 , .00000000) DX= .00000000
KOORD= 1

BND = 0. IFRCT = 1 ITCNT = 2 VELOCITY BOUNDARY CONDITIONS 6 6 12 3
IDUCT = 1 IMACH = 1 JFRCT = 1 DENSITY BOUNDARY CONDITIONS 6 6 12 20
VELOCITY VECTOR DISPLAYED IN COMPUTATIONAL COORDINATES

Initial Values of
Streamwise Velocity

LEVEL 1 ***** U-VEL

IZ=	1	2	3	4	5	6	7	8	9	10
Z =	.0000	.7143-01	.1429+00	.2143+00	.2857+00	.3571+00	.4286+00	.5000+00	.5714+00	.6429+00
IY Y										
15 .10000+01	.10000+01	.10000+01	.10000+01	.10000+01	.10000+01	.10000+01	.10000+01	.99683+00	.97422+00	.91697+00
14 .92857+00	.10000+01	.10000+01	.10000+01	.10000+01	.10000+01	.10000+01	.10000+01	.99732+00	.97589+00	.91986+00
13 .85714+00	.10000+01	.10000+01	.10000+01	.10000+01	.10000+01	.10000+01	.10000+01	.99855+00	.98077+00	.92873+00
12 .78571+00	.10000+01	.10000+01	.10000+01	.10000+01	.10000+01	.10000+01	.10000+01	.99874+00	.98824+00	.94395+00
11 .71429+00	.10000+01	.10000+01	.10000+01	.10000+01	.10000+01	.10000+01	.10000+01	.10000+01	.99614+00	.96497+00
10 .64286+00	.10000+01	.10000+01	.10000+01	.10000+01	.10000+01	.10000+01	.10000+01	.10000+01	.99993+00	.98887+00
9 .57143+00	.10000+01	.10000+01	.10000+01	.10000+01	.10000+01	.10000+01	.10000+01	.10000+01	.10000+01	.99861+00
8 .50000+00	.10000+01	.10000+01	.10000+01	.10000+01	.10000+01	.10000+01	.10000+01	.10000+01	.10000+01	.99994+00
7 .42857+00	.10000+01	.10000+01	.10000+01	.10000+01	.10000+01	.10000+01	.10000+01	.10000+01	.10000+01	.99861+00
6 .35714+00	.10000+01	.10000+01	.10000+01	.10000+01	.10000+01	.10000+01	.10000+01	.10000+01	.99993+00	.98887+00
5 .28571+00	.10000+01	.10000+01	.10000+01	.10000+01	.10000+01	.10000+01	.10000+01	.10000+01	.99614+00	.96497+00
4 .21429+00	.10000+01	.10000+01	.10000+01	.10000+01	.10000+01	.10000+01	.10000+01	.99874+00	.98824+00	.94395+00
3 .14286+00	.10000+01	.10000+01	.10000+01	.10000+01	.10000+01	.10000+01	.10000+01	.99855+00	.98077+00	.92873+00
2 .71429-01	.10000+01	.10000+01	.10000+01	.10000+01	.10000+01	.10000+01	.10000+01	.99732+00	.97589+00	.91986+00
1 .00000	.10000+01	.10000+01	.10000+01	.10000+01	.10000+01	.10000+01	.10000+01	.99683+00	.97422+00	.91697+00

IZ=	11	12	13	14	15
Z =	.7143+00	.7857+00	.8571+00	.9286+00	.1000+01
15 .10000+01	.81588+00	.66779+00	.47552+00	.24797+00	.00000
14 .92857+00	.81969+00	.67161+00	.47869+00	.24976+00	.00000
13 .85714+00	.83120+00	.68375+00	.48880+00	.25553+00	.00000
12 .78571+00	.85217+00	.70631+00	.50788+00	.26653+00	.00000
11 .71429+00	.88614+00	.74283+00	.53976+00	.28521+00	.00000
10 .64286+00	.92642+00	.79587+00	.58875+00	.31480+00	.00000
9 .57143+00	.96523+00	.85533+00	.64910+00	.35104+00	.00000
8 .50000+00	.97991+00	.88418+00	.68152+00	.37459+00	.00000
7 .42857+00	.96523+00	.85533+00	.64910+00	.35104+00	.00000
6 .35714+00	.92642+00	.79587+00	.58875+00	.31480+00	.00000
5 .28571+00	.88614+00	.74283+00	.53976+00	.28521+00	.00000
4 .21429+00	.85217+00	.70631+00	.50788+00	.26653+00	.00000
3 .14286+00	.83120+00	.68375+00	.48880+00	.25553+00	.00000
2 .71429-01	.81969+00	.67161+00	.47869+00	.24976+00	.00000
1 .00000	.81588+00	.66779+00	.47552+00	.24797+00	.00000

Microfilmed From
Best Available Copy

LEVEL 1 ***** V-VEL *****

Initial Values of
Circumferential Velocity

I= / Z =	1 .0000	2 .7143-01	3 .1429+00	4 .2143+00	5 .2857+00	6 .3571+00	7 .4286+00	8 .5000+00	9 .5714+00	10 .6429+00
17										
16	.10000+01	.00000	.00000	.00000	.00000	.00000	.00000	.00000	.00000	.00000
15	.92857+00	.00000	.00000	.00000	.00000	.00000	.00000	.00000	.00000	.00000
14	.85714+00	.00000	.00000	.00000	.00000	.00000	.00000	.00000	.00000	.00000
13	.78571+00	.00000	.00000	.00000	.00000	.00000	.00000	.00000	.00000	.00000
12	.71429+00	.00000	.00000	.00000	.00000	.00000	.00000	.00000	.00000	.00000
11	.64286+00	.00000	.00000	.00000	.00000	.00000	.00000	.00000	.00000	.00000
10	.57143+00	.00000	.00000	.00000	.00000	.00000	.00000	.00000	.00000	.00000
9	.50000+00	.00000	.00000	.00000	.00000	.00000	.00000	.00000	.00000	.00000
8	.42857+00	.00000	.00000	.00000	.00000	.00000	.00000	.00000	.00000	.00000
7	.35714+00	.00000	.00000	.00000	.00000	.00000	.00000	.00000	.00000	.00000
6	.28571+00	.00000	.00000	.00000	.00000	.00000	.00000	.00000	.00000	.00000
5	.21429+00	.00000	.00000	.00000	.00000	.00000	.00000	.00000	.00000	.00000
4	.14286+00	.00000	.00000	.00000	.00000	.00000	.00000	.00000	.00000	.00000
3	.71429-01	.00000	.00000	.00000	.00000	.00000	.00000	.00000	.00000	.00000
2	.00000	.00000	.00000	.00000	.00000	.00000	.00000	.00000	.00000	.00000
1										

I= / Z =	11 .7143+00	12 .7857+00	13 .8571+00	14 .9286+00	15 .1000+01
16	.10000+01	.00000	.00000	.00000	.00000
15	.92857+00	.00000	.00000	.00000	.00000
14	.85714+00	.00000	.00000	.00000	.00000
13	.78571+00	.00000	.00000	.00000	.00000
12	.71429+00	.00000	.00000	.00000	.00000
11	.64286+00	.00000	.00000	.00000	.00000
10	.57143+00	.00000	.00000	.00000	.00000
9	.50000+00	.00000	.00000	.00000	.00000
8	.42857+00	.00000	.00000	.00000	.00000
7	.35714+00	.00000	.00000	.00000	.00000
6	.28571+00	.00000	.00000	.00000	.00000
5	.21429+00	.00000	.00000	.00000	.00000
4	.14286+00	.00000	.00000	.00000	.00000
3	.71429-01	.00000	.00000	.00000	.00000
2	.00000	.00000	.00000	.00000	.00000
1					

LEVEL 1 ***** V-VEL *****

Microfilmed From
Best Available Copy

IZ= / J=	1 .0000	2 .7143-01	3 .1429+00	4 .2143+00	5 .2857+00	6 .3571+00	7 .4286+00	8 .5000+00	9 .5714+00	10 .6429+00
17										
15	.10000+01	.00000	.07400	.00000	.00000	.00000	.00000	.00000	.00000	.00000
14	.92857+00	.00000	.07400	.00000	.00000	.00000	.00000	.00000	.00000	.00000
13	.85714+00	.00000	.07400	.00000	.00000	.00000	.00000	.00000	.00000	.00000
12	.78571+00	.00000	.07400	.00000	.00000	.00000	.00000	.00000	.00000	.00000
11	.71429+00	.00000	.07400	.00000	.00000	.00000	.00000	.00000	.00000	.00000
10	.64286+00	.00000	.07400	.00000	.00000	.00000	.00000	.00000	.00000	.00000
9	.57143+00	.00000	.07400	.00000	.00000	.00000	.00000	.00000	.00000	.00000
8	.50000+00	.00000	.07400	.00000	.00000	.00000	.00000	.00000	.00000	.00000
7	.42857+00	.00000	.07400	.00000	.00000	.00000	.00000	.00000	.00000	.00000
6	.35714+00	.00000	.07400	.00000	.00000	.00000	.00000	.00000	.00000	.00000
5	.28571+00	.00000	.07400	.00000	.00000	.00000	.00000	.00000	.00000	.00000
4	.21429+00	.00000	.07400	.00000	.00000	.00000	.00000	.00000	.00000	.00000
3	.14286+00	.00000	.07400	.00000	.00000	.00000	.00000	.00000	.00000	.00000
2	.71429-01	.00000	.07400	.00000	.00000	.00000	.00000	.00000	.00000	.00000
1	.00000	.00000	.07400	.00000	.00000	.00000	.00000	.00000	.00000	.00000

IZ= / J=	11 .7143+00	12 .7857+00	13 .8571+00	14 .9286+00	15 .1000+01
15	.00000	.00000	.00000	.00000	.00000
14	.00000	.00000	.00000	.00000	.00000
13	.00000	.00000	.00000	.00000	.00000
12	.00000	.00000	.00000	.00000	.00000
11	.00000	.00000	.00000	.00000	.00000
10	.00000	.00000	.00000	.00000	.00000
9	.00000	.00000	.00000	.00000	.00000
8	.00000	.00000	.00000	.00000	.00000
7	.00000	.00000	.00000	.00000	.00000
6	.00000	.00000	.00000	.00000	.00000
5	.00000	.00000	.00000	.00000	.00000
4	.00000	.00000	.00000	.00000	.00000
3	.00000	.00000	.00000	.00000	.00000
2	.00000	.00000	.00000	.00000	.00000
1	.00000	.00000	.00000	.00000	.00000

Initial Values of
Radial Velocity

Microfilmed From
Best Available Copy

LOCATION OF CENTERLINE (.00000000 , .00000000 , .00000000) DX: .00000000

I-TH STATION , S: .00000000

NSURF = 1

BWD = 0. IFACT = 1 IPCNT = 2
IBUCT = 1 IMACH = 1 NOMACH = 0

LEVEL 1 ***** BWD ******

Initial Values of
Density

I7: / 7 :	1 .0000	2 .7143-01	3 .1429+00	4 .2143+00	5 .2857+00	6 .3571+00	7 .4286+00	8 .5000+00	9 .5714+00	10 .6429+00
17	9									
16	.10000+01	.10000+01	.10000+01	.10000+01	.10000+01	.10000+01	.10000+01	.10000+01	.99999+00	.99999+00	.99998+00
15	.92857+00	.10000+01	.10000+01	.10000+01	.10000+01	.10000+01	.10000+01	.10000+01	.99999+00	.99999+00	.99997+00
14	.85714+00	.10000+01	.10000+01	.10000+01	.10000+01	.10000+01	.10000+01	.10000+01	.99999+00	.99999+00	.99993+00
13	.78571+00	.10000+01	.10000+01	.10000+01	.10000+01	.10000+01	.10000+01	.10000+01	.99999+00	.99998+00	.99978+00
12	.71429+00	.10000+01	.10000+01	.10000+01	.10000+01	.10000+01	.10000+01	.10000+01	.99999+00	.99994+00	.99946+00
11	.64286+00	.10000+01	.10000+01	.10000+01	.10000+01	.10000+01	.10000+01	.10000+01	.99999+00	.99984+00	.99865+00
10	.57143+00	.10000+01	.10000+01	.10000+01	.10000+01	.10000+01	.10000+01	.10000+01	.99999+00	.99951+00	.99595+00
9	.50000+00	.10000+01	.10000+01	.10000+01	.10000+01	.10000+01	.10000+01	.10000+01	.99999+00	.99854+00	.98966+00
8	.42857+00	.10000+01	.10000+01	.10000+01	.10000+01	.10000+01	.10000+01	.10000+01	.99999+00	.99561+00	.97437+00
7	.35714+00	.10000+01	.10000+01	.10000+01	.10000+01	.10000+01	.10000+01	.10000+01	.99999+00	.98684+00	.92308+00
6	.28571+00	.10000+01	.10000+01	.10000+01	.10000+01	.10000+01	.10000+01	.10000+01	.99999+00	.96053+00	.76923+00
5	.21429+00	.10000+01	.10000+01	.10000+01	.10000+01	.10000+01	.10000+01	.10000+01	.99999+00	.90789+00	.53846+00
4	.14286+00	.10000+01	.10000+01	.10000+01	.10000+01	.10000+01	.10000+01	.10000+01	.99999+00	.81579+00	.30769+00
3	.71429-01	.10000+01	.10000+01	.10000+01	.10000+01	.10000+01	.10000+01	.10000+01	.99999+00	.72368+00	.15385+00
2	.0000	.10000+01	.10000+01	.10000+01	.10000+01	.10000+01	.10000+01	.10000+01	.99999+00	.69737+00	.07692+00

I7: / 7 :	11 .7143+00	12 .7857+00	13 .8571+00	14 .9286+00	15 .1000+01
16	.10000+01	.99993+00	.99988+00	.99984+00	.99981+00	.99801+00
15	.99971+00	.99989+00	.99984+00	.99981+00	.99801+00
14	.99913+00	.99986+00	.99981+00	.99801+00
13	.99855+00	.99983+00	.99801+00
12	.99797+00	.99801+00
11	.99739+00	.99801+00
10	.99681+00	.99801+00
9	.99623+00	.99801+00
8	.99565+00	.99801+00
7	.99507+00	.99801+00
6	.99449+00	.99801+00
5	.99391+00	.99801+00
4	.99333+00	.99801+00
3	.99275+00	.99801+00
2	.99217+00	.99801+00

Microfilmed From
Best Available Copy

PEPSIS CURVED CENTERLINE TEST CASE RALPH LEVY DATE 011078 PAGE 26

LOCATION OF CENTERLINE : .00000000 I-IN STATION : .00000000 . .00000000 . .00000000 DX: .00000000

BND : 0. IFACT : 1 ITCNT : 2
IDUCT : 1 IMACH : 1 NOMACH : 0

LEVEL 1 ***** PRESS *****

Initial Values of
Pressure

J2=	1 .0000	2 .7143-01	3 .1429+00	4 .2143+00	5 .2857+00	6 .3571+00	7 .4286+00	8 .5000+00	9 .5714+00	10 .6429+00
19										
18										
17										
16										
15										
14										
13										
12										
11										
10										
9										
8										
7										
6										
5										
4										
3										
2										
1	.0000									

J2=	11 .7143+00	12 .7857+00	13 .8571+00	14 .9286+00	15 .1000+01
15					
14					
13					
12					
11					
10					
9					
8					
7					
6					
5					
4					
3					
2					
1	.0000				

Microfilmed From
Best Available Copy

PEPSIS CURVED CENTERLINE TEST CASE RALPH LEVY — DATE 011079 — PAGE 27

LEVEL 1 ***** CP/2 *****

Initial Values of
Pressure Coefficient

I2= / J=	1 .0000	2 .7143-01	3 .1429+00	4 .2143+00	5 .2857+00	6 .3571+00	7 .4286+00	8 .5000+00	9 .5714+00	10 .6429+00
17	.10000+01	.64634-06	.64634-06	.64634-06	.64634-06	.64634-06	.64634-06	-.30734-06	-.30734-06	-.30734-06
16	.92857+00	.64634-06	.64634-06	.64634-06	.64634-06	.64634-06	.64634-06	-.30734-06	-.30734-06	-.30734-06
15	.85714+00	.64634-06	.64634-06	.64634-06	.64634-06	.64634-06	.64634-06	-.30734-06	-.30734-06	-.30734-06
14	.78571+00	.64634-06	.64634-06	.64634-06	.64634-06	.64634-06	.64634-06	-.30734-06	-.30734-06	-.30734-06
13	.71429+00	.64634-06	.64634-06	.64634-06	.64634-06	.64634-06	.64634-06	-.30734-06	-.30734-06	-.30734-06
12	.64286+00	.64634-06	.64634-06	.64634-06	.64634-06	.64634-06	.64634-06	-.30734-06	-.30734-06	-.30734-06
11	.57143+00	.64634-06	.64634-06	.64634-06	.64634-06	.64634-06	.64634-06	-.30734-06	-.30734-06	-.30734-06
10	.50000+00	.64634-06	.64634-06	.64634-06	.64634-06	.64634-06	.64634-06	-.30734-06	-.30734-06	-.30734-06
9	.42857+00	.64634-06	.64634-06	.64634-06	.64634-06	.64634-06	.64634-06	-.30734-06	-.30734-06	-.30734-06
8	.35714+00	.64634-06	.64634-06	.64634-06	.64634-06	.64634-06	.64634-06	-.30734-06	-.30734-06	-.30734-06
7	.28571+00	.64634-06	.64634-06	.64634-06	.64634-06	.64634-06	.64634-06	-.30734-06	-.30734-06	-.30734-06
6	.21429+00	.64634-06	.64634-06	.64634-06	.64634-06	.64634-06	.64634-06	-.30734-06	-.30734-06	-.30734-06
5	.14286+00	.64634-06	.64634-06	.64634-06	.64634-06	.64634-06	.64634-06	-.30734-06	-.30734-06	-.30734-06
4	.71429-01	.64634-06	.64634-06	.64634-06	.64634-06	.64634-06	.64634-06	-.30734-06	-.30734-06	-.30734-06
3	.00000	.64634-06	.64634-06	.64634-06	.64634-06	.64634-06	.64634-06	-.30734-06	-.30734-06	-.30734-06

I2= / J=	11 .7143+00	12 .7857+00	13 .8571+00	14 .9286+00	15 .1000+01
17	.10000+01	-.30734-06	-.30734-06	-.30734-06	-.30734-06	-.30734-06
16	.92857+00	-.30734-06	-.30734-06	-.30734-06	-.30734-06	-.30734-06
15	.85714+00	-.30734-06	-.30734-06	-.30734-06	-.30734-06	-.30734-06
14	.78571+00	-.30734-06	-.30734-06	-.30734-06	-.30734-06	-.30734-06
13	.71429+00	-.30734-06	-.30734-06	-.30734-06	-.30734-06	-.30734-06
12	.64286+00	-.30734-06	-.30734-06	-.30734-06	-.30734-06	-.30734-06
11	.57143+00	-.30734-06	-.30734-06	-.30734-06	-.30734-06	-.30734-06
10	.50000+00	-.30734-06	-.30734-06	-.30734-06	-.30734-06	-.30734-06
9	.42857+00	-.30734-06	-.30734-06	-.30734-06	-.30734-06	-.30734-06
8	.35714+00	-.30734-06	-.30734-06	-.30734-06	-.30734-06	-.30734-06
7	.28571+00	-.30734-06	-.30734-06	-.30734-06	-.30734-06	-.30734-06
6	.21429+00	-.30734-06	-.30734-06	-.30734-06	-.30734-06	-.30734-06
5	.14286+00	-.30734-06	-.30734-06	-.30734-06	-.30734-06	-.30734-06
4	.71429-01	-.30734-06	-.30734-06	-.30734-06	-.30734-06	-.30734-06
3	.00000	-.30734-06	-.30734-06	-.30734-06	-.30734-06	-.30734-06

LEVEL 1 ***** MACH *****

Microfilmed From
Best Available Copy

IZ=	1	2	3	4	5	6	7	8	9	10
Z =	.0000	.7143-01	.1429+00	.2143+00	.2857+00	.3571+00	.4286+00	.5000+00	.5714+00	.6429+00
IY Y										
15 .10000+01	.10000+00	.10000+00	.10000+00	.10000+00	.10000+00	.10000+00	.10000+00	.99682-01	.97417-01	.91683-01
14 .92857+00	.10000+00	.10000+00	.10000+00	.10000+00	.10000+00	.10000+00	.10000+00	.99731-01	.97584-01	.91972-01
13 .85714+00	.10000+00	.10000+00	.10000+00	.10000+00	.10000+00	.10000+00	.10000+00	.99854-01	.98073-01	.92860-01
12 .78571+00	.10000+00	.10000+00	.10000+00	.10000+00	.10000+00	.10000+00	.10000+00	.99974-01	.98822-01	.94385-01
11 .71429+00	.10000+00	.10000+00	.10000+00	.10000+00	.10000+00	.10000+00	.10000+00	.10000+00	.99613-01	.96491-01
10 .64286+00	.10000+00	.10000+00	.10000+00	.10000+00	.10000+00	.10000+00	.10000+00	.10000+00	.99993-01	.98684-01
9 .57143+00	.10000+00	.10000+00	.10000+00	.10000+00	.10000+00	.10000+00	.10000+00	.10000+00	.10000+00	.99860-01
8 .50000+00	.10000+00	.10000+00	.10000+00	.10000+00	.10000+00	.10000+00	.10000+00	.10000+00	.10000+00	.99994-01
7 .42857+00	.10000+00	.10000+00	.10000+00	.10000+00	.10000+00	.10000+00	.10000+00	.10000+00	.10000+00	.99860-01
6 .35714+00	.10000+00	.10000+00	.10000+00	.10000+00	.10000+00	.10000+00	.10000+00	.10000+00	.99993-01	.98684-01
5 .28571+00	.10000+00	.10000+00	.10000+00	.10000+00	.10000+00	.10000+00	.10000+00	.10000+00	.99613-01	.96491-01
4 .21429+00	.10000+00	.10000+00	.10000+00	.10000+00	.10000+00	.10000+00	.10000+00	.99974-01	.98822-01	.94385-01
3 .14286+00	.10000+00	.10000+00	.10000+00	.10000+00	.10000+00	.10000+00	.10000+00	.99854-01	.98073-01	.92860-01
2 .71429-01	.10000+00	.10000+00	.10000+00	.10000+00	.10000+00	.10000+00	.10000+00	.99731-01	.97584-01	.91972-01
1 .00000	.10000+00	.10000+00	.10000+00	.10000+00	.10000+00	.10000+00	.10000+00	.99682-01	.97417-01	.91683-01

IZ=	11	12	13	14	15
Z =	.7143+00	.7857+00	.8571+00	.9286+00	.1000+01
15 .10000+01	.81561-01	.66742-01	.47516-01	.24773-01	.00000
14 .92857+00	.81932-01	.67124-01	.47832-01	.24953-01	.00000
13 .85714+00	.83094-01	.68339-01	.48842-01	.25530-01	.00000
12 .78571+00	.85194-01	.70595-01	.50751-01	.26629-01	.00000
11 .71429+00	.88415-01	.74249-01	.53938-01	.28495-01	.00000
10 .64286+00	.92629-01	.79558-01	.58837-01	.31452-01	.00000
9 .57143+00	.96516-01	.85510-01	.64872-01	.35273-01	.00000
8 .50000+00	.97967-01	.88399-01	.68115-01	.37427-01	.00000
7 .42857+00	.96516-01	.85510-01	.64872-01	.35273-01	.00000
6 .35714+00	.92629-01	.79558-01	.58837-01	.31452-01	.00000
5 .28571+00	.88415-01	.74249-01	.53938-01	.28495-01	.00000
4 .21429+00	.85194-01	.70595-01	.50751-01	.26629-01	.00000
3 .14286+00	.83094-01	.68339-01	.48842-01	.25530-01	.00000
2 .71429-01	.81932-01	.67124-01	.47832-01	.24953-01	.00000
1 .00000	.81561-01	.66742-01	.47516-01	.24773-01	.00000

Initial Values of
Mach Number

INTEGRATED PROPERTIES AT STATION 2

Check on Mass Conservation

FLOW AREA= .52164 SQ.FT. MASS FLUX= .36799-01LBM/SEC.

LOCAL TO ORIGINAL AREA RATIO 1.0000
LOCAL TO ORIGINAL MASS FLUX RATIO 1.0000

Microfilmed From
Best Available Copy

Results of 1st Marching Step

2-TH STATION , S= .00000000

LOCATION OF CENTERLINE (.00000000 , .00000000 , .40000000+001 DX= .40000000+00

KOORD= 1

RWD = 0. IFACT = 1 IICNT = 2 VELOCITY BOUNDARY CONDITIONS 4 4 12 3
IDUCT = 1 IMACH = 1 JFACT = 1 DENSITY BOUNDARY CONDITIONS 4 11 12 20

LEVEL 1 ***** RADIUS *****

IZ= / J=	1 .0000	2 .7143-01	3 .1429+00	4 .2143+00	5 .2857+00	6 .3571+00	7 .4286+00	8 .5000+00	9 .5714+00	10 .6429+00
17										
15	.10000+01	.50000-01	.94048-01	.13810+00	.18214+00	.22619+00	.27024+00	.31429+00	.35833+00	.40238+00
14	.92857+00	.50000-01	.94716-01	.13963+00	.18415+00	.22867+00	.27358+00	.31830+00	.36301+00	.40773+00
13	.85714+00	.50000-01	.94752-01	.14350+00	.19026+00	.23701+00	.28376+00	.33051+00	.37726+00	.42401+00
12	.78571+00	.50000-01	.10021+00	.15042+00	.20062+00	.25083+00	.30104+00	.35125+00	.40145+00	.45166+00
11	.71429+00	.50000-01	.10503+00	.16005+00	.21508+00	.27010+00	.32513+00	.38015+00	.43518+00	.49020+00
10	.64286+00	.50000-01	.11169+00	.17139+00	.23208+00	.29277+00	.35347+00	.41417+00	.47486+00	.53556+00
9	.57143+00	.50000-01	.11574+00	.18469+00	.24923+00	.31298+00	.37672+00	.44047+00	.51021+00	.57595+00
8	.50000+00	.50000-01	.11786+00	.18571+00	.25557+00	.32143+00	.38929+00	.45714+00	.52500+00	.59286+00
7	.42857+00	.50000-01	.11574+00	.18469+00	.24923+00	.31298+00	.37672+00	.44047+00	.51021+00	.57595+00
6	.35714+00	.50000-01	.11169+00	.17139+00	.23208+00	.29278+00	.35347+00	.41417+00	.47486+00	.53556+00
5	.28571+00	.50000-01	.10503+00	.16005+00	.21508+00	.27017+00	.32513+00	.38015+00	.43518+00	.49020+00
4	.21429+00	.50000-01	.10021+00	.15042+00	.20062+00	.25083+00	.30104+00	.35125+00	.40145+00	.45166+00
3	.14286+00	.50000-01	.96752-01	.14350+00	.19026+00	.23701+00	.28376+00	.33051+00	.37726+00	.42401+00
2	.71429-01	.50000-01	.94716-01	.13963+00	.18415+00	.22867+00	.27358+00	.31830+00	.36301+00	.40773+00
1	.00000	.50000-01	.94048-01	.13810+00	.18214+00	.22619+00	.27024+00	.31429+00	.35833+00	.40238+00

IZ= / J=	11 .7143+00	12 .7857+00	13 .85714+00	14 .9286+00	15 .1000+01
15	.40048+00	.45452+00	.57857+00	.62262+00	.66667+00
14	.40716+00	.54188+00	.58666+00	.62434+00	.67603+00
13	.41752+00	.56427+00	.61102+00	.65777+00	.70453+00
12	.43208+00	.60228+00	.65249+00	.70270+00	.75291+00
11	.45028+00	.65528+00	.71030+00	.76531+00	.82034+00
10	.46969+00	.71764+00	.77834+00	.83903+00	.89973+00
9	.47744+00	.77119+00	.83893+00	.90667+00	.97442+00
8	.47857+00	.79643+00	.86429+00	.93214+00	.10000+01
7	.47744+00	.77119+00	.83893+00	.90667+00	.97442+00
6	.46969+00	.71764+00	.77834+00	.83903+00	.89973+00
5	.45028+00	.65528+00	.71030+00	.76531+00	.82034+00
4	.43208+00	.60228+00	.65249+00	.70270+00	.75291+00
3	.41752+00	.56427+00	.61102+00	.65777+00	.70453+00
2	.40716+00	.54188+00	.58666+00	.63134+00	.67603+00
1	.40048+00	.53452+00	.57857+00	.62262+00	.66667+00

Microfilmed From
Best Available Copy

LEVEL 1 ***** THETA *****

J \ I2=	1 .0000	2 .7143-01	3 .1429+00	4 .2143+00	5 .2857+00	6 .3571+00	7 .4286+00	8 .5000+00	9 .5714+00	10 .6429+00
17										
16 .10000+01	180.00	180.00	180.00	180.00	180.00	180.00	180.00	180.00	180.00	180.00
15 .92857+00	167.14	167.14	167.14	167.14	167.14	167.14	167.14	167.14	167.14	167.14
14 .85714+00	154.29	154.29	154.29	154.29	154.29	154.29	154.29	154.29	154.29	154.29
13 .78571+00	141.43	141.43	141.43	141.43	141.43	141.43	141.43	141.43	141.43	141.43
12 .71429+00	128.57	128.57	128.57	128.57	128.57	128.57	128.57	128.57	128.57	128.57
11 .64286+00	115.71	115.71	115.71	115.71	115.71	115.71	115.71	115.71	115.71	115.71
10 .57143+00	102.86	102.86	102.86	102.86	102.86	102.86	102.86	102.86	102.86	102.86
9 .50000+00	90.00	90.00	90.00	90.00	90.00	90.00	90.00	90.00	90.00	90.00
8 .42857+00	77.14	77.14	77.14	77.14	77.14	77.14	77.14	77.14	77.14	77.14
7 .35714+00	64.29	64.29	64.29	64.29	64.29	64.29	64.29	64.29	64.29	64.29
6 .28571+00	51.43	51.43	51.43	51.43	51.43	51.43	51.43	51.43	51.43	51.43
5 .21429+00	38.57	38.57	38.57	38.57	38.57	38.57	38.57	38.57	38.57	38.57
4 .14286+00	25.71	25.71	25.71	25.71	25.71	25.71	25.71	25.71	25.71	25.71
3 .71429-01	12.86	12.86	12.86	12.86	12.86	12.86	12.86	12.86	12.86	12.86
2 .00000	.00	.00	.00	.00	.00	.00	.00	.00	.00	.00

J \ I2=	11 .7143+00	12 .7857+00	13 .8571+00	14 .9286+00	15 .1000+01
16 .10000+01	180.00	180.00	180.00	180.00	180.00
15 .92857+00	167.14	167.14	167.14	167.14	167.14
14 .85714+00	154.29	154.29	154.29	154.29	154.29
13 .78571+00	141.43	141.43	141.43	141.43	141.43
12 .71429+00	128.57	128.57	128.57	128.57	128.57
11 .64286+00	115.71	115.71	115.71	115.71	115.71
10 .57143+00	102.86	102.86	102.86	102.86	102.86
9 .50000+00	90.00	90.00	90.00	90.00	90.00
8 .42857+00	77.14	77.14	77.14	77.14	77.14
7 .35714+00	64.29	64.29	64.29	64.29	64.29
6 .28571+00	51.43	51.43	51.43	51.43	51.43
5 .21429+00	38.57	38.57	38.57	38.57	38.57
4 .14286+00	25.71	25.71	25.71	25.71	25.71
3 .71429-01	12.86	12.86	12.86	12.86	12.86
2 .00000	.00	.00	.00	.00	.00

Microfilmed From
Best Available Copy

LOCATION OF CENTERLINE (.00000000 2-TH STATION , S= .00000000
.00000000 , .4U000000+001) DX= .40000000+00
*OORD= 1

NND = 9. IFACT = 1 ITCNT = 2 VELOCITY BOUNDARY CONDITIONS 6 6 12 1
IDUCT = 1 IMACH = 1 JFACT = 1 DENSITY BOUNDARY CONDITIONS 6 11 12 20
VELOCITY VECTOR DISPLAYED IN COMPUTATIONAL COORDINATES

LEVEL 1 ***** U-VEL *****

I=	1	2	3	4	5	6	7	8	9	10
J=	.0000	.7143-01	.1429+00	.2143+00	.2857+00	.3571+00	.4286+00	.5000+00	.5714+00	.6429+00
17										
16	.10000+01	.10015+01	.10015+01	.10014+01	.10014+01	.10013+01	.10011+01	.99747+00	.97420+00	.91634+00
15	.92857+00	.10015+01	.10015+01	.10014+01	.10014+01	.10013+01	.10012+01	.99789+00	.97583+00	.91929+00
14	.85714+00	.10015+01	.10015+01	.10014+01	.10014+01	.10013+01	.10012+01	.99819+00	.97699+00	.92015+00
13	.78571+00	.10015+01	.10015+01	.10014+01	.10014+01	.10013+01	.10012+01	.10005+01	.98819+00	.96335+00
12	.71429+00	.10016+01	.10015+01	.10014+01	.10014+01	.10013+01	.10013+01	.10010+01	.99630+00	.96437+00
11	.64286+00	.10016+01	.10015+01	.10014+01	.10014+01	.10014+01	.10014+01	.10012+01	.10007+01	.98857+00
10	.57143+00	.10016+01	.10016+01	.10015+01	.10015+01	.10015+01	.10015+01	.10014+01	.10014+01	.99913+00
9	.50000+00	.10016+01	.10016+01	.10016+01	.10016+01	.10016+01	.10016+01	.10016+01	.10016+01	.10016+01
8	.42857+00	.10016+01	.10016+01	.10016+01	.10016+01	.10016+01	.10016+01	.10015+01	.10014+01	.99913+00
7	.35714+00	.10016+01	.10015+01	.10014+01	.10014+01	.10014+01	.10014+01	.10013+01	.10007+01	.98857+00
6	.28571+00	.10016+01	.10015+01	.10014+01	.10013+01	.10013+01	.10013+01	.10012+01	.99630+00	.96437+00
5	.21429+00	.10015+01	.10015+01	.10014+01	.10013+01	.10013+01	.10012+01	.10005+01	.98819+00	.96335+00
4	.14286+00	.10015+01	.10015+01	.10014+01	.10013+01	.10012+01	.10012+01	.99819+00	.97699+00	.92015+00
3	.71429-01	.10015+01	.10015+01	.10014+01	.10013+01	.10012+01	.10011+01	.99789+00	.97583+00	.91929+00
2	.00000	.10015+01	.10015+01	.10014+01	.10013+01	.10012+01	.10011+01	.99747+00	.97420+00	.91634+00
1										

I=	11	12	13	14	15
J=	.7143+00	.7857+00	.8571+00	.9286+00	.1000+01
16	.81441+00	.66654+00	.47461+00	.24832+00	.00000
15	.81888+00	.67001+00	.47801+00	.24999+00	.00000
14	.82032+00	.67142+00	.47924+00	.25000+00	.00000
13	.81515+00	.66737+00	.47535+00	.24701+00	.00000
12	.80135+00	.65678+00	.46562+00	.24062+00	.00000
11	.78002+00	.63987+00	.45098+00	.23151+00	.00000
10	.75233+00	.61747+00	.43268+00	.22111+00	.00000
9	.71964+00	.59068+00	.41177+00	.21073+00	.00000
8	.68346+00	.56078+00	.38966+00	.20119+00	.00000
7	.64541+00	.52929+00	.36779+00	.19351+00	.00000
6	.60715+00	.49777+00	.34747+00	.18851+00	.00000
5	.57031+00	.46774+00	.32991+00	.18662+00	.00000
4	.53633+00	.44045+00	.31587+00	.18701+00	.00000
3	.50635+00	.41677+00	.30562+00	.18832+00	.00000
2	.48121+00	.39715+00	.29882+00	.18999+00	.00000
1	.46135+00	.38178+00	.29461+00	.19082+00	.00000

Microfilmed From
Best Available Copy

LEVEL 1 ***** W-VEL *****

IZ:	1	2	3	4	5	6	7	8	9	10
Z :	.0000	.7143-01	.1429+00	.2143+00	.2857+00	.3571+00	.4286+00	.5000+00	.5714+00	.6429+00
17										
16	.10000+01	.000000	-.334407-20	-.788872-20	-.818105-20	-.165317-19	-.164778-19	-.162688-19	-.197711-19	-.241501-19
15	.92857+00	.000000	-.772422-05	-.200211-04	-.190487-04	-.409137-04	-.419886-04	-.405648-04	-.450511-04	-.490279-04
14	.85714+00	.000000	-.157848-04	-.418611-04	-.459555-04	-.112641-03	-.116311-03	-.112052-03	-.121224-03	-.129869-03
13	.78571+00	.000000	-.307272-04	-.836437-04	-.950285-04	-.122784-03	-.126507-03	-.122844-03	-.132644-03	-.142154-03
12	.71429+00	.000000	-.536417-04	-.146337-03	-.166555-03	-.154637-03	-.159465-03	-.154896-03	-.167246-03	-.179537-03
11	.64286+00	.000000	-.761154-04	-.207835-03	-.236537-03	-.196465-03	-.202811-03	-.196946-03	-.212596-03	-.228037-03
10	.57143+00	.000000	-.876499-04	-.239075-03	-.272307-03	-.225907-03	-.233170-03	-.226411-03	-.244370-03	-.262108-03
9	.50000+00	.000000	-.876499-04	-.239075-03	-.272307-03	-.225907-03	-.233170-03	-.226411-03	-.244370-03	-.262108-03
8	.42857+00	.000000	-.761154-04	-.207835-03	-.236537-03	-.196465-03	-.202811-03	-.196946-03	-.212596-03	-.228037-03
7	.35714+00	.000000	-.536417-04	-.146337-03	-.166555-03	-.154637-03	-.159465-03	-.154896-03	-.167246-03	-.179537-03
6	.28571+00	.000000	-.307272-04	-.836437-04	-.950285-04	-.122784-03	-.126507-03	-.122844-03	-.132644-03	-.142154-03
5	.21429+00	.000000	-.157848-04	-.418611-04	-.459555-04	-.112641-03	-.116311-03	-.112052-03	-.121224-03	-.129869-03
4	.14286+00	.000000	-.772422-05	-.200211-04	-.190487-04	-.409137-04	-.419886-04	-.405648-04	-.450511-04	-.490279-04
3	.71429-01	.000000	-.334407-20	-.788872-20	-.818105-20	-.165317-19	-.164778-19	-.162688-19	-.197711-19	-.241501-19
2	.00000	.000000	-.333343-20	-.788801-20	-.817945-20	-.165307-19	-.164667-19	-.160781-19	-.147706-19	-.241411-19
1										

IZ:	11	12	13	14	15
Z :	.7143+00	.7857+00	.8571+00	.9286+00	.1000+01
15	.10000+01	-.104119-19	-.434631-20	-.257951-21	-.586421-21	.000000
14	.92857+00	-.145574-04	-.929385-05	-.899471-05	-.749155-04	.000000
13	.85714+00	-.172644-04	-.422051-05	-.110503-04	-.170444-04	.000000
12	.78571+00	-.321084-04	-.784241-05	-.439684-04	-.106871-04	.000000
11	.71429+00	-.725118-04	-.199480-04	-.756264-04	-.722237-04	.000000
10	.64286+00	-.149884-03	-.412241-04	-.204176-04	-.165284-03	.000000
9	.57143+00	-.166864-03	-.459284-04	-.227406-04	-.184058-03	.000000
8	.50000+00	-.110641-20	-.433933-05	-.887230-07	-.372568-07	.000000
7	.42857+00	-.166734-03	-.459284-04	-.265654-04	-.184058-03	.000000
6	.35714+00	-.149884-03	-.412241-04	-.204176-04	-.165284-03	.000000
5	.28571+00	-.321084-04	-.784241-05	-.439684-04	-.106871-04	.000000
4	.21429+00	-.725118-04	-.199480-04	-.756264-04	-.722237-04	.000000
3	.14286+00	-.172644-04	-.422051-05	-.110503-04	-.170444-04	.000000
2	.71429-01	-.145574-04	-.929385-05	-.899471-05	-.749155-04	.000000
1		-.104119-19	-.434631-20	-.257951-21	-.586421-21	.000000

LEVEL 1 ***** W-VEL *****

Microfilmed From
Best Available Copy

J2 =	1	2	3	4	5	6	7	8	9	10
J1 =	.0000	.7143-01	.1429+00	.2143+00	.2857+00	.3571+00	.4286+00	.5000+00	.5714+00	.6429+00
17	1									
16	.1000+01	.00000	-.13387-01	-.23169-01	-.31698-01	-.39726-01	-.47359-01	-.54688-01	-.61817-01	-.68841-
15	.9286+00	.00000	-.11594-01	-.20439-01	-.28220-01	-.35439-01	-.42366-01	-.49037-01	-.55563-01	-.61954-
14	.8571+00	.00000	-.10000-01	-.17639-01	-.24359-01	-.30594-01	-.36588-01	-.42366-01	-.48000-01	-.53507-
13	.7857+00	.00000	-.85194-02	-.15028-01	-.20756-01	-.26069-01	-.31169-01	-.36088-01	-.40894-01	-.45594-
12	.7143+00	.00000	-.71866-02	-.12675-01	-.17505-01	-.21988-01	-.26294-01	-.30444-01	-.34494-01	-.38456-
11	.6429+00	.00000	-.59697-02	-.10527-01	-.14539-01	-.18263-01	-.21838-01	-.25281-01	-.28644-01	-.31938-
10	.5714+00	.00000	-.48160-02	-.84939-02	-.11729-01	-.14734-01	-.17619-01	-.20400-01	-.23113-01	-.25769-
9	.5000+00	.00000	-.37140-02	-.65506-02	-.90469-02	-.11363-01	-.13589-01	-.15733-01	-.17825-01	-.19869-
8	.4286+00	.00000	-.27017-02	-.47648-02	-.65803-02	-.82653-02	-.98846-02	-.11443-01	-.12966-01	-.14455-
7	.3571+00	.00000	-.18063-02	-.31850-02	-.43988-02	-.55259-02	-.66091-02	-.76520-02	-.86697-02	-.96656-
6	.2857+00	.00000	-.10483-02	-.18486-02	-.25529-02	-.32069-02	-.38353-02	-.44405-02	-.50309-02	-.56091-
5	.2143+00	.00000	-.46837-03	-.82607-03	-.11408-02	-.14329-02	-.17137-02	-.19841-02	-.22479-02	-.25067-
4	.1429+00	.00000	-.11713-03	-.20659-03	-.28526-03	-.35832-03	-.42853-03	-.49610-03	-.56199-03	-.62667-
3	.7143-01	.00000	-.11713-03	-.20659-03	-.28526-03	-.35832-03	-.42853-03	-.49610-03	-.56199-03	-.62667-
2	.0000	.00000	-.11713-03	-.20659-03	-.28526-03	-.35832-03	-.42853-03	-.49610-03	-.56199-03	-.62667-
1	.0000	.00000	-.11713-03	-.20659-03	-.28526-03	-.35832-03	-.42853-03	-.49610-03	-.56199-03	-.62667-

J2 =	11	12	13	14	15
J1 =	.7143+00	.7857+00	.8571+00	.9286+00	.1000+01
17	1				
16	.1000+01	-.27176-01	-.17355-01	-.77822-01	.19417-04	.00000
15	.9286+00	-.23116-01	-.14769-01	-.66224-01	.16524-04	.00000
14	.8571+00	-.19274-01	-.12315-01	-.55224-01	.13778-04	.00000
13	.7857+00	-.15677-01	-.10019-01	-.44931-01	.11209-04	.00000
12	.7143+00	-.12350-01	-.78935-02	-.35398-01	.88305-05	.00000
11	.6429+00	-.93127-02	-.59520-02	-.26693-01	.66594-05	.00000
10	.5714+00	-.68116-02	-.43538-02	-.19524-01	.48717-05	.00000
9	.5000+00	-.47000-02	-.30040-02	-.13473-01	.33617-05	.00000
8	.4286+00	-.30124-02	-.19254-02	-.86349-02	.21544-05	.00000
7	.3571+00	-.17090-02	-.10922-02	-.48988-02	.12222-05	.00000
6	.2857+00	-.75999-03	-.48582-03	-.21789-02	.54362-06	.00000
5	.2143+00	-.19000-03	-.12145-03	-.54473-03	.13591-06	.00000
4	.1429+00	-.19000-03	-.12145-03	-.54473-03	.13591-06	.00000
3	.7143-01	-.19000-03	-.12145-03	-.54473-03	.13591-06	.00000
2	.0000	-.19000-03	-.12145-03	-.54473-03	.13591-06	.00000
1	.0000	-.19000-03	-.12145-03	-.54473-03	.13591-06	.00000

Microfilmed From
Best Available Copy

PEPSIB CURVED CENTERLINE TEST CASE RALPH LEVY DATE 011078 PAGE 48

2-TH STATION , S: .0000000

LOCATION OF CENTERLINE : .0000000 , .0000000 , .4000000E+001 DH: .40000000E+00

NOSE: 1

BND = 0. IFACT = 1 ITCNT = 2

IDUCT = 1 IMACH = 1 NOMACH = 0

LEVEL 1 ***** RHO *****

JZ=	1 .0000	2 .7143-01	3 .1429+00	4 .2143+00	5 .2857+00	6 .3571+00	7 .4286+00	8 .5000+00	9 .5714+00	10 .6429+00
17	.10000E+01	.10000E+01	.10000E+01	.10000E+01	.10000E+01	.10000E+01	.10000E+01	.99999+00	.99999+00	.99998+00
16	.99857+00	.10000E+01	.10000E+01	.10000E+01	.10000E+01	.10000E+01	.10000E+01	.99999+00	.99999+00	.99997+00
15	.99571+00	.10000E+01	.10000E+01	.10000E+01	.10000E+01	.10000E+01	.10000E+01	.99999+00	.99999+00	.99997+00
14	.99286+00	.10000E+01	.10000E+01	.10000E+01	.10000E+01	.10000E+01	.10000E+01	.99999+00	.99999+00	.99996+00
13	.99000+00	.10000E+01	.10000E+01	.10000E+01	.10000E+01	.10000E+01	.10000E+01	.99999+00	.99999+00	.99996+00
12	.98714+00	.10000E+01	.10000E+01	.10000E+01	.10000E+01	.10000E+01	.10000E+01	.99999+00	.99999+00	.99995+00
11	.98429+00	.10000E+01	.10000E+01	.10000E+01	.10000E+01	.10000E+01	.10000E+01	.99999+00	.99999+00	.99995+00
10	.98143+00	.10000E+01	.10000E+01	.10000E+01	.10000E+01	.10000E+01	.10000E+01	.99999+00	.99999+00	.99994+00
9	.97857+00	.10000E+01	.10000E+01	.10000E+01	.10000E+01	.10000E+01	.10000E+01	.99999+00	.99999+00	.99994+00
8	.97571+00	.10000E+01	.10000E+01	.10000E+01	.10000E+01	.10000E+01	.10000E+01	.99999+00	.99999+00	.99993+00
7	.97286+00	.10000E+01	.10000E+01	.10000E+01	.10000E+01	.10000E+01	.10000E+01	.99999+00	.99999+00	.99993+00
6	.97000+00	.10000E+01	.10000E+01	.10000E+01	.10000E+01	.10000E+01	.10000E+01	.99999+00	.99999+00	.99992+00
5	.96714+00	.10000E+01	.10000E+01	.10000E+01	.10000E+01	.10000E+01	.10000E+01	.99999+00	.99999+00	.99992+00
4	.96429+00	.10000E+01	.10000E+01	.10000E+01	.10000E+01	.10000E+01	.10000E+01	.99999+00	.99999+00	.99991+00
3	.96143+00	.10000E+01	.10000E+01	.10000E+01	.10000E+01	.10000E+01	.10000E+01	.99999+00	.99999+00	.99991+00
2	.95857+00	.10000E+01	.10000E+01	.10000E+01	.10000E+01	.10000E+01	.10000E+01	.99999+00	.99999+00	.99990+00
1	.95571+00	.10000E+01	.10000E+01	.10000E+01	.10000E+01	.10000E+01	.10000E+01	.99999+00	.99999+00	.99990+00

JZ=	11 .7143+00	12 .7857+00	13 .8571+00	14 .9286+00	15 .1000+01
17	.10026E+01	.99891+00	.99865+00	.99841+00	.99801+00
16	.10026E+01	.99891+00	.99865+00	.99841+00	.99801+00
15	.10026E+01	.99891+00	.99865+00	.99841+00	.99801+00
14	.10026E+01	.99891+00	.99865+00	.99841+00	.99801+00
13	.10026E+01	.99891+00	.99865+00	.99841+00	.99801+00
12	.10026E+01	.99891+00	.99865+00	.99841+00	.99801+00
11	.10026E+01	.99891+00	.99865+00	.99841+00	.99801+00
10	.10026E+01	.99891+00	.99865+00	.99841+00	.99801+00
9	.10026E+01	.99891+00	.99865+00	.99841+00	.99801+00
8	.10026E+01	.99891+00	.99865+00	.99841+00	.99801+00
7	.10026E+01	.99891+00	.99865+00	.99841+00	.99801+00
6	.10026E+01	.99891+00	.99865+00	.99841+00	.99801+00
5	.10026E+01	.99891+00	.99865+00	.99841+00	.99801+00
4	.10026E+01	.99891+00	.99865+00	.99841+00	.99801+00
3	.10026E+01	.99891+00	.99865+00	.99841+00	.99801+00
2	.10026E+01	.99891+00	.99865+00	.99841+00	.99801+00
1	.10026E+01	.99891+00	.99865+00	.99841+00	.99801+00

Microfilmed From
Best Available Copy

2-TH STATION , S= .70000000
LOCATION OF CENTERLINE (.70000000 , .00000000 , .40000000+001) DX= .40000000+00
KOORD= 1
BWD = 0. IFACT = 1 IICNT = 2
IDUCT = 1 IMACH = 1 NOMACH = 0

LEVEL 1 ***** PRESS *****

IY	Y \ IX=	1	2	3	4	5	6	7	8	9	10
	Z =	.0000	.7143-01	.1429+00	.2143+00	.2857+00	.3571+00	.4286+00	.5000+00	.5714+00	.6429+00
15	.10000+01	.71453+02	.71453+02	.71454+02	.71454+02	.71454+02	.71454+02	.71454+02	.71454+02	.71454+02	.71454+02
14	.92857+00	.71453+02	.71453+02	.71453+02	.71454+02	.71454+02	.71454+02	.71454+02	.71454+02	.71454+02	.71454+02
13	.85714+00	.71453+02	.71453+02	.71453+02	.71454+02	.71454+02	.71454+02	.71454+02	.71454+02	.71454+02	.71454+02
12	.78571+00	.71453+02	.71453+02	.71453+02	.71453+02	.71453+02	.71454+02	.71454+02	.71454+02	.71454+02	.71454+02
11	.71429+00	.71453+02	.71453+02	.71453+02	.71453+02	.71453+02	.71453+02	.71453+02	.71454+02	.71454+02	.71454+02
10	.64286+00	.71453+02	.71453+02	.71453+02	.71453+02	.71453+02	.71453+02	.71453+02	.71453+02	.71454+02	.71454+02
9	.57143+00	.71453+02	.71453+02	.71453+02	.71453+02	.71453+02	.71453+02	.71453+02	.71453+02	.71453+02	.71453+02
8	.50000+00	.71452+02	.71452+02	.71452+02	.71452+02	.71453+02	.71453+02	.71453+02	.71453+02	.71453+02	.71453+02
7	.42857+00	.71453+02	.71453+02	.71453+02	.71453+02	.71453+02	.71453+02	.71453+02	.71453+02	.71453+02	.71453+02
6	.35714+00	.71453+02	.71453+02	.71453+02	.71453+02	.71453+02	.71453+02	.71453+02	.71453+02	.71454+02	.71454+02
5	.28571+00	.71453+02	.71453+02	.71453+02	.71453+02	.71453+02	.71453+02	.71453+02	.71454+02	.71454+02	.71454+02
4	.21429+00	.71453+02	.71453+02	.71453+02	.71453+02	.71453+02	.71454+02	.71454+02	.71454+02	.71454+02	.71454+02
3	.14286+00	.71453+02	.71453+02	.71453+02	.71453+02	.71454+02	.71454+02	.71454+02	.71454+02	.71454+02	.71454+02
2	.71429-01	.71453+02	.71453+02	.71453+02	.71454+02	.71454+02	.71454+02	.71454+02	.71454+02	.71454+02	.71454+02
1	.00000	.71453+02	.71453+02	.71454+02	.71454+02	.71454+02	.71454+02	.71454+02	.71454+02	.71454+02	.71454+02

IY	Y \ IX=	11	12	13	14	15
	Z =	.7143+00	.7857+00	.8571+00	.9286+00	.1000+01
15	.10000+01	.71454+02	.71454+02	.71454+02	.71454+02	.71454+02
14	.92857+00	.71454+02	.71454+02	.71454+02	.71454+02	.71454+02
13	.85714+00	.71454+02	.71454+02	.71454+02	.71454+02	.71454+02
12	.78571+00	.71454+02	.71454+02	.71454+02	.71454+02	.71454+02
11	.71429+00	.71454+02	.71454+02	.71454+02	.71454+02	.71454+02
10	.64286+00	.71454+02	.71454+02	.71454+02	.71454+02	.71454+02
9	.57143+00	.71454+02	.71454+02	.71454+02	.71454+02	.71454+02
8	.50000+00	.71454+02	.71454+02	.71454+02	.71454+02	.71454+02
7	.42857+00	.71454+02	.71454+02	.71454+02	.71454+02	.71454+02
6	.35714+00	.71454+02	.71454+02	.71454+02	.71454+02	.71454+02
5	.28571+00	.71454+02	.71454+02	.71454+02	.71454+02	.71454+02
4	.21429+00	.71454+02	.71454+02	.71454+02	.71454+02	.71454+02
3	.14286+00	.71454+02	.71454+02	.71454+02	.71454+02	.71454+02
2	.71429-01	.71454+02	.71454+02	.71454+02	.71454+02	.71454+02
1	.00000	.71454+02	.71454+02	.71454+02	.71454+02	.71454+02

Microfilmed From
Best Available Copy

LEVEL 1 ***** CP/2 *****

IZ=	1 .0000	2 .7143-01	3 .1429+00	4 .2143+00	5 .2857+00	6 .3571+00	7 .4286+00	8 .5000+00	9 .5714+00	10 .6429+00
17	.10000E+01	-.43200E-03	-.43516E-03	-.42088E-03	-.39947E-03	-.37794E-03	-.35811E-03	-.34071E-03	-.32588E-03	-.31369E-03
16	.92857E+00	-.44660E-03	-.44972E-03	-.43495E-03	-.41280E-03	-.39067E-03	-.37044E-03	-.35258E-03	-.33705E-03	-.32421E-03
15	.85714E+00	-.47333E-03	-.47647E-03	-.46130E-03	-.43869E-03	-.41557E-03	-.39422E-03	-.37506E-03	-.35855E-03	-.34505E-03
14	.78571E+00	-.53627E-03	-.53941E-03	-.52429E-03	-.49877E-03	-.44377E-03	-.39322E-03	-.33403E-03	-.28638E-03	-.24747E-03
13	.71429E+00	-.66216E-03	-.65930E-03	-.63736E-03	-.60208E-03	-.55439E-03	-.49622E-03	-.42851E-03	-.35031E-03	-.26352E-03
12	.64286E+00	-.89546E-03	-.88265E-03	-.86013E-03	-.82583E-03	-.77183E-03	-.70221E-03	-.61971E-03	-.52101E-03	-.41039E-03
11	.57143E+00	-.14925E-02	-.14768E-02	-.14429E-02	-.13955E-02	-.13276E-02	-.12386E-02	-.11320E-02	-.10052E-02	-.86025E-03
10	.50000E+00	-.15357E-02	-.15433E-02	-.14775E-02	-.14289E-02	-.13555E-02	-.12592E-02	-.11395E-02	-.10052E-02	-.86025E-03
9	.42857E+00	-.14944E-02	-.14698E-02	-.14268E-02	-.13993E-02	-.13276E-02	-.12386E-02	-.11320E-02	-.99404E-03	-.82524E-03
8	.35714E+00	-.90344E-03	-.88610E-03	-.86374E-03	-.83776E-03	-.77089E-03	-.70271E-03	-.61733E-03	-.52101E-03	-.41039E-03
7	.28571E+00	-.66216E-03	-.65930E-03	-.63736E-03	-.60208E-03	-.55535E-03	-.49717E-03	-.42851E-03	-.35126E-03	-.26498E-03
6	.21429E+00	-.53436E-03	-.53244E-03	-.52429E-03	-.49882E-03	-.44281E-03	-.39227E-03	-.33314E-03	-.28641E-03	-.24747E-03
5	.14286E+00	-.44853E-03	-.44681E-03	-.44028E-03	-.42665E-03	-.38845E-03	-.34268E-03	-.28641E-03	-.22347E-03	-.15671E-03
4	.71429E-01	-.44853E-03	-.44681E-03	-.44028E-03	-.42665E-03	-.38766E-03	-.31788E-03	-.25760E-03	-.19676E-03	-.13573E-03
3	.00000E	-.43908E-03	-.43726E-03	-.41706E-03	-.39131E-03	-.35507E-03	-.31025E-03	-.25760E-03	-.19676E-03	-.13573E-03

IZ=	11 .7143+00	12 .7857+00	13 .8571+00	14 .9286+00	15 .1000+01
15	-.30176E-03	-.28336E-03	-.26904E-05	-.50757E-05	-.31684E-05
14	-.31058E-03	-.12705E-04	-.31684E-05	-.31684E-05	-.31684E-05
13	-.34113E-03	-.26568E-04	-.41220E-05	-.31684E-05	-.31684E-05
12	-.62796E-03	-.24149E-04	-.26831E-05	-.41220E-05	-.31684E-05
11	-.98136E-03	-.49323E-04	-.14642E-04	-.80294E-05	-.31684E-05
10	-.17674E-02	-.65548E-04	-.29871E-04	-.79367E-05	-.31684E-05
9	-.32472E-02	-.16720E-03	-.81342E-04	-.12705E-04	-.31684E-05
8	-.62976E-02	-.25208E-03	-.26831E-04	-.16522E-04	-.31684E-05
7	-.12265E-01	-.46720E-03	-.81342E-04	-.12705E-04	-.31684E-05
6	-.17674E-02	-.65548E-04	-.29871E-04	-.79367E-05	-.31684E-05
5	-.98136E-03	-.49323E-04	-.14642E-04	-.80294E-05	-.31684E-05
4	-.61342E-03	-.24149E-04	-.26831E-05	-.31684E-05	-.31684E-05
3	-.45138E-03	-.15568E-04	-.41220E-05	-.31684E-05	-.31684E-05
2	-.38654E-03	-.12705E-04	-.31684E-05	-.31684E-05	-.31684E-05
1	-.45137E-03	-.27334E-04	-.26904E-05	-.41220E-05	-.31684E-05

LEVEL 1 ***** MACH *****

Microfilmed From
Best Available Copy

PEPS16 CURVED CENTERLINE TEST CASE RALPH LEVY DATE 011078 PAGE 43

IZ=	1	2	3	4	5	6	7	8	9	10
Z =	.0000	.7143-01	.1429+00	.2143+00	.2857+00	.3571+00	.4286+00	.5000+00	.5714+00	.6429+00
IY Y										
15 .10000+01	.10015+00	.10015+00	.10014+00	.10014+00	.10014+00	.10014+00	.10011+00	.99747-01	.97415-01	.91619-01
14 .92857+00	.10015+00	.10015+00	.10014+00	.10014+00	.10014+00	.10013+00	.10012+00	.99789-01	.97578-01	.91915-01
13 .85714+00	.10015+00	.10015+00	.10014+00	.10014+00	.10013+00	.10013+00	.10012+00	.99914-01	.97885-01	.92803-01
12 .78571+00	.10015+00	.10015+00	.10014+00	.10014+00	.10013+00	.10013+00	.10012+00	.10005+00	.98817-01	.94325-01
11 .71429+00	.10015+00	.10015+00	.10014+00	.10014+00	.10013+00	.10013+00	.10013+00	.10010+00	.99629-01	.96411-01
10 .64286+00	.10016+00	.10015+00	.10015+00	.10014+00	.10014+00	.10014+00	.10014+00	.10013+00	.10007+00	.98655-01
9 .57143+00	.10016+00	.10016+00	.10015+00	.10015+00	.10014+00	.10015+00	.10015+00	.10015+00	.10014+00	.99913-01
8 .50000E-00	.10015+00	.10015+00	.10016+00	.10016+00	.10016+00	.10016+00	.10016+00	.10017+00	.10016+00	.10010+00
7 .42857+00	.10015+00	.10016+00	.10016+00	.10016+00	.10016+00	.10016+00	.10016+00	.10015+00	.10014+00	.99913-01
6 .35714+00	.10014+00	.10016+00	.10015+00	.10014+00	.10014+00	.10014+00	.10014+00	.10013+00	.10007+00	.98655-01
5 .28571+00	.10014+00	.10015+00	.10014+00	.10014+00	.10013+00	.10013+00	.10013+00	.10010+00	.99629-01	.96411-01
4 .21429+00	.10015+00	.10015+00	.10014+00	.10014+00	.10013+00	.10013+00	.10012+00	.10005+00	.98817-01	.94325-01
3 .14286+00	.10015+00	.10015+00	.10014+00	.10014+00	.10013+00	.10013+00	.10012+00	.99914-01	.97885-01	.92803-01
2 .71429-01	.10015+00	.10015+00	.10014+00	.10014+00	.10013+00	.10013+00	.10012+00	.99789-01	.97578-01	.91915-01
1 .00000	.10015+00	.10015+00	.10014+00	.10014+00	.10014+00	.10014+00	.10011+00	.99747-01	.97415-01	.91619-01

IZ=	11	12	13	14	15
Z =	.7143+00	.7857+00	.8571+00	.9286+00	.1000+01
15 .10000+01	.81452-01	.66618-01	.47424-01	.24779-01	.00000
14 .92857+00	.81841-01	.67125-01	.47764-01	.24976-01	.00000
13 .85714+00	.83006-01	.68286-01	.48784-01	.25566-01	.00000
12 .78571+00	.85103-01	.70501-01	.50696-01	.26677-01	.00000
11 .71429+00	.88113-01	.74141-01	.53868-01	.28535-01	.00000
10 .64286+00	.92520-01	.79413-01	.58709-01	.31423-01	.00000
9 .57143+00	.94436-01	.85327-01	.64642-01	.35088-01	.00000
8 .50000E-00	.97042-01	.88.06-01	.67828-01	.37141-01	.00000
7 .42857+00	.94436-01	.85327-01	.64642-01	.35088-01	.00000
6 .35714+00	.92520-01	.79413-01	.58709-01	.31423-01	.00000
5 .28571+00	.88113-01	.74141-01	.53868-01	.28535-01	.00000
4 .21429+00	.85103-01	.70501-01	.50696-01	.26677-01	.00000
3 .14286+00	.83006-01	.68286-01	.48784-01	.25566-01	.00000
2 .71429-01	.81841-01	.67125-01	.47764-01	.24976-01	.00000
1 .00000	.81452-01	.66618-01	.47424-01	.24779-01	.00000

Microfilmed From
Best Available Copy

Check on Mass Conservation
at Station 13

INTEGRATED PROPERTIES AT STATION 13

FLOW AREA= .52286 SQ.FT. MASS FLUX= .34839-01LBM/SEC

LOCAL TO ORIGINAL AREA RATIO 1.0004
LOCAL TO ORIGINAL MASS FLUX RATIO 1.0011

Microfilmed From
Best Available Copy

Results of Calculation at

Station 13

PEPSIS CURVED CENTERLINE TEST CASE PALPW LEVY DATE 01/1978 PAGE 231

13-IN STATION , S: .4001680E+01

LOCATION OF CENTERLINE (.7000000D .6873722+0-01. .4000000D+01) DX: .5000000D-00

NWD: 1

NWD = 7. IFACT = 1 IICNT = 0 VELOCITY BOUNDARY CONDITIONS 6 6 12 3

IDUCT = 1 I-PACH = 1 JFACT = 1 DENSITY BOUNDARY CONDITIONS 6 11 12 20

LEVEL 1 ***** RADIUS *****

I2: J	1 .0000	2 .7143-01	3 .1429+00	4 .2143+00	5 .2857+00	6 .3571+00	7 .4286+00	8 .5000+00	9 .5714+00	10 .6429+00
17	.10000+01	.96282-01	.91648-01	.17810+00	.18219+00	.22619+00	.27024+00	.31429+00	.35833+00	.40238+00
16	.92857+00	.89446-01	.85116-01	.16544+00	.16915+00	.20987+00	.25060+00	.29132+00	.33204+00	.37276+00
15	.85714+00	.82610-01	.78584-01	.15278+00	.15611+00	.19350+00	.23089+00	.26828+00	.30567+00	.34307+00
14	.78571+00	.75774-01	.72052-01	.14011+00	.14328+00	.17714+00	.21101+00	.24488+00	.28075+00	.31662+00
13	.71429+00	.68938-01	.65520-01	.12745+00	.13024+00	.16077+00	.19130+00	.22183+00	.25236+00	.28289+00
12	.64286+00	.62102-01	.58988-01	.11478+00	.11737+00	.14441+00	.17144+00	.19847+00	.22551+00	.25254+00
11	.57143+00	.55266-01	.52456-01	.10212+00	.10441+00	.12804+00	.15159+00	.17513+00	.19868+00	.22223+00
10	.50000+00	.48430-01	.45924-01	.89457-01	.91450-01	.11168+00	.13173+00	.15178+00	.17183+00	.19188+00
9	.42857+00	.41594-01	.39392-01	.76791-01	.78494-01	.95317+00	.11288+00	.13044+00	.14799+00	.16555+00
8	.35714+00	.34758-01	.32860-01	.64125-01	.65538-01	.79560+00	.94188+00	.10882+00	.12345+00	.13808+00
7	.28571+00	.27922-01	.26328-01	.51459-01	.52582-01	.63804+00	.75499+00	.87194+00	.98889+00	.11058+00
6	.21429+00	.21086-01	.19796-01	.38793-01	.39626-01	.48047+00	.56810+00	.65573+00	.74336+00	.83099+00
5	.14286+00	.14250-01	.13264-01	.26127-01	.26670-01	.32291+00	.38121+00	.43952+00	.49782+00	.55612+00
4	.71429-01	.71414-02	.66319-02	.13461-01	.13714-01	.16535+00	.19432+00	.22329+00	.25226+00	.28123+00
3	.14286-01	.14286-02	.13264-02	.26922-02	.27428-02	.33070-01	.38864-01	.44658-01	.50452-01	.56246-01
2	.71429-02	.71429-03	.66319-03	.13461-02	.13714-02	.16535-01	.19432-01	.22329-01	.25226-01	.28123-01
1	.00000	.00000+00	.00000+00	.00000+00	.00000+00	.00000+00	.00000+00	.00000+00	.00000+00	.00000+00

I2: J	11 .7857+00	12 .8571+00	13 .9286+00	14 .1000+01
17	.44053+00	.47857+00	.51662+00	.55467+00
16	.40848+00	.44419+00	.47990+00	.51561+00
15	.37643+00	.40981+00	.44319+00	.47657+00
14	.34438+00	.37543+00	.40648+00	.43753+00
13	.31233+00	.34105+00	.36977+00	.39849+00
12	.28028+00	.30667+00	.33306+00	.35945+00
11	.24823+00	.27229+00	.29635+00	.32041+00
10	.21618+00	.23791+00	.25964+00	.28137+00
9	.18310+00	.20352+00	.22393+00	.24234+00
8	.15073+00	.16914+00	.18755+00	.20596+00
7	.11838+00	.12775+00	.13712+00	.14649+00
6	.90022+01	.96369+01	.10272+00	.10907+00
5	.61667+01	.67963+01	.74259+01	.80555+01
4	.31224+01	.34557+01	.37890+01	.41223+01
3	.62440+00	.69114+00	.75788+00	.82462+00
2	.31224+00	.34557+00	.37890+00	.41223+00
1	.00000+00	.00000+00	.00000+00	.00000+00

Microfilmed From
Best Available Copy

LEVEL 1 ***** THETA *****

J	1	2	3	4	5	6	7	8	9	10
I	.0000	.7143-01	.1429+00	.2143+00	.2857+00	.3571+00	.4286+00	.5000+00	.5714+00	.6429+00
17	180.00	180.00	180.00	180.00	180.00	180.00	180.00	180.00	180.00	180.00
16	167.18	167.18	167.18	167.18	167.18	167.18	167.18	167.18	167.18	167.18
15	154.37	154.37	154.37	154.37	154.37	154.37	154.37	154.37	154.37	154.37
14	141.55	141.55	141.55	141.55	141.55	141.55	141.55	141.55	141.55	141.55
13	128.74	128.74	128.74	128.74	128.74	128.74	128.74	128.74	128.74	128.74
12	115.92	115.92	115.92	115.92	115.92	115.92	115.92	115.92	115.92	115.92
11	103.11	103.11	103.11	103.11	103.11	103.11	103.11	103.11	103.11	103.11
10	90.29	90.29	90.29	90.29	90.29	90.29	90.29	90.29	90.29	90.29
9	77.48	77.48	77.48	77.48	77.48	77.48	77.48	77.48	77.48	77.48
8	64.66	64.66	64.66	64.66	64.66	64.66	64.66	64.66	64.66	64.66
7	51.85	51.85	51.85	51.85	51.85	51.85	51.85	51.85	51.85	51.85
6	39.03	39.03	39.03	39.03	39.03	39.03	39.03	39.03	39.03	39.03
5	26.22	26.22	26.22	26.22	26.22	26.22	26.22	26.22	26.22	26.22
4	13.40	13.40	13.40	13.40	13.40	13.40	13.40	13.40	13.40	13.40
3	.59	.00	.00	.00	.00	.00	.00	.00	.00	.00

J	11	12	13	14	15
I	.7143+00	.7857+00	.8571+00	.9286+00	.1000+01
17	180.00	180.00	180.00	180.00	180.00
16	167.18	167.18	167.18	167.18	167.18
15	154.37	154.37	154.37	154.37	154.37
14	141.55	141.55	141.55	141.55	141.55
13	128.74	128.74	128.74	128.74	128.74
12	115.92	115.92	115.92	115.92	115.92
11	103.11	103.11	103.11	103.11	103.11
10	90.29	90.29	90.29	90.29	90.29
9	77.48	77.48	77.48	77.48	77.48
8	64.66	64.66	64.66	64.66	64.66
7	51.85	51.85	51.85	51.85	51.85
6	39.03	39.03	39.03	39.03	39.03
5	26.22	26.22	26.22	26.22	26.22
4	13.40	13.40	13.40	13.40	13.40
3	.59	.00	.00	.00	.00

Microfilmed From
Best Available Copy

12-TH STATION , S: .4OF16805+01

LOCATION OF CENTERLINE : .00000000 , .6836724D-01, .4000000D+01) DX: .50000000-00

KODE: 1

NAD : 0. IFCI : 1 IICNI : 0 VELOCITY BOUNDARY CONDITIONS 4 4 12 3

IDUCT : 1 IPACH : 1 JFCI : 1 DENSITY BOUNDARY CONDITIONS 4 11 12 20

VELOCITY VECTOR DISPLAYED IN COMPUTATIONAL COORDINATES

LEVEL 1 ***** U-SEL *****

J7 :	1 .0000	2 .7143-01	3 .1429+00	4 .2143+00	5 .2857+00	6 .3571+00	7 .4286+00	8 .5000+00	9 .5714+00	10 .6429+00
17										
16										
15										
14										
13										
12										
11										
10										
9										
8										
7										
6										
5										
4										
3										
2										
1										

J7 :	11 .7143+00	12 .7857+00	13 .8571+00	14 .9286+00	15 .1000+01
15					
14					
13					
12					
11					
10					
9					
8					
7					
6					
5					
4					
3					
2					
1					

Microfilmed From
Best Available Copy

LEVEL 1 ***** V-VEL *****

IZ=	1 .0000	2 .7143-01	3 .1429+00	4 .2143+00	5 .2857+00	6 .3571+00	7 .4286+00	8 .5000+00	9 .5714+00	10 .6429+00
IY Y										
15 .10000+01	.26545-09	-.16099-19	-.31778-19	-.38335-19	-.22304-19	-.22311-19	-.33025-20	-.17624-20	-.88180-20	-.95197-20
14 .92857+00	.32672-03	-.14207-03	-.64091-03	-.93720-03	-.11328-02	-.12805-02	-.14037-02	-.15003-02	-.15706-02	-.16121-02
13 .85714+00	.63712-03	-.17617-03	-.10861-02	-.16223-02	-.19938-02	-.22684-02	-.25148-02	-.27170-02	-.28698-02	-.29856-02
12 .78571+00	.91570-03	.60983-04	-.10842-02	-.17826-02	-.22367-02	-.26226-02	-.29874-02	-.32574-02	-.35330-02	-.38019-02
11 .71429+00	.11485-02	.77798-03	-.33177-03	-.10137-02	-.15799-02	-.19342-02	-.23093-02	-.27016-02	-.31169-02	-.35960-02
10 .64286+00	.13239-02	.13794-02	.15950-02	.85360-03	.42217-03	.70372-05	-.39500-03	-.83158-03	-.13475-02	-.20651-02
9 .57143+00	.14330-02	.37943-02	.34795-02	.31809-02	.28668-02	.25449-02	.21552-02	.17207-02	.11790-02	.36979-03
8 .50000+00	.14704-02	.44864-02	.43906-02	.42062-02	.39635-02	.36752-02	.33416-02	.29489-02	.24306-02	.16418-02
7 .42857+00	.14340-02	.35706-02	.32981-02	.30362-02	.27875-02	.24846-02	.21290-02	.17422-02	.12344-02	.44659-03
6 .35714+00	.13256-02	.20355-02	.13536-02	.86719-03	.46991-03	.10944-03	-.25927-03	-.65311-03	-.11559-02	-.19178-02
5 .28571+00	.11506-02	.99499-03	-.25237-03	-.90852-03	-.13956-02	-.18053-02	-.21863-02	-.25761-02	-.30335-02	-.36168-02
4 .21429+00	.91760-03	.89598-04	-.10719-02	-.17653-02	-.22390-02	-.26168-02	-.29557-02	-.32647-02	-.35806-02	-.39403-02
3 .14286+00	.63881-03	-.48610-03	-.11485-02	-.17113-02	-.20852-02	-.23674-02	-.25996-02	-.28130-02	-.30021-02	-.31754-02
2 .71429-01	.32755-03	-.15988-03	-.70241-03	-.10117-02	-.12142-02	-.13639-02	-.14866-02	-.15911-02	-.16742-02	-.17425-02
1 .00000	.00000	-.22623-19	-.28410-19	-.24226-19	-.45884-19	-.44603-19	-.43269-19	-.40867-19	-.74809-19	-.66378-19

IZ=	11 .7143+00	12 .7857+00	13 .8571+00	14 .9286+00	15 .1000+01
15 .10000+01	.70449-20	.19553-20	-.38653-20	-.29002-20	.00000
14 .92857+00	-.16226-02	-.16515-02	-.16759-02	-.14693-02	.00000
13 .85714+00	-.30971-02	-.32117-02	-.33733-02	-.30412-02	.00000
12 .78571+00	-.41026-02	-.44996-02	-.50454-02	-.48903-02	.00000
11 .71429+00	-.42365-02	-.51549-02	-.64670-02	-.69133-02	.00000
10 .64286+00	-.31177-02	-.47349-02	-.71103-02	-.88980-02	.00000
9 .57143+00	-.95324-03	-.31543-02	-.66185-02	-.10366-01	.00000
8 .50000+00	-.28864-03	-.20679-02	-.60289-02	-.11270-01	.00000
7 .42857+00	-.87169-03	-.31060-02	-.69057-02	-.12343-01	.00000
6 .35714+00	-.19742-02	-.49493-02	-.80931-02	-.12863-01	.00000
5 .28571+00	-.34289-02	-.56206-02	-.78118-02	-.11330-01	.00000
4 .21429+00	-.43831-02	-.60483-02	-.63130-02	-.84792-02	.00000
3 .14286+00	-.33679-02	-.34429-02	-.42669-02	-.54466-02	.00000
2 .71429-01	-.17956-02	-.18878-02	-.21262-02	-.26192-02	.00000
1 .00000	-.57815-19	-.50151-19	-.81578-19	-.36862-19	.00000

LEVEL 1 ***** W-VEL *****

Microfilmed From
Best Available Copy

PEPSIG CURVED CENTERLINE TEST CASE PALPW LEVY DATE 011078 PAGE 201

IZ= / Z =	1 .0000	2 .7143-01	3 .1429+00	4 .2143+00	5 .2857+00	6 .3571+00	7 .4286+00	8 .5000+00	9 .5714+00	10 .6429+00
17 Y										
15	.10000+01	-.19682-02	-.11293-02	-.99207-03	-.75165-03	-.59985-03	-.32691-03	-.11271-03	-.88776-04	-.78937-03	-.23275-03
14	.92857+00	-.19319-02	-.11127-02	-.97821-03	-.74669-03	-.57875-03	-.31716-03	-.17687-03	-.51221-05	-.10941-03	-.15066-03
13	.85714+00	-.13230-02	-.76651-03	-.67393-03	-.51297-03	-.38611-03	-.53806-03	-.38060-03	-.26042-03	-.19540-03	-.11103-03
12	.78571+00	-.11483-02	-.92220-03	-.81400-03	-.74919-03	-.67072-03	-.56421-03	-.43961-03	-.32187-03	-.24348-03	-.22457-03
11	.71429+00	-.91591-03	-.[illegible]	-.[illegible]	-.[illegible]	-.[illegible]	-.[illegible]	-.10557-04	-.12559-03	-.21330-03	-.21170-03
10	.64286+00	-.61756-03	-.[illegible]	-.70583-04	-.26207-03	-.51946-03	-.75145-03	-.97787-03	-.11823-02	-.13226-02	-.13924-02
9	.57143+00	-.32708-03	-.15366-03	-.19354-03	-.55024-03	-.88888-03	-.12106-02	-.15160-02	-.17960-02	-.20198-02	-.21154-02
8	.50000+00	-.67169-10	-.55470-33	-.57565-03	-.40346-03	-.15169-03	-.13029-03	-.42501-03	-.71373-03	-.98185-03	-.11790-02
7	.42857+00	-.32729-03	-.76417-03	-.11333-02	-.11394-02	-.98598-03	-.76269-03	-.50661-03	-.23806-03	-.22171-04	-.23724-03
6	.35714+00	-.63837-03	-.92277-03	-.[illegible]	-.70773-03	-.50692-03	-.25322-03	-.[illegible]	-.27283-03	-.49868-03	-.65693-03
5	.28571+00	-.91759-03	-.74237-04	-.92496-04	-.78742-04	-.36181-03	-.66685-03	-.[illegible]	-.12109-02	-.13925-02	-.14768-02
4	.21429+00	-.11509-02	-.46767-03	-.[illegible]	-.61425-03	-.91350-03	-.12184-02	-.14955-02	-.17153-02	-.18952-02	-.19689-02
3	.14286+00	-.13765-02	-.71974-03	-.66849-33	-.84656-03	-.10907-02	-.13923-02	-.15671-02	-.17546-02	-.18166-02	-.18068-02
2	.71429-01	-.14355-02	-.85700-03	-.78966-03	-.90803-03	-.11887-02	-.12796-02	-.14510-02	-.15727-02	-.16209-02	-.15967-02
1	.00000	-.14704-02	-.89954-03	-.82693-03	-.92736-03	-.10874-02	-.12591-02	-.14136-02	-.15208-02	-.15584-02	-.15296-02

IZ= / Z =	11 .7143+00	12 .7857+00	13 .8571+00	14 .9286+00	15 .1000+01
15	.10000+01	-.16978-03	-.56981-04	.12354-03	.10004-03	.00000
14	.92857+00	-.11775-03	-.12297-34	.17538-23	.12096-03	.00000
13	.85714+00	.14112-03	.22286-03	.38009-03	.18715-03	.00000
12	.78571+00	.26692-03	.36113-03	.47426-03	.25924-03	.00000
11	.71429+00	-.11408-03	.75661-04	.29352-03	.19104-03	.00000
10	.64286+00	-.11572-02	-.78628-03	-.28018-03	-.15988-04	.00000
9	.57143+00	-.10855-02	-.15659-02	-.87852-03	-.25560-03	.00000
8	.50000+00	-.12250-02	-.10585-02	-.67131-03	-.22820-03	.00000
7	.42857+00	-.36693-03	-.40586-03	-.35981-33	-.16510-03	.00000
6	.35714+00	-.73743-03	-.76177-03	-.71188-03	-.34886-03	.00000
5	.28571+00	-.14678-02	-.13892-02	-.12093-02	-.56316-03	.00000
4	.21429+00	-.17999-02	-.16695-02	-.14229-02	-.65517-03	.00000
3	.14286+00	-.17250-02	-.15984-02	-.13613-02	-.64302-03	.00000
2	.71429-01	-.15236-02	-.14295-02	-.12677-02	-.59942-03	.00000
1	.00000	-.14594-02	-.13755-02	-.12306-02	-.58533-03	.00000

Microfilmed From
Best Available Copy

13-IH STATION : S= .9001660E+01

LOCATION OF CENTERLINE = .0000000E+00 , .6836224E-01, .4000000E+01) DX= .5000000E+00

ROORD= 1

RHO = 0. TRACT = 1 ITCN1 = 0

IDUCT = 1 ITSCH = 1 NOMACH = 0

LEVEL 1 ***** RHO *****

Z=	1 .0000	2 .7143-01	3 .1429+00	4 .2143+00	5 .2857+00	6 .3571+00	7 .4286+00	8 .5000+00	9 .5714+00	10 .6429+00
17										
15	.1000E+01	.9996E+00	.9997E+00	.9997E+00	.9998E+00	.9998E+00	.9998E+00	.9998E+00	.9996E+00	.9996E+00
14	.9286E+00	.9996E+00	.9997E+00	.9997E+00	.9998E+00	.9998E+00	.9998E+00	.9998E+00	.9996E+00	.9996E+00
13	.8571E+00	.9997E+00	.9997E+00	.9997E+00	.9998E+00	.9998E+00	.9998E+00	.9998E+00	.9997E+00	.9996E+00
12	.7857E+00	.9997E+00	.9997E+00	.9997E+00	.9998E+00	.9998E+00	.9998E+00	.9998E+00	.9997E+00	.9995E+00
11	.7143E+00	.9997E+00	.9997E+00	.9997E+00	.9998E+00	.9998E+00	.9998E+00	.9998E+00	.9997E+00	.9995E+00
10	.6429E+00	.9997E+00	.9997E+00	.9997E+00	.9998E+00	.9998E+00	.9998E+00	.9998E+00	.9997E+00	.9995E+00
9	.5714E+00	.9997E+00	.9997E+00	.9997E+00	.9998E+00	.9998E+00	.9998E+00	.9998E+00	.9997E+00	.9995E+00
8	.5000E+00	.9997E+00	.9997E+00	.9997E+00	.9998E+00	.9998E+00	.9998E+00	.9998E+00	.9997E+00	.9995E+00
7	.4286E+00	.9996E+00	.9996E+00	.9996E+00	.9997E+00	.9997E+00	.9997E+00	.9997E+00	.9996E+00	.9994E+00
6	.3571E+00	.9996E+00	.9996E+00	.9996E+00	.9997E+00	.9997E+00	.9997E+00	.9997E+00	.9996E+00	.9994E+00
5	.2857E+00	.9996E+00	.9996E+00	.9996E+00	.9997E+00	.9997E+00	.9997E+00	.9997E+00	.9996E+00	.9994E+00
4	.2143E+00	.9996E+00	.9996E+00	.9996E+00	.9997E+00	.9997E+00	.9997E+00	.9997E+00	.9996E+00	.9994E+00
3	.1429E+00	.9996E+00	.9996E+00	.9996E+00	.9997E+00	.9997E+00	.9997E+00	.9997E+00	.9996E+00	.9994E+00
2	.7143E-01	.9996E+00	.9996E+00	.9996E+00	.9997E+00	.9997E+00	.9997E+00	.9997E+00	.9996E+00	.9994E+00
1	.0000E	.9996E+00	.9996E+00	.9996E+00	.9997E+00	.9997E+00	.9997E+00	.9997E+00	.9996E+00	.9994E+00

Z=	11 .7143+00	12 .7857+00	13 .8571+00	14 .9286+00	15 .1000+01
15	.1000E+01	.9988E+00	.9982E+00	.9979E+00	.9979E+00
14	.9286E+00	.9986E+00	.9982E+00	.9979E+00	.9979E+00
13	.8571E+00	.9986E+00	.9982E+00	.9979E+00	.9979E+00
12	.7857E+00	.9986E+00	.9982E+00	.9979E+00	.9979E+00
11	.7143E+00	.9986E+00	.9982E+00	.9979E+00	.9979E+00
10	.6429E+00	.9985E+00	.9982E+00	.9979E+00	.9979E+00
9	.5714E+00	.9985E+00	.9982E+00	.9979E+00	.9979E+00
8	.5000E+00	.9985E+00	.9982E+00	.9979E+00	.9979E+00
7	.4286E+00	.9984E+00	.9981E+00	.9978E+00	.9977E+00
6	.3571E+00	.9984E+00	.9981E+00	.9978E+00	.9977E+00
5	.2857E+00	.9984E+00	.9981E+00	.9978E+00	.9977E+00
4	.2143E+00	.9984E+00	.9981E+00	.9978E+00	.9977E+00
3	.1429E+00	.9984E+00	.9981E+00	.9978E+00	.9977E+00
2	.7143E-01	.9984E+00	.9981E+00	.9978E+00	.9977E+00
1	.0000E	.9984E+00	.9981E+00	.9978E+00	.9977E+00

Microfilmed From
Best Available Copy

12-IN STATION I S= .8071685-01

LOCATION OF CENTERLINE (.00000000 , .6836240-01, .40000000-01) DX= .50000000-00

NCORD= 1

BND = 0. IFACT = 1 ITCNT = 0

IDUCT = 1 IMACH = 1 NOMACH = 0

LEVEL 1 ***** PRESS *****

IZ=	1	2	3	4	5	6	7	8	9	10
Z =	.0000	.7143-01	.1429+00	.2143+00	.2857+00	.3571+00	.4286+00	.5000+00	.5714+00	.6429+00
17										
15	.1000E+01	.71433+02	.71435+02	.71436+02	.71438+02	.71439+02	.71440+02	.71442+02	.71443+02	.71446+02	.71446+02
14	.9286E+00	.71433+02	.71435+02	.71436+02	.71438+02	.71439+02	.71440+02	.71442+02	.71443+02	.71446+02	.71446+02
13	.8571E+00	.71433+02	.71435+02	.71436+02	.71437+02	.71438+02	.71440+02	.71441+02	.71442+02	.71445+02	.71445+02
12	.7857E+00	.71433+02	.71434+02	.71435+02	.71436+02	.71437+02	.71438+02	.71440+02	.71441+02	.71442+02	.71443+02
11	.7143E+00	.71431+02	.71433+02	.71433+02	.71434+02	.71435+02	.71437+02	.71438+02	.71439+02	.71440+02	.71441+02
10	.6429E+00	.71429+02	.71431+02	.71431+02	.71432+02	.71433+02	.71434+02	.71435+02	.71436+02	.71437+02	.71438+02
9	.5714E+00	.71427+02	.71428+02	.71429+02	.71429+02	.71430+02	.71431+02	.71432+02	.71433+02	.71434+02	.71435+02
8	.5000E+00	.71427+02	.71427+02	.71427+02	.71427+02	.71427+02	.71427+02	.71427+02	.71427+02	.71427+02	.71427+02
7	.4286E+00	.71426+02	.71428+02	.71428+02	.71425+02	.71424+02	.71424+02	.71423+02	.71423+02	.71422+02	.71422+02
6	.3571E+00	.71426+02	.71427+02	.71427+02	.71422+02	.71421+02	.71420+02	.71419+02	.71418+02	.71417+02	.71417+02
5	.2857E+00	.71422+02	.71422+02	.71421+02	.71420+02	.71418+02	.71416+02	.71416+02	.71416+02	.71415+02	.71413+02
4	.2143E+00	.71421+02	.71421+02	.71420+02	.71418+02	.71417+02	.71416+02	.71414+02	.71413+02	.71412+02	.71410+02
3	.1429E+00	.71421+02	.71420+02	.71418+02	.71418+02	.71416+02	.71415+02	.71413+02	.71412+02	.71410+02	.71409+02
2	.7143E-01	.71421+02	.71420+02	.71419+02	.71417+02	.71416+02	.71414+02	.71413+02	.71411+02	.71410+02	.71408+02
1	.0000E	.71421+02	.71420+02	.71419+02	.71417+02	.71415+02	.71414+02	.71412+02	.71411+02	.71409+02	.71408+02

IZ=	11	12	13	14	15
Z =	.7143+00	.7857+00	.8571+00	.9286+00	.1000+01
15	.1000E+01	.71447+02	.71448+02	.71448+02	.71449+02	.71449+02
14	.9286E+00	.71447+02	.71448+02	.71448+02	.71448+02	.71448+02
13	.8571E+00	.71447+02	.71447+02	.71448+02	.71448+02	.71448+02
12	.7857E+00	.71446+02	.71446+02	.71446+02	.71446+02	.71446+02
11	.7143E+00	.71443+02	.71443+02	.71444+02	.71444+02	.71444+02
10	.6429E+00	.71439+02	.71439+02	.71440+02	.71440+02	.71440+02
9	.5714E+00	.71433+02	.71434+02	.71434+02	.71434+02	.71434+02
8	.5000E+00	.71427+02	.71427+02	.71427+02	.71427+02	.71427+02
7	.4286E+00	.71421+02	.71422+02	.71420+02	.71420+02	.71420+02
6	.3571E+00	.71416+02	.71415+02	.71414+02	.71414+02	.71414+02
5	.2857E+00	.71411+02	.71410+02	.71410+02	.71409+02	.71409+02
4	.2143E+00	.71408+02	.71408+02	.71407+02	.71407+02	.71407+02
3	.1429E+00	.71407+02	.71406+02	.71405+02	.71405+02	.71405+02
2	.7143E-01	.71406+02	.71405+02	.71404+02	.71404+02	.71404+02
1	.0000E	.71406+02	.71405+02	.71404+02	.71404+02	.71404+02

Microfilmed From
Best Available Copy

LEVEL 1 ***** CP/2 *****

IZ=	1 .0000	2 .7143-01	3 .1429+00	4 .2143+00	5 .2857+00	6 .3571+00	7 .4286+00	8 .5000+00	9 .5714+00	10 .6429+00
17										
16	.10000+01	-.20741-01	-.18011-01	-.17519-01	-.16211-01	-.14896-01	-.13544-01	-.12185-01	-.10827-01	-.94834-02
15	.92857+00	-.20741-01	-.18011-01	-.17519-01	-.16211-01	-.14896-01	-.13544-01	-.12185-01	-.10827-01	-.94834-02
14	.85714+00	-.20831-01	-.18035-01	-.17537-01	-.16210-01	-.14896-01	-.13544-01	-.12185-01	-.10827-01	-.94834-02
13	.78571+00	-.21295-01	-.18327-01	-.17934-01	-.16722-01	-.15501-01	-.14280-01	-.12960-01	-.11569-01	-.10171-01
12	.71429+00	-.22526-01	-.19152-01	-.18784-01	-.17607-01	-.16308-01	-.15018-01	-.13640-01	-.12183-01	-.10718-01
11	.64286+00	-.24377-01	-.20701-01	-.19634-01	-.18501-01	-.17097-01	-.15718-01	-.14320-01	-.12820-01	-.11284-01
10	.57143+00	-.26650-01	-.22629-01	-.21349-01	-.20133-01	-.18665-01	-.17159-01	-.15575-01	-.13987-01	-.12317-01
9	.50000+00	-.27135-01	-.23076-01	-.21704-01	-.20253-01	-.18759-01	-.17191-01	-.15593-01	-.13987-01	-.12317-01
8	.42857+00	-.26626-01	-.22634-01	-.21177-01	-.19651-01	-.18128-01	-.16528-01	-.14983-01	-.13437-01	-.11847-01
7	.35714+00	-.26610-01	-.22666-01	-.21177-01	-.19651-01	-.18128-01	-.16528-01	-.14983-01	-.13437-01	-.11847-01
6	.28571+00	-.26668-01	-.22726-01	-.21178-01	-.19651-01	-.18128-01	-.16528-01	-.14983-01	-.13437-01	-.11847-01
5	.21429+00	-.26778-01	-.22826-01	-.21277-01	-.19751-01	-.18227-01	-.16627-01	-.15082-01	-.13536-01	-.11946-01
4	.14286+00	-.26927-01	-.22967-01	-.21418-01	-.19892-01	-.18368-01	-.16768-01	-.15223-01	-.13677-01	-.12087-01
3	.71429-01	-.27107-01	-.23138-01	-.21589-01	-.20063-01	-.18539-01	-.16939-01	-.15394-01	-.13848-01	-.12258-01
2	.00000	-.27306-01	-.23326-01	-.21777-01	-.20251-01	-.18727-01	-.17127-01	-.15582-01	-.14036-01	-.12446-01
1	.00000	-.27306-01	-.23326-01	-.21777-01	-.20251-01	-.18727-01	-.17127-01	-.15582-01	-.14036-01	-.12446-01

IZ=	11 .7143+00	12 .7857+00	13 .8571+00	14 .9286+00	15 .1000+01
17					
16	.10000+01	-.70852-02	-.67049-02	-.56727-02	-.53630-02	-.53294-02
15	.92857+00	-.73407-02	-.69388-02	-.58835-02	-.56138-02	-.55867-02
14	.85714+00	-.81237-02	-.72435-02	-.66579-02	-.63704-02	-.63376-02
13	.78571+00	-.95990-02	-.87285-02	-.81285-02	-.78328-02	-.77756-02
12	.71429+00	-.12042-01	-.11197-01	-.10598-01	-.10282-01	-.10217-01
11	.64286+00	-.15827-01	-.15169-01	-.14500-01	-.14172-01	-.14093-01
10	.57143+00	-.21018-01	-.20121-01	-.19462-01	-.19767-01
9	.50000+00	-.21018-01	-.20121-01	-.19462-01	-.19767-01
8	.42857+00	-.32949-01	-.31896-01	-.34188-01	-.34267-01
7	.35714+00	-.38265-01	-.39116-01	-.39675-01	-.40121-01	-.40296-01
6	.28571+00	-.42139-01	-.43683-01	-.43826-01	-.44218-01	-.44536-01
5	.21429+00	-.44733-01	-.46578-01	-.46537-01	-.47028-01	-.47260-01
4	.14286+00	-.46315-01	-.47379-01	-.48168-01	-.48862-01	-.48896-01
3	.71429-01	-.47153-01	-.48439-01	-.49035-01	-.49529-01	-.49762-01
2	.00000	-.47445-01	-.48539-01	-.49134-01	-.49822-01	-.50032-01
1	.00000	-.47445-01	-.48539-01	-.49134-01	-.49822-01	-.50032-01

LEVEL 1 ***** MACH *****

Microfilmed From
Best Available Copy

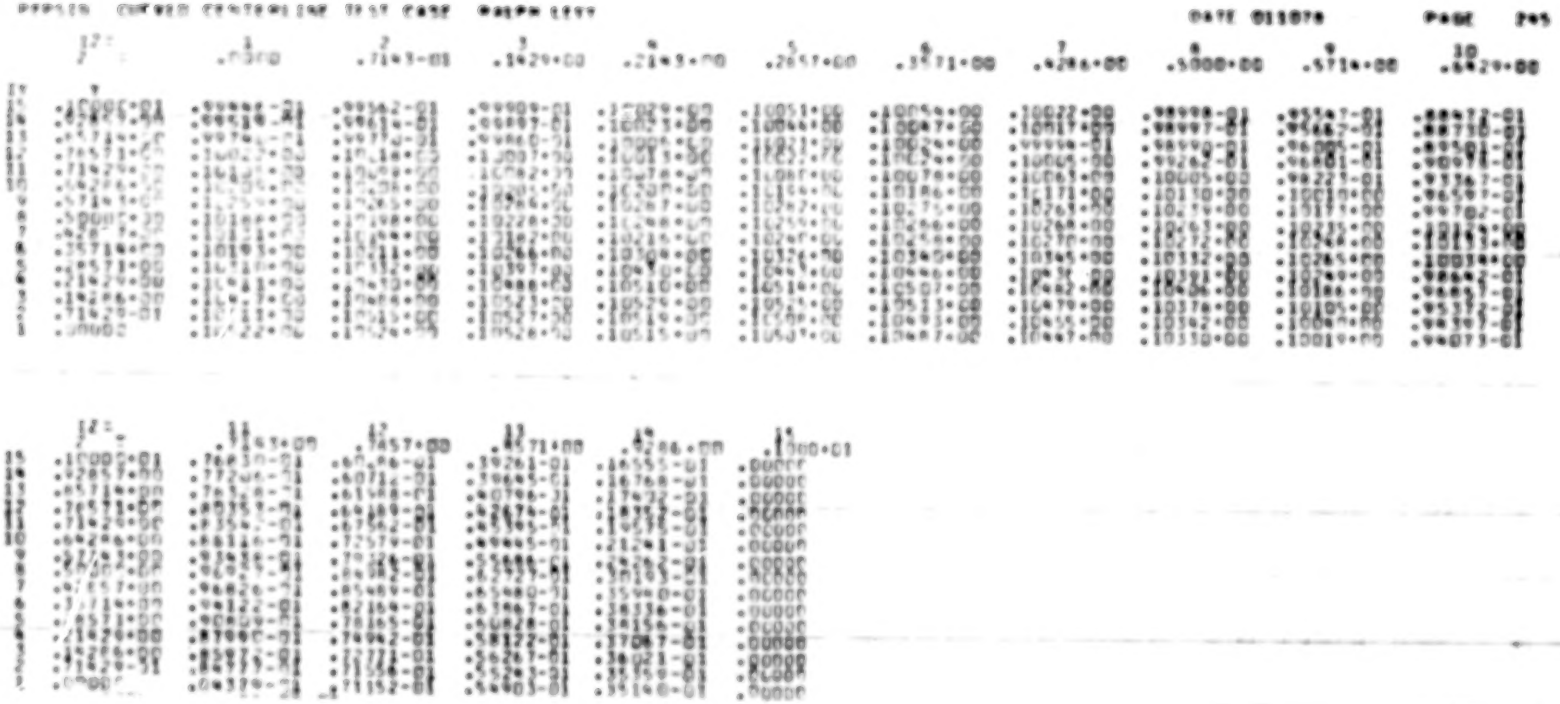

REFERENCES

1. Hawthorne, W. R.: The Applicability of Secondary Flow Analyses to the Solution of Internal Flow Problems. Fluid Mechanics of Internal Flow, Gino Sovran, Ed.; Elsevier Publishing Co., New York, New York, 1967.

2. Stuart, A. R. and R. Hetherington: The Solution of the Three Variable Duct Flow Equations. In Fluid Mechanics, Acoustics and Design of Turbomachinery, NASA SP-304, 1974, pp. 135-154.

3. Nash, J. F. and V. C. Patel: Three-dimensional Turbulent Boundary Layers, SBC Technical Books, Atlanta, 1972.

4. Patankar, S. V. and D. B. Spalding: A Calculation Procedure for Heat, Mass, and Momentum Transfer in Three-dimensional Parabolic Flows. Int. J. Heat and Mass Transfer, Vol. 15, 1972, p. 1787.

5. Caretto, L. S., R. M. Curr, and D. B. Spalding: Computational Methods in Applied Mechanics and Engineering, Vol. 1, 1973, p. 39.

6. Briley, W. R.: Numerical Method for Predicting Three-dimensional Steady Viscous Flow in Ducts. Journal of Computational Physics, Vol. 14, 1974, p. 8.

7. Patankar, S. V., V. S. Pratap, and D. B. Spalding: Prediction of Laminar Flow and Heat Transfer in Helically Coiled Pipes. Journal of Fluid Mechanics Vol. 62, 1974, p. 539.

8. Patankar, S. V., V. S. Pratap, and D. B. Spalding: Prediction of Turbulent Flow in Curved Pipes. Journal of Fluid Mechanics, Vol. 67, 1975, p. 583.

9. Ghia, K. N., V. Ghia, and C. J. Studerus: Analytical Formulation of Three-Dimensional Laminar Viscous Flow Through Turbine Cascades Using Surface-Oriented Coordinates. ASME Paper No. 76-FE-22, 1976.

10. Briley, W. R. and H. McDonald: Computation of Three-dimensional Turbulent Subsonic Flow in Curved Passages. United Technologies Research Center Report R75-911596-8, 1975.

11. Briley, W. R. and H. McDonald: An Implicit Numerical Method for the Multidimensional Compressible Navier-Stokes Equations. United Aircraft Research Laboratories Report M911363-6, November 1973.

12. McDonald H. and W. R. Briley: Three-dimensional Supersonic Flow of a Viscous or Inviscid Gas. Journal of Computational Physics, Vol. 19, No. 2, 1975, p. 150.

13. Briley, W. R., J. P. Kreskovsky and H. McDonald: Computation of Three-Dimensional Viscous Flow in Straight and Curved Passages. United Technologies Research Center Report R76-911841-9, August 1976.

14. Eiseman, P. R., H. McDonald and W. R. Briley: Method for Computing Three-Dimensional Viscous Diffuser Flows. United Technologies Research Center Report R76-911737-1, July 1975.

15. Eiseman, P. R.: The Numerical Solution of the Fluid Dynamic Equations in Curvilinear Coordinates. Air Force Weapons Laboratory Technical Report AFWL-TR-73-172, August 1973.

16. Hinze, J. O.: Turbulence, McGraw-Hill Book Company, Inc., New York, 1959.

17. Beer, J. M. and N. A. Chigier: Combustion Aerodynamics. Wiley, New York, 1972.

18. McDonald, H. and F. J. Camarata: An Extended Mixing Length Approach for Computing the Turbulent Boundary-Layer Development. In Proceedings, Stanford Conference on Computation of Turbulent Boundary Layers, Vol. I, Published by Stanford University, 1969, pp. 83-98.

19. Laugwitz, D.: Differential and Riemannian Geometry. Academic Press, Inc., New York, 1965.

20. Isaacson, E. and H. B. Keller: Analysis of Numerical Methods, John Wiley & Sons, Inc., New York, 1966.

21. Naot, D., A. Shavit, and M. Wolfshtein: Numerical Calculation of Reynolds Stresses in a Square Duct with Secondary Flow. Warme-und Stoffubertragung, Vol. 7, 1974, p. 151.

22. Coles, D.: The Law of the Wake in the Turbulent Boundary Layer. Journal of Fluid Mechanics, Vol. I, 1956, p. 191.

23. Maise, G. and McDonald, H.: Mixing Length and Kinematic Eddy Viscosity in a Compressible Boundary Layer. AIAA Journal, Vol. 6, 1968, p. 73.

24. Waltz, A.: Boundary Layers of Flow and Temperature. MIT Press, 1969, p. 115.

TABLE OF CONTENTS

	Page	
SUMMARY	1	1/A5
INTRODUCTION	3	1/A7
GOVERNING EQUATIONS	6	1/A10
Turbulence Model	8	1/A12
CURVILINEAR COORDINATE SYSTEM	11	1/B1
METHOD OF SOLUTION	15	1/B5
Background	15	1/B5
Computation of Mean Pressure Drop	15	1/B5
Integral Mass Flux Condition	17	1/B7
Solution of the Split Difference Equations	19	1/B9
APPLICATION TO INTERNAL SUBSONIC FLOWS	21	1/B11
Boundary and Initial Conditions	23	1/B12
DISCUSSION OF RESULTS	25	1/C1
RESUME	29	1/C5
APPENDIX - COMPUTER CODE INPUT AND OUTPUT	31	1/C7
REFERENCES	64	1/G13

25. Reshotko, E.: Experimental Study of the Stability of Pipe Flow, Pt. 1 Establishment of an Axially Symmetric Poiseville Flow. Jet Propulsion Laboratory Progress Report No. 20-364, October 1958.

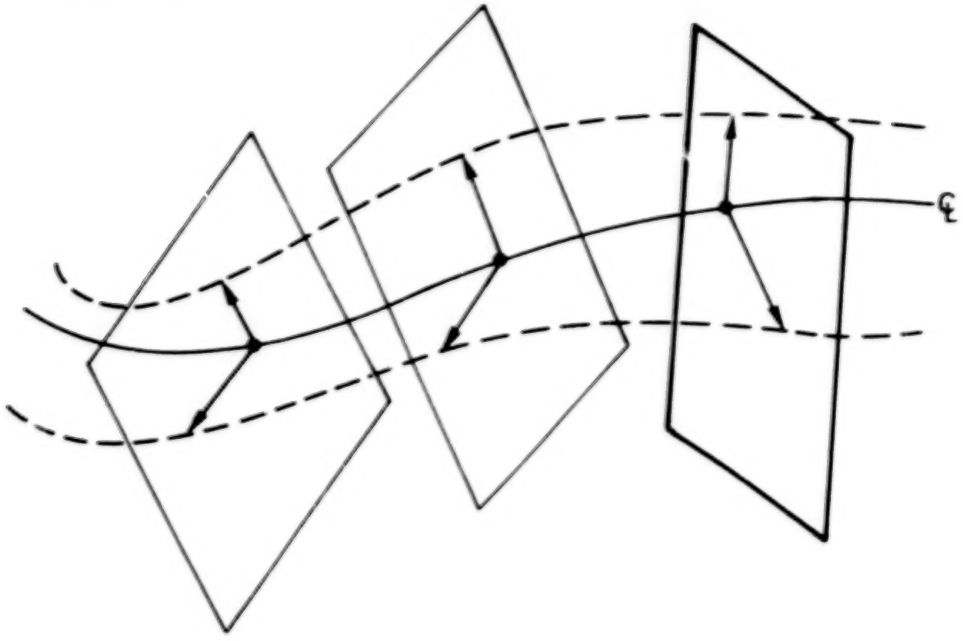

Figure 1. Generation of Transverse Planes from Two Vector Fields

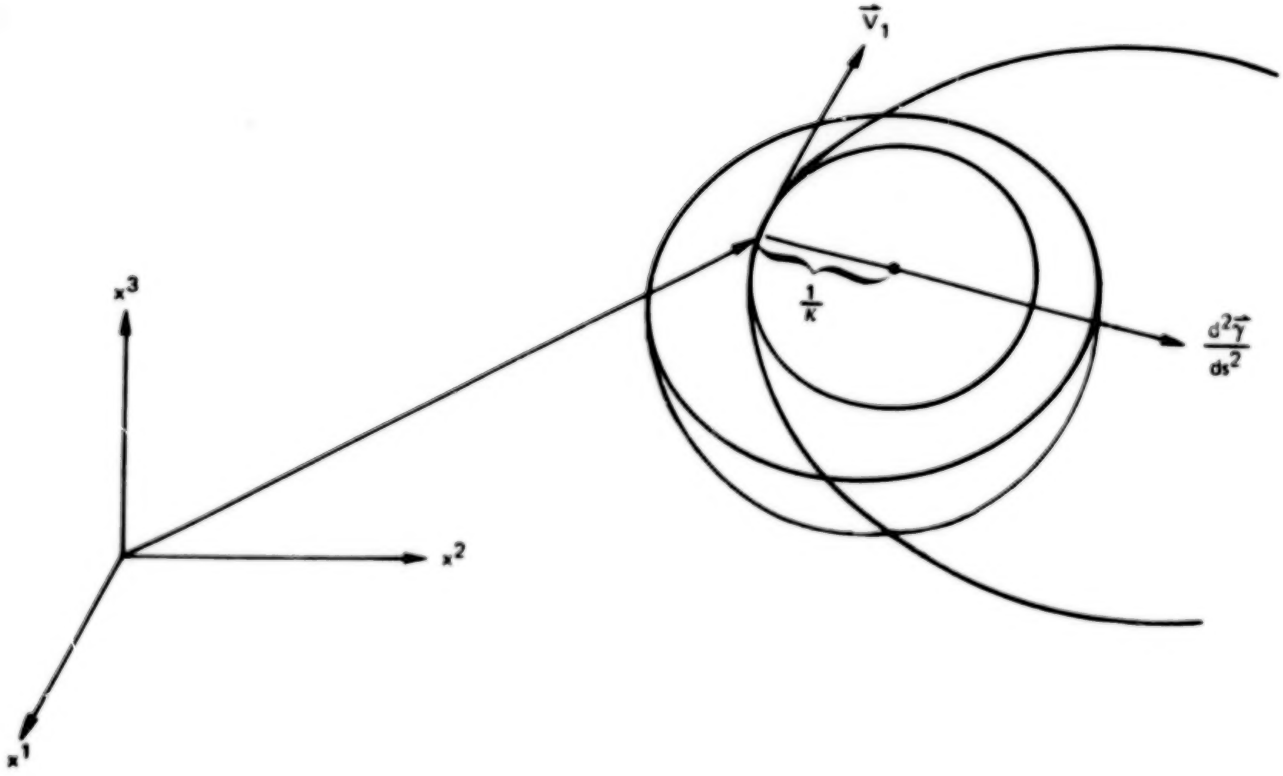

Figure 2. The Osculating Sphere

78-01-128-4

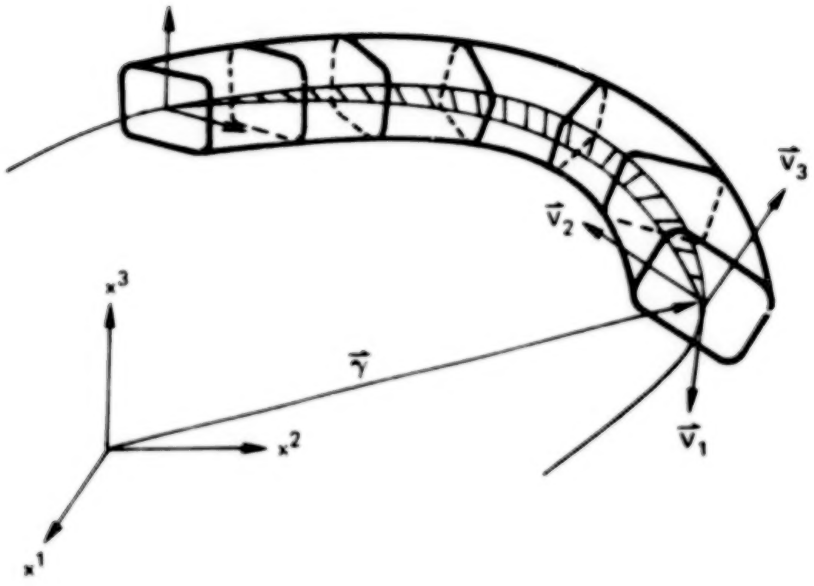

Figure 3. Transformation as an Embedding into Three Dimensional Euclidian Space

78-01-128-5

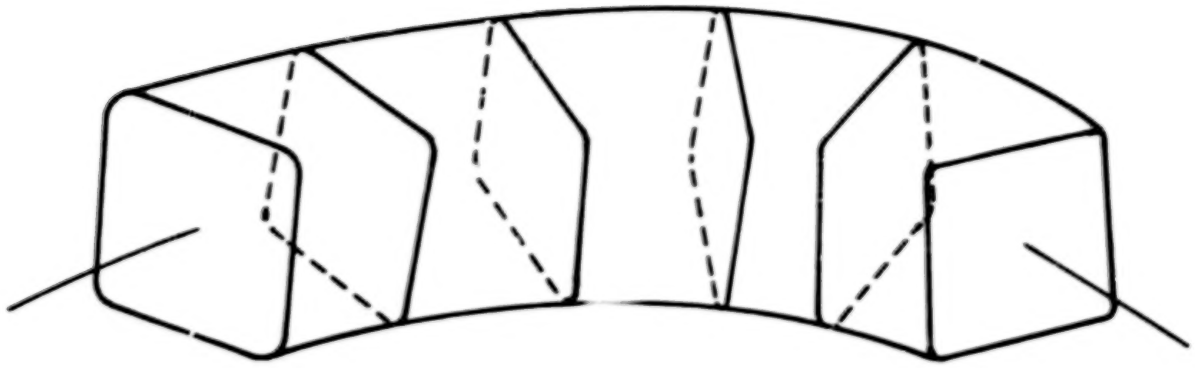

Figure 4a. Transverse Planar Cuts of Constant Axial Location y^3

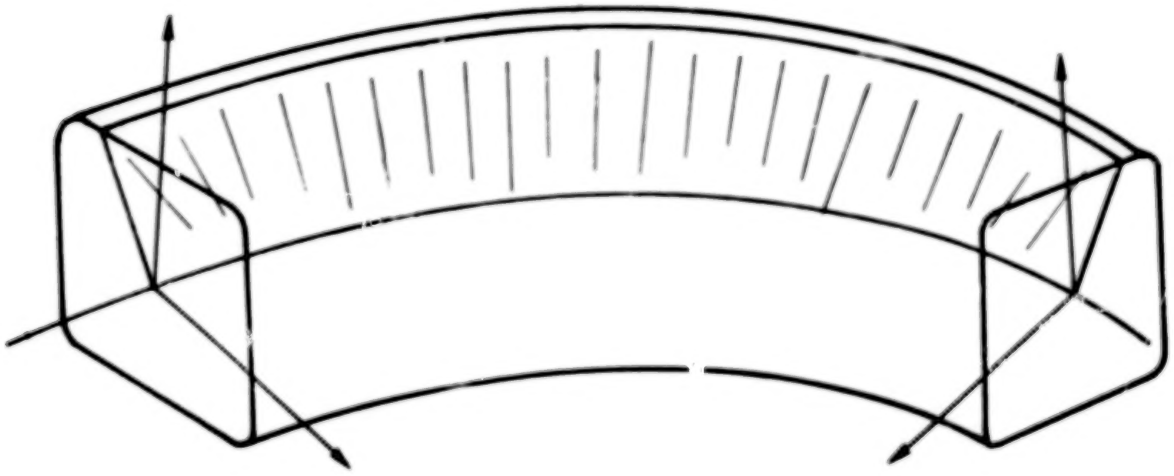

Figure 4b. Ruled Surface of Constant Pseudo–Angle y^1

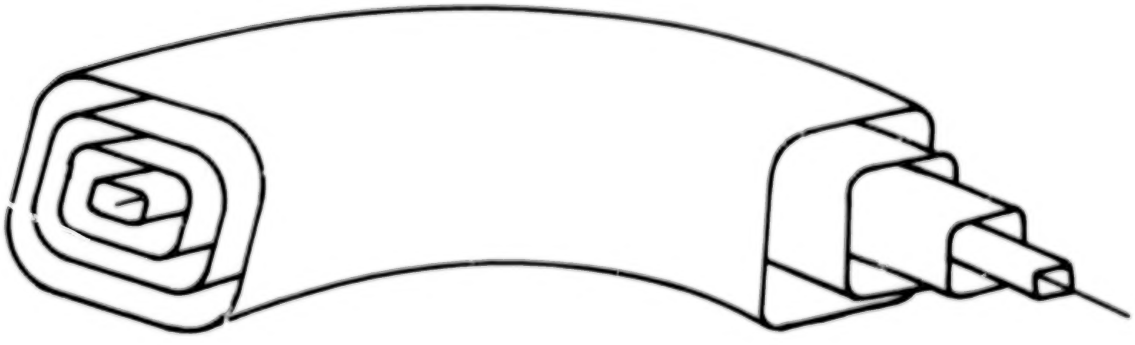

Figure 4c. Tube–Like Surfaces of Constant Pseudo–Radius y^2

78–01–128–3

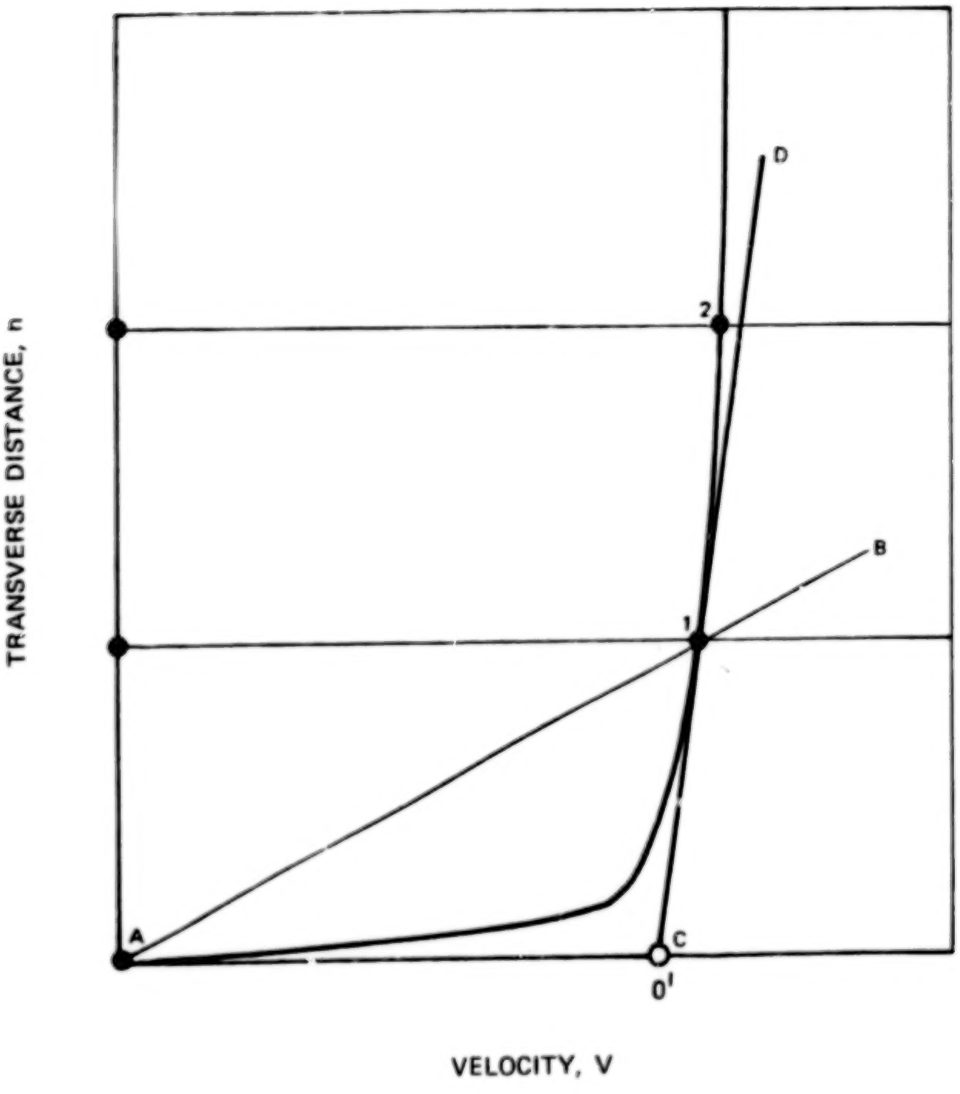

Figure 5. Schematic of Wall Function Treatment

78-01-128-6

Microfilmed From
Best Available Copy

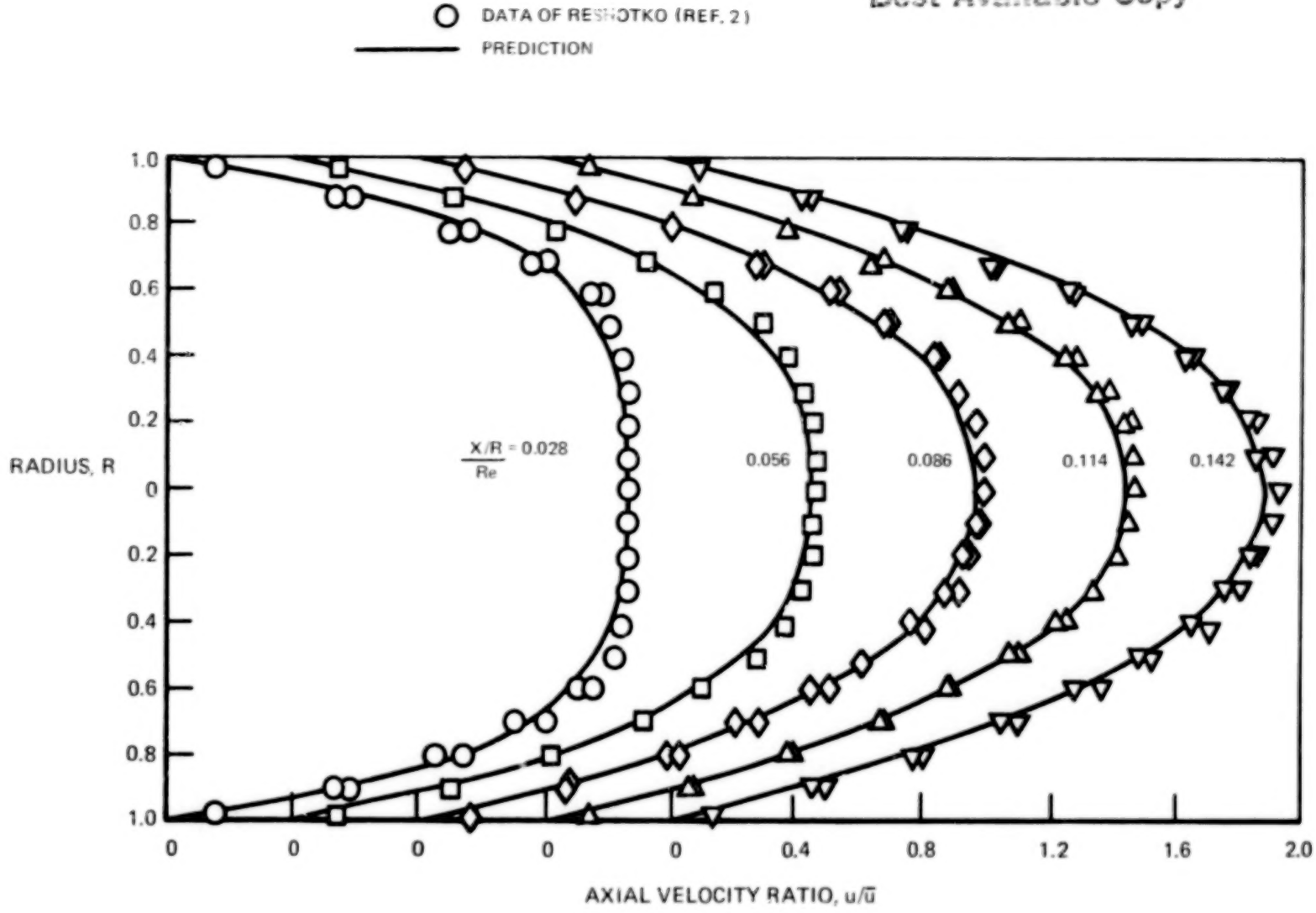

Figure 6. Velocity Profiles in the Entrance Region of a Circular Pipe

78-01-125-7

Microfilmed From
Best Available Copy

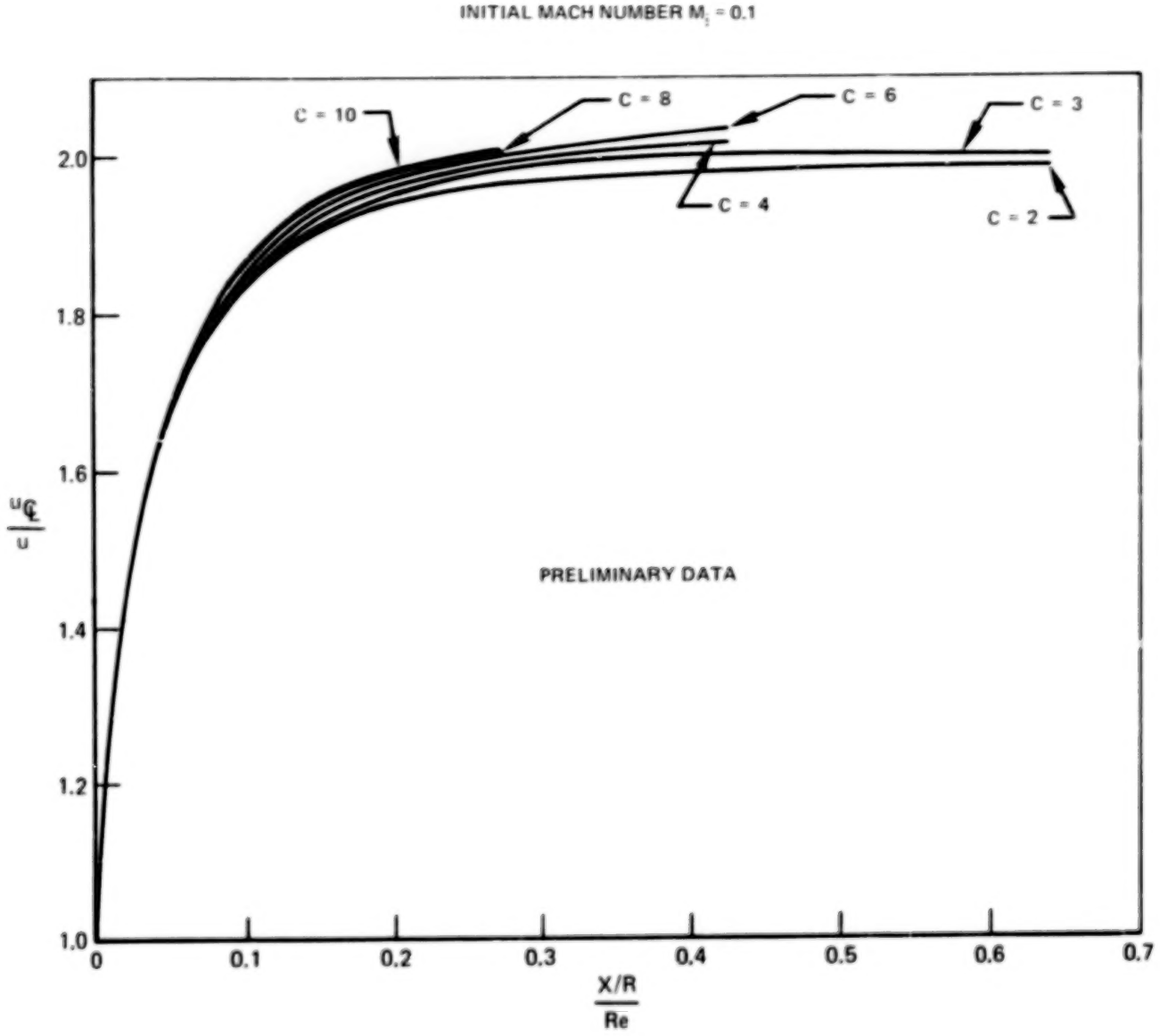

Figure 7. Effect of Superelliptic Exponent on Centerline Velocity Ratio

Microfilmed From
Best Available Copy

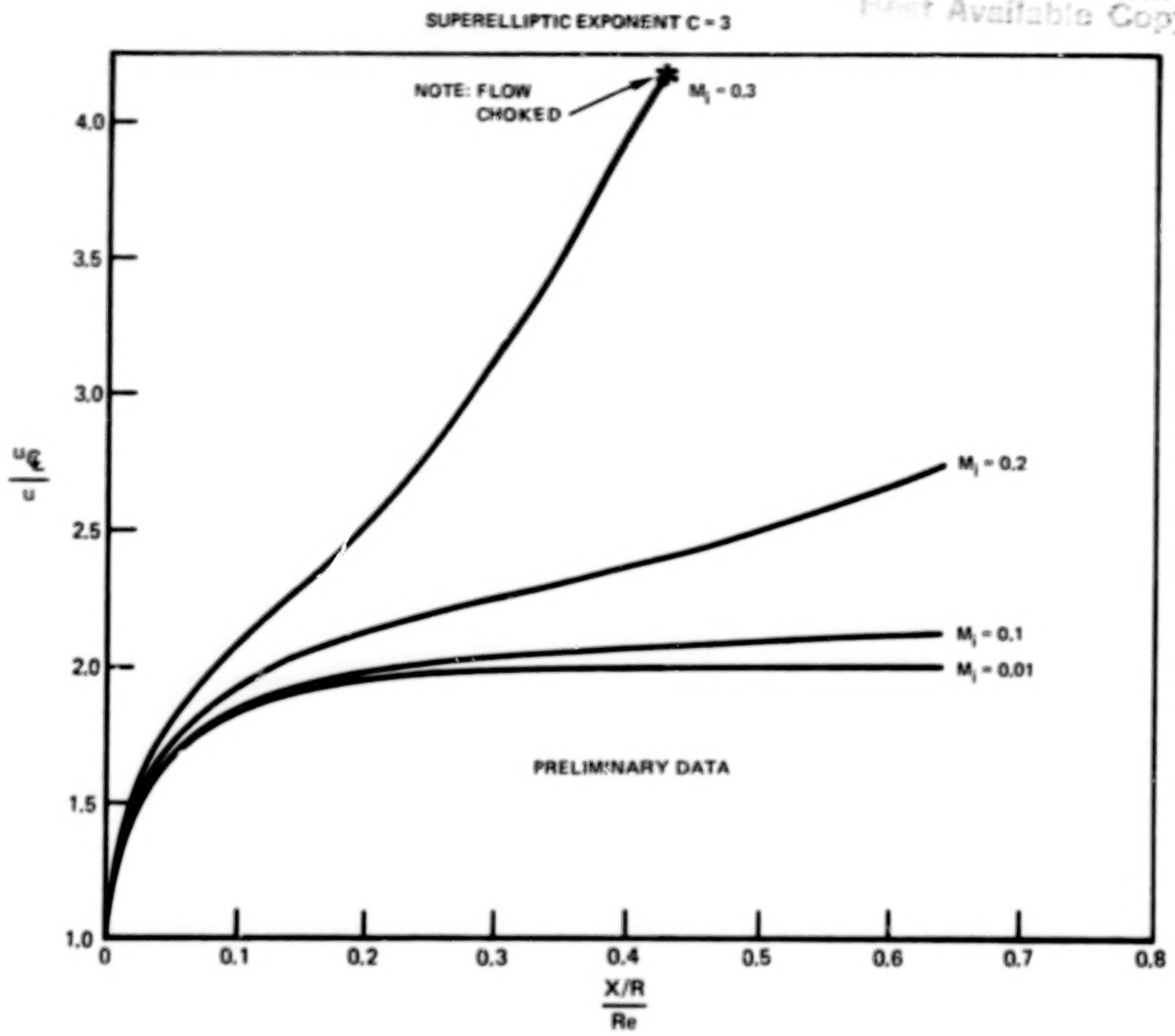

Figure 8. Effect of Mach Number on Centerline Velocity Ratio

78-01-128-2

Microfilmed From
Best Available Copy

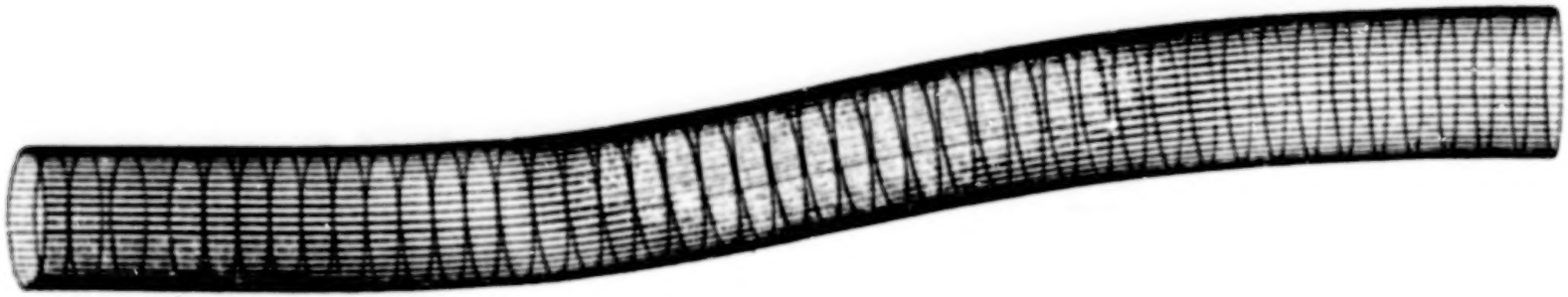

Figure 9. S–Shaped Bend with Circular Cross Section

(FLOW LEFT TO RIGHT)

Microfilmed From
Best Available Copy

SCALE: VMAX = 10.-03 ——→
STATION NO. 5 READ AT (.0000 .0000 .2475+01)

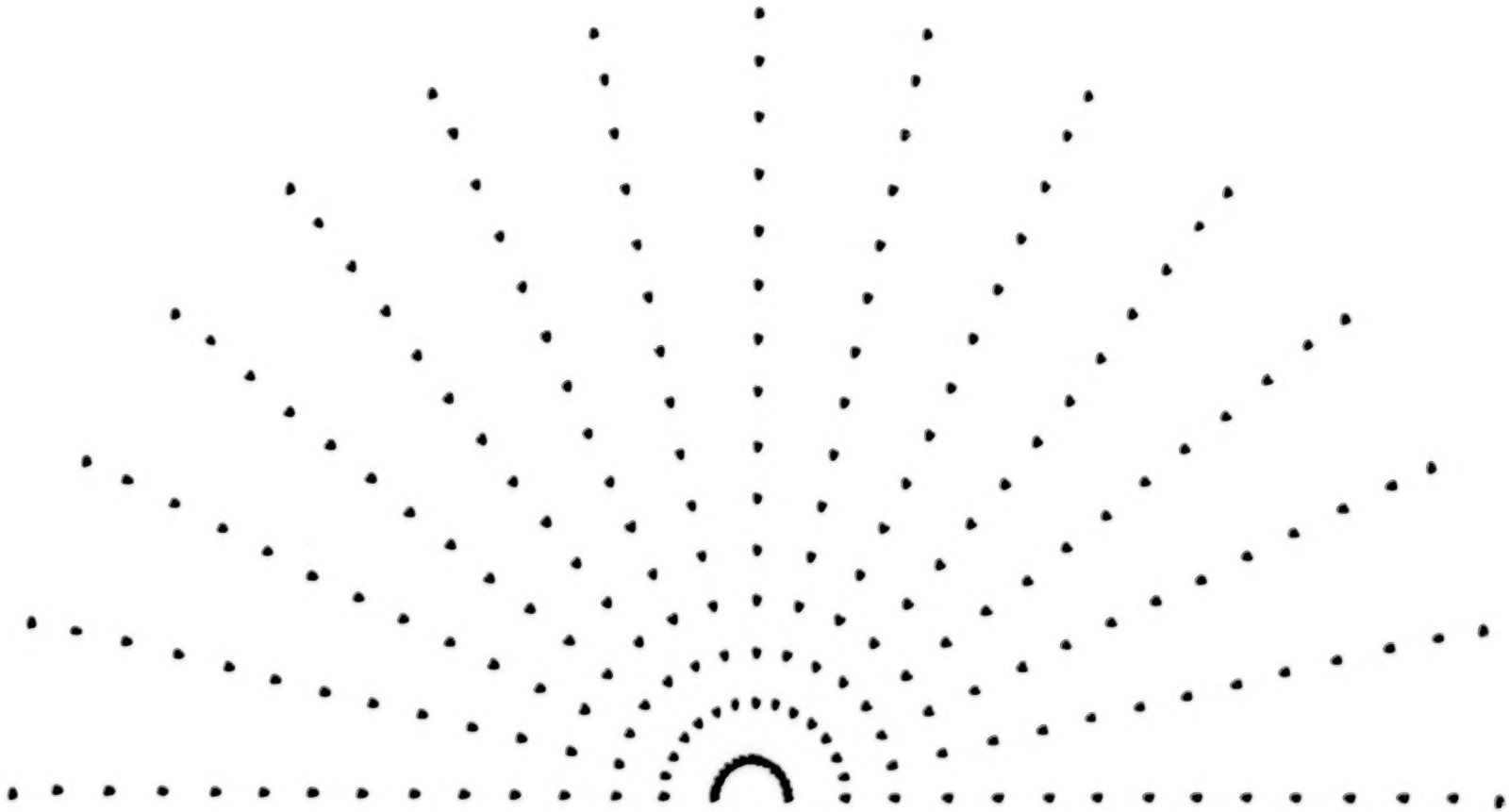

78-01-128-12

Figure 10a. – Cross Flow Velocity Vector in a Curved Circular Duct
,Sta. No. 5

Microfilmed From
Best Available Copy

SCALE: VMAX = 10.-03 ——→
STATION NO. 6 READ AT (.0000 .0000 .2475+01)

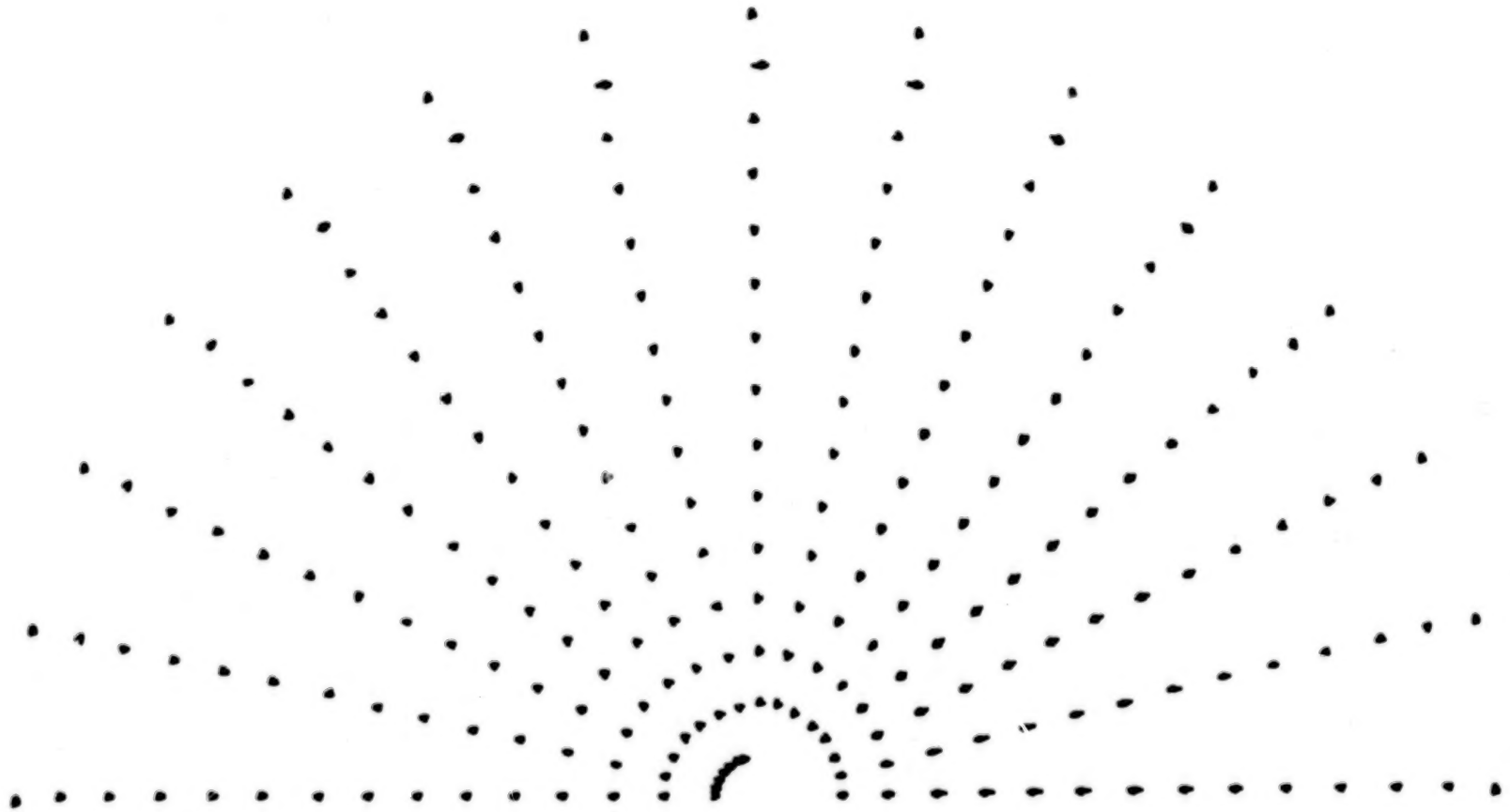

78-01-128-13

Figure 10b. – Cross Flow Velocity Vector in a Curved Circular Duct
, Sta. No. 6

Microfilmed From
Best Available Copy

SCALE: VMAX = 10.-03
STATION NO. 7 READ AT (.0000 .3894-03 .1000+01)

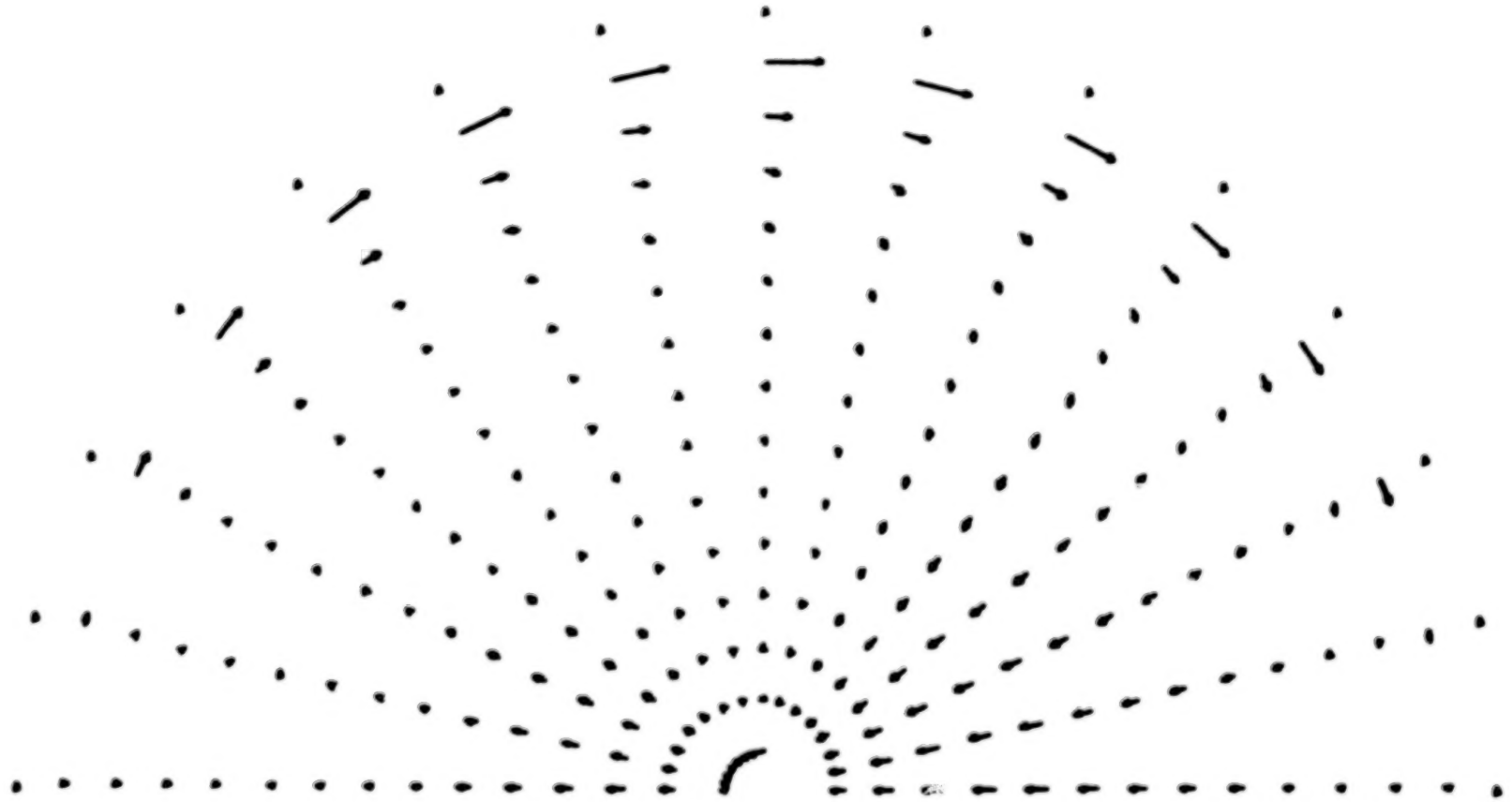

78-01-128-14

Figure 10c. – Cross Flow Velocity Vector in a Curved Circular Duct
Sta. No. 7

Microfilmed From
Best Available Copy

SCALE: VMAX = 10.-03 ——→
STATION NO. 8 READ AT (.0000 .1859-02 .1500+01)

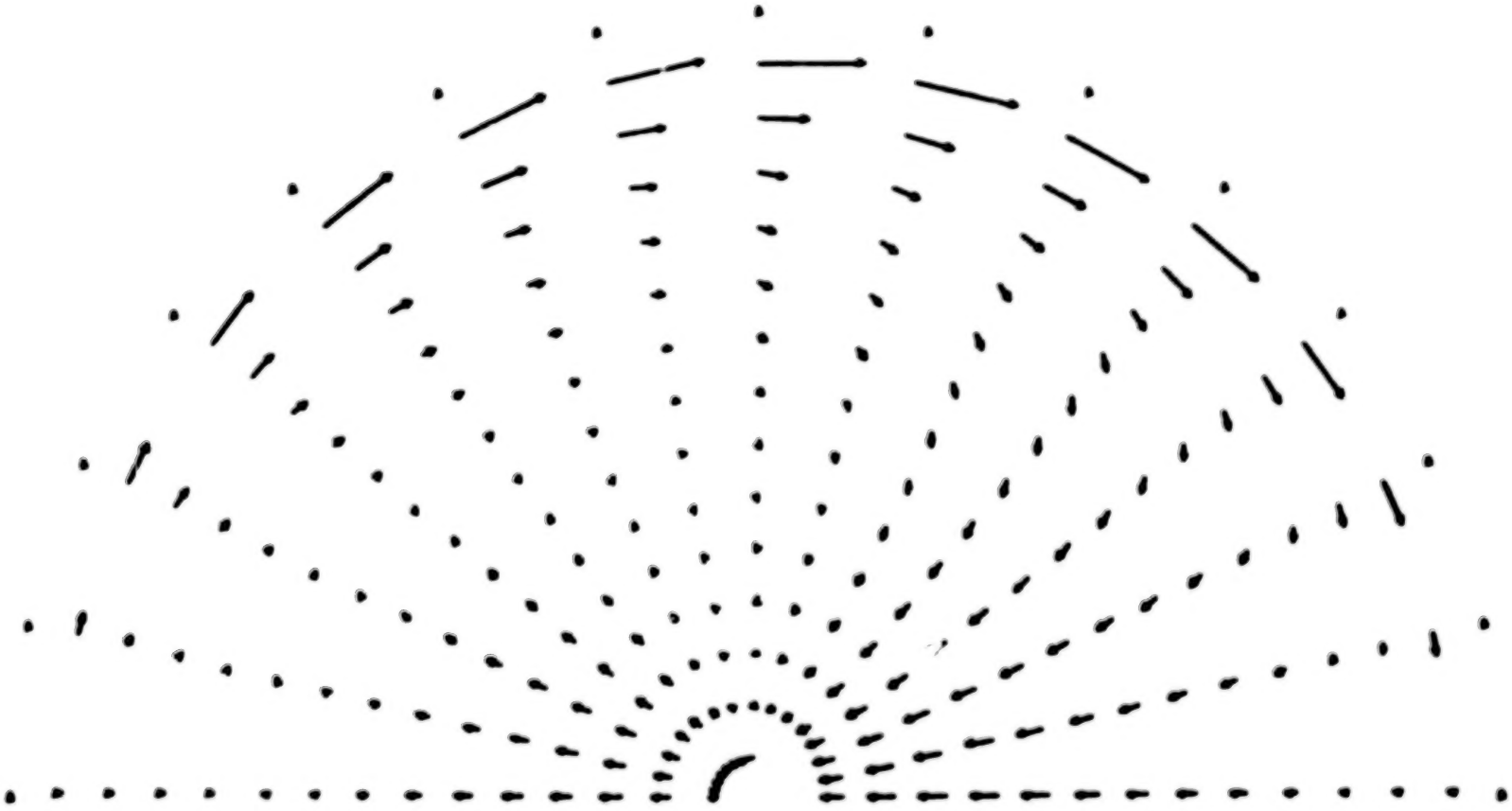

78-01-128-15

Figure 10d. Cross Flow Velocity Vector in a Curved Circular Duct
, Sta. No. 8

Microfilmed From
Best Available Copy

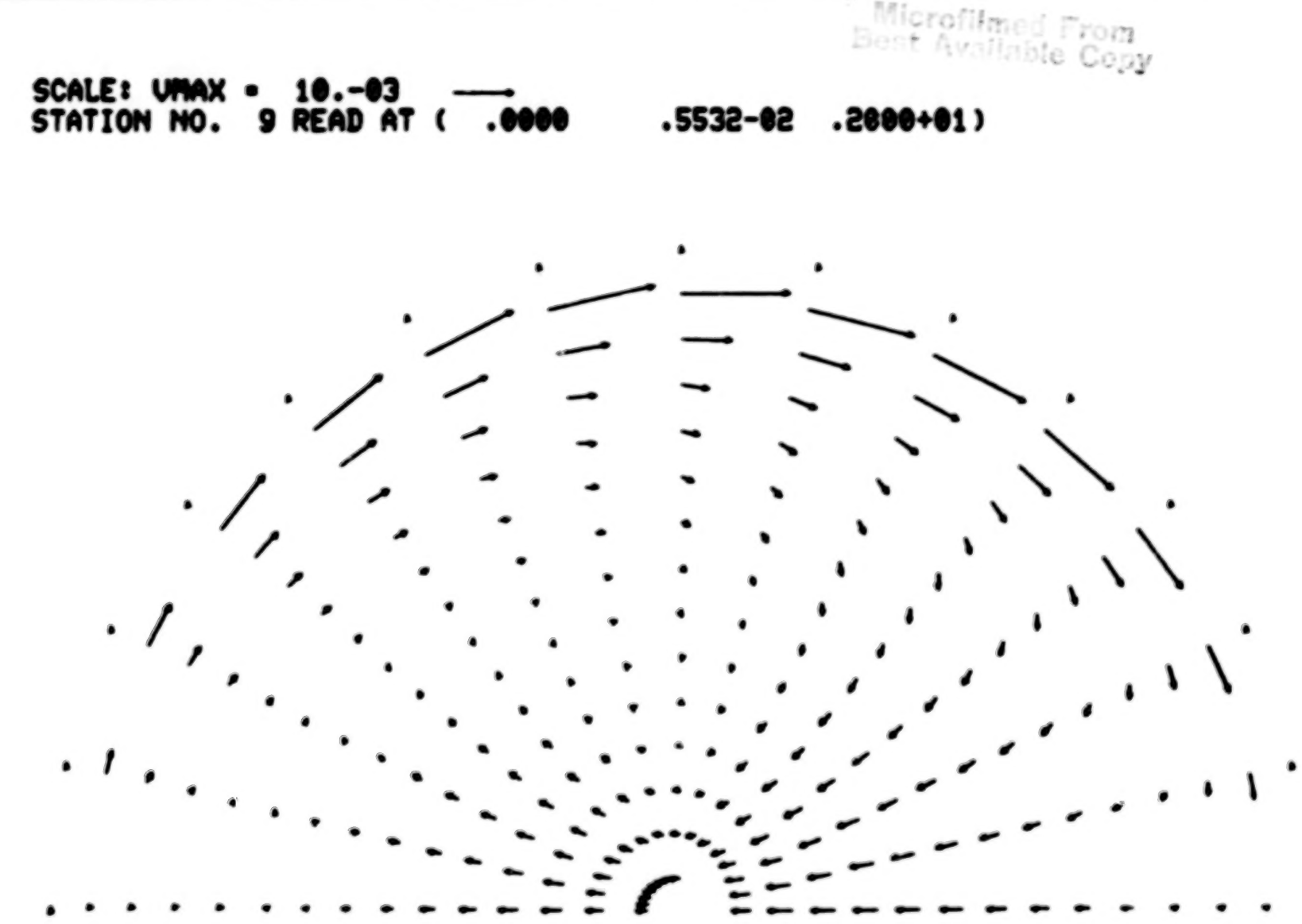

78-01-128-16

Figure 10e. – Cross Flow Velocity Vector in a Curved Circular Duct
, Sta. No. 9

Microfilmed From
Best Available Copy

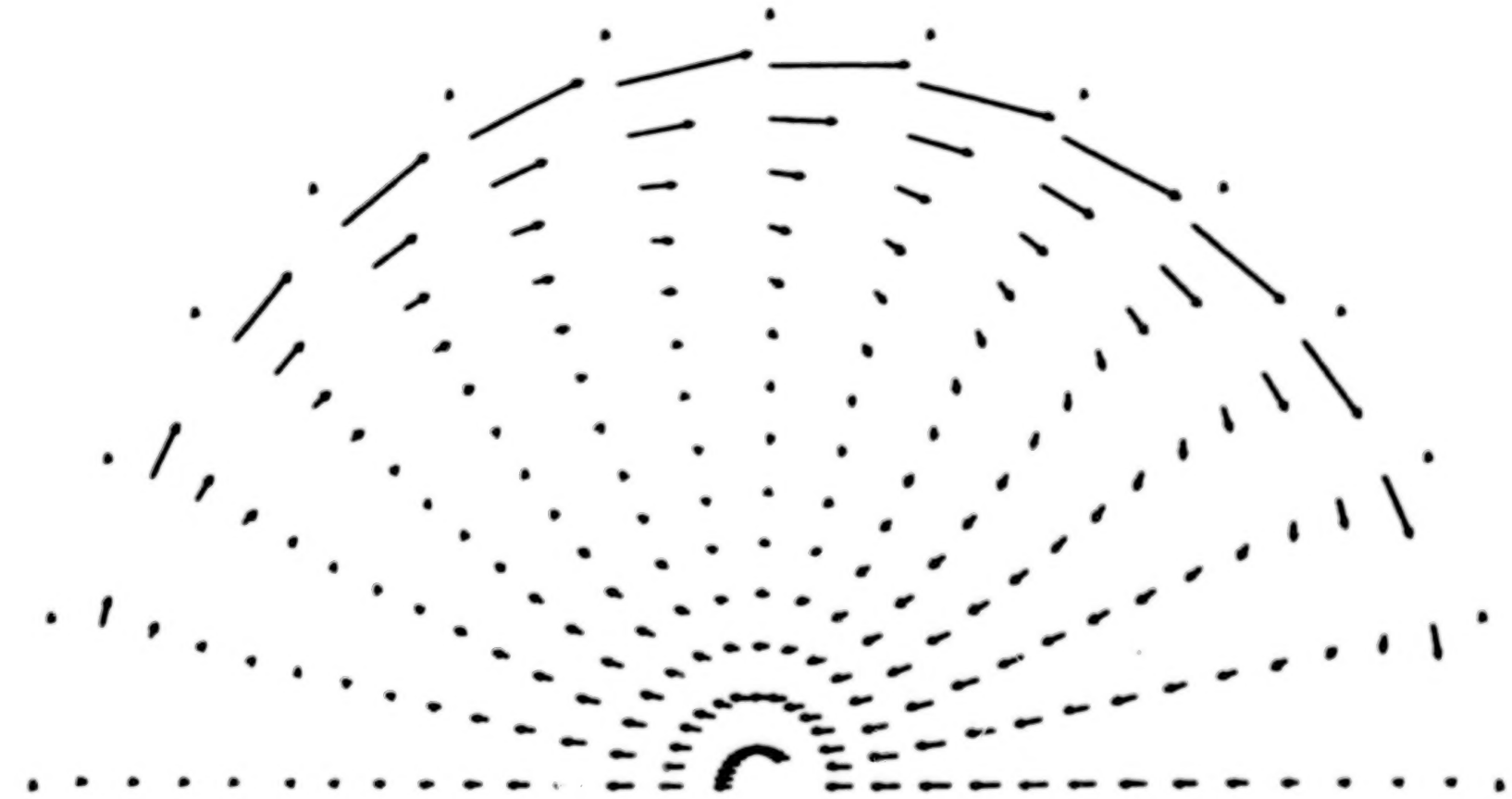

78-01-128-17

Figure 10f. – Cross Flow Velocity Vector in a Curved Circular Duct , Sta. No. 10

Microfilmed From
Best Available Copy

SCALE: VMAX = 10.-03 ——→
STATION NO. 11 READ AT (.0000 .2470-01 .3000+01)

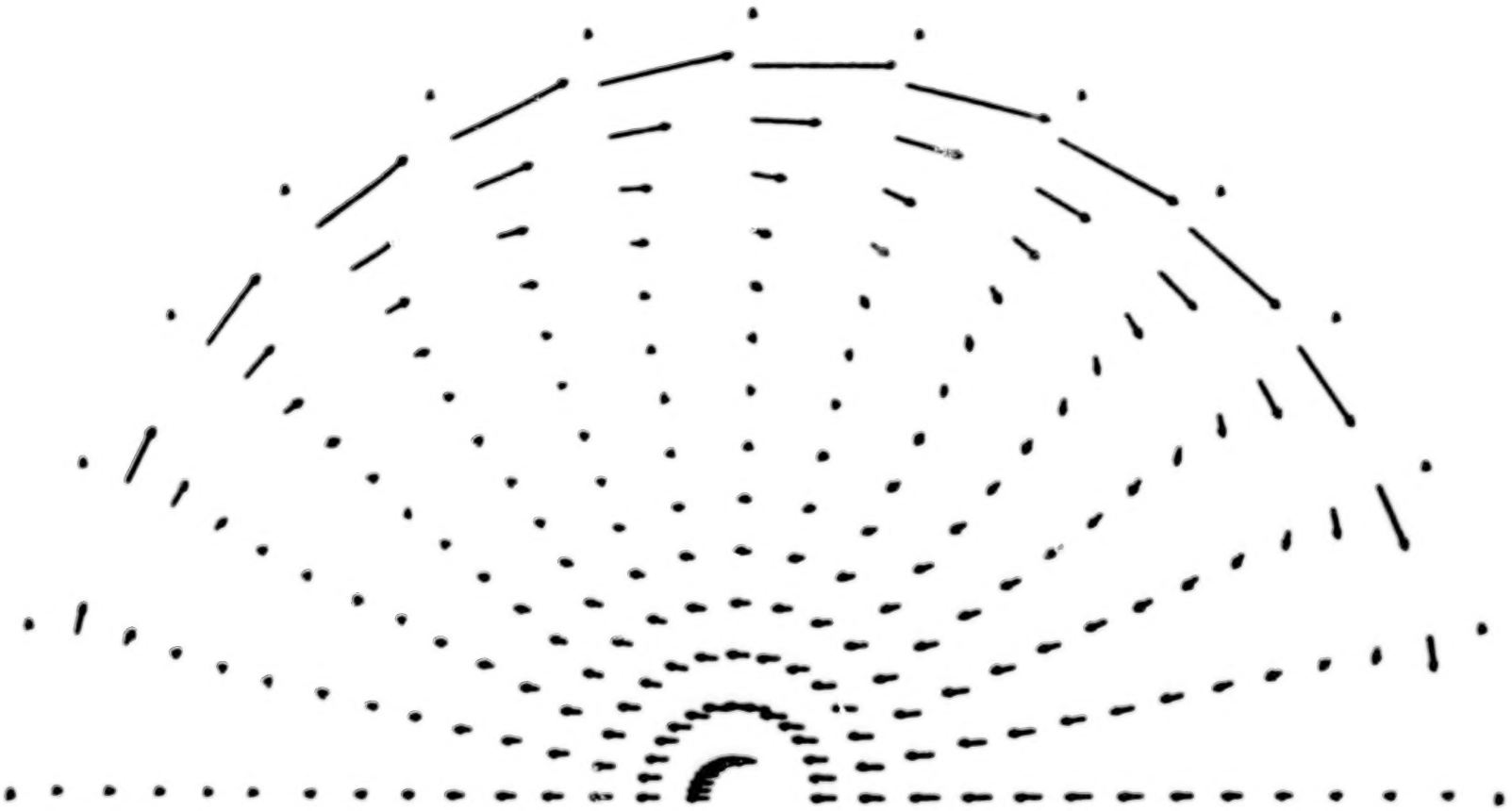

Figure 10g. – Cross Flow Velocity Vector in a Curved Circular Duct
, Sta. No. 11

Microfilmed From
Best Available Copy

SCALE: VMAX = 10.-03 ——
STATION NO. 12 READ AT (.0000 .4286-01 .3500+01)

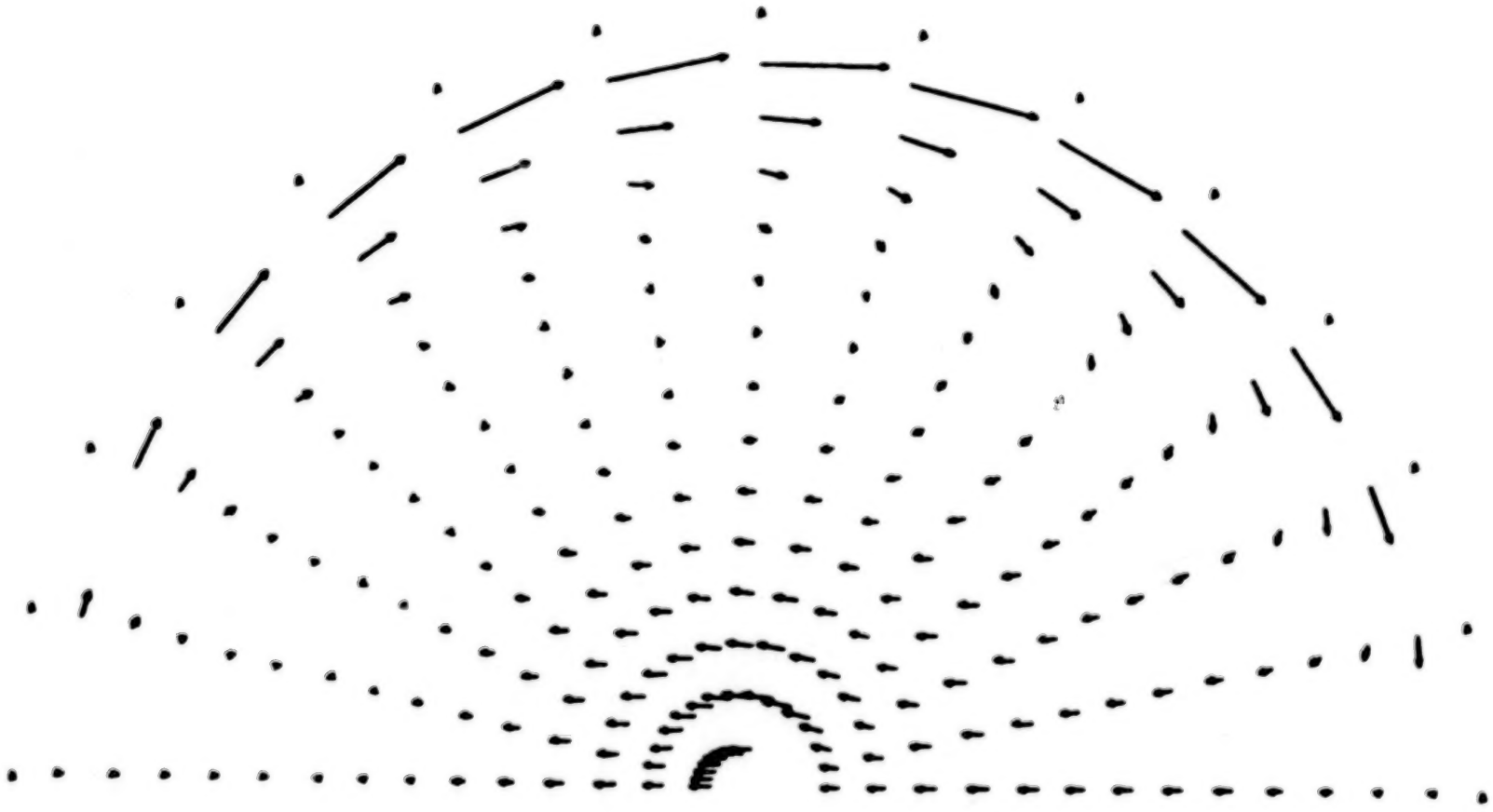

78-01-128-19

Figure 10h. – Cross Flow Velocity Vector in a Curved Circular Duct
, Sta. No. 12

Microfilmed From
Best Available Copy

SCALE: VMAX = 10.-03
STATION NO. 13 READ AT (.0000 .6836-01 .4000+01)

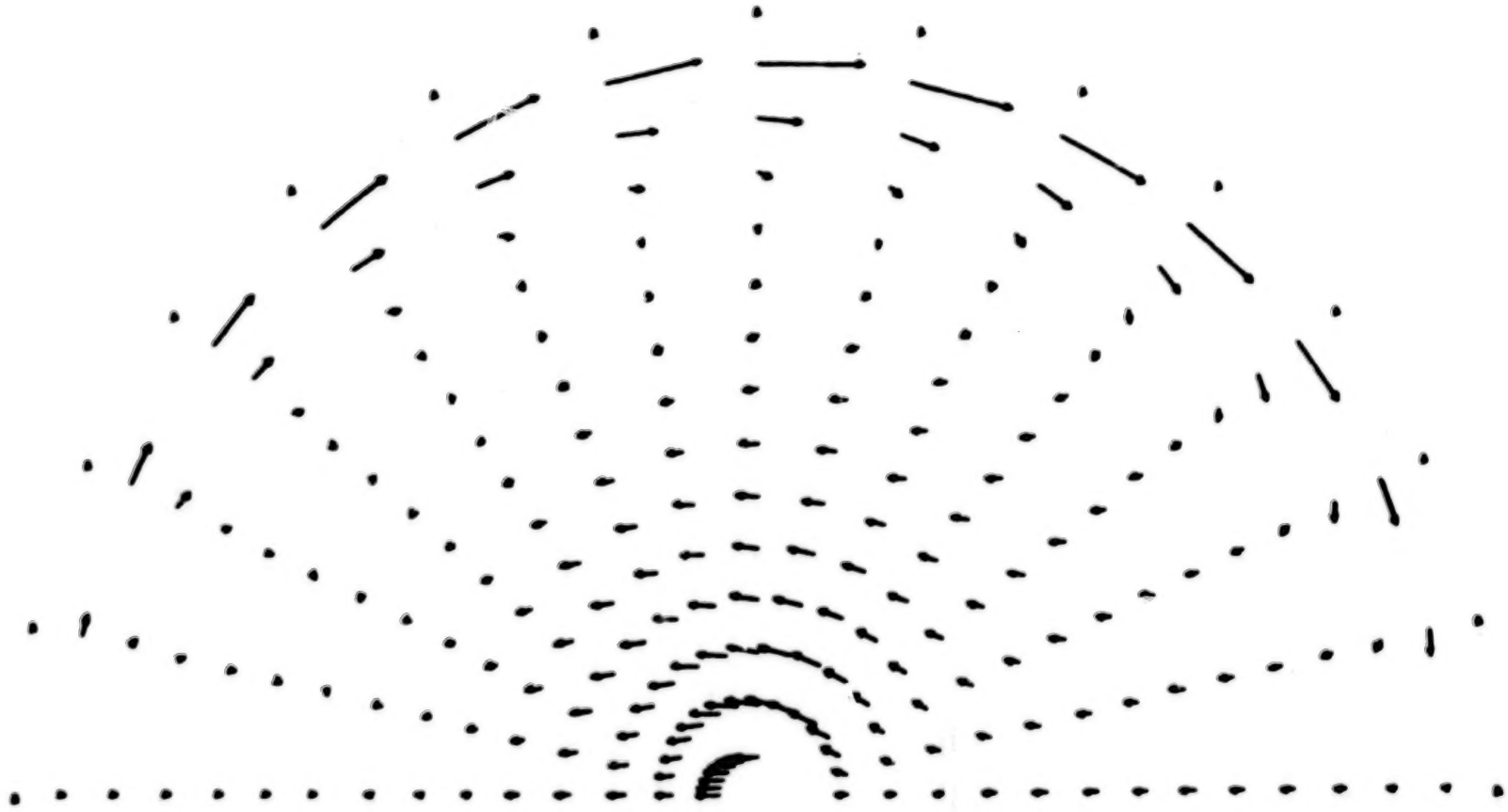

78-01-128-20

Figure 10i. – Cross Flow Velocity Vector in a Curved Circular Duct
, Sta. No. 13

Microfilmed From
Best Available Copy

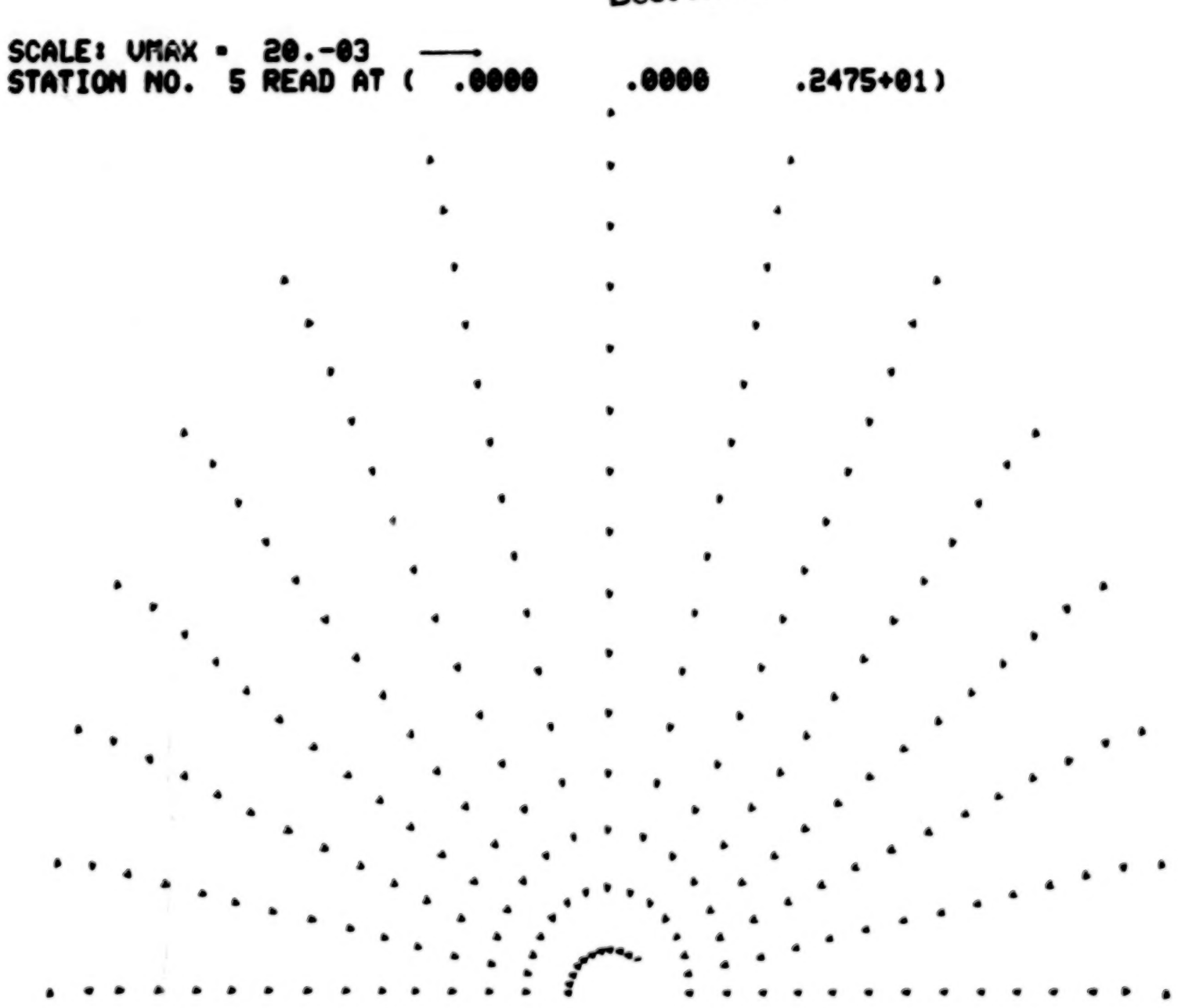

Figure 11a. – Cross Flow Velocity in a Curved Elliptic Duct, Shape = 0.667
,Sta. No. 5

78-01-128-21

Microfilmed From
Best Available Copy

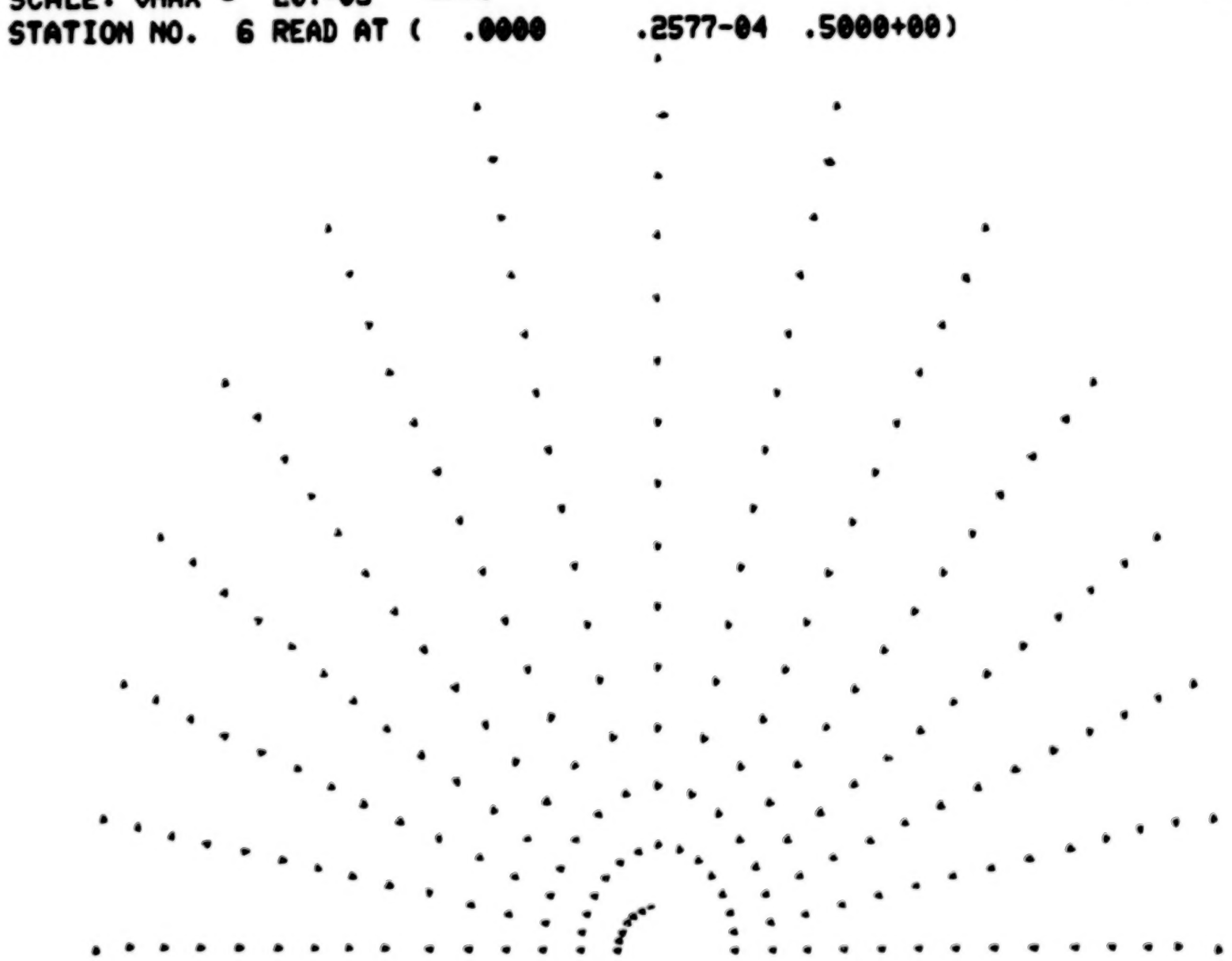

78-01-128-22

Figure 11b. — Cross Flow Velocity in a Elliptic Duct, Shape = 0.667
, Sta. No. 6

Microfilmed From
Best Available Copy

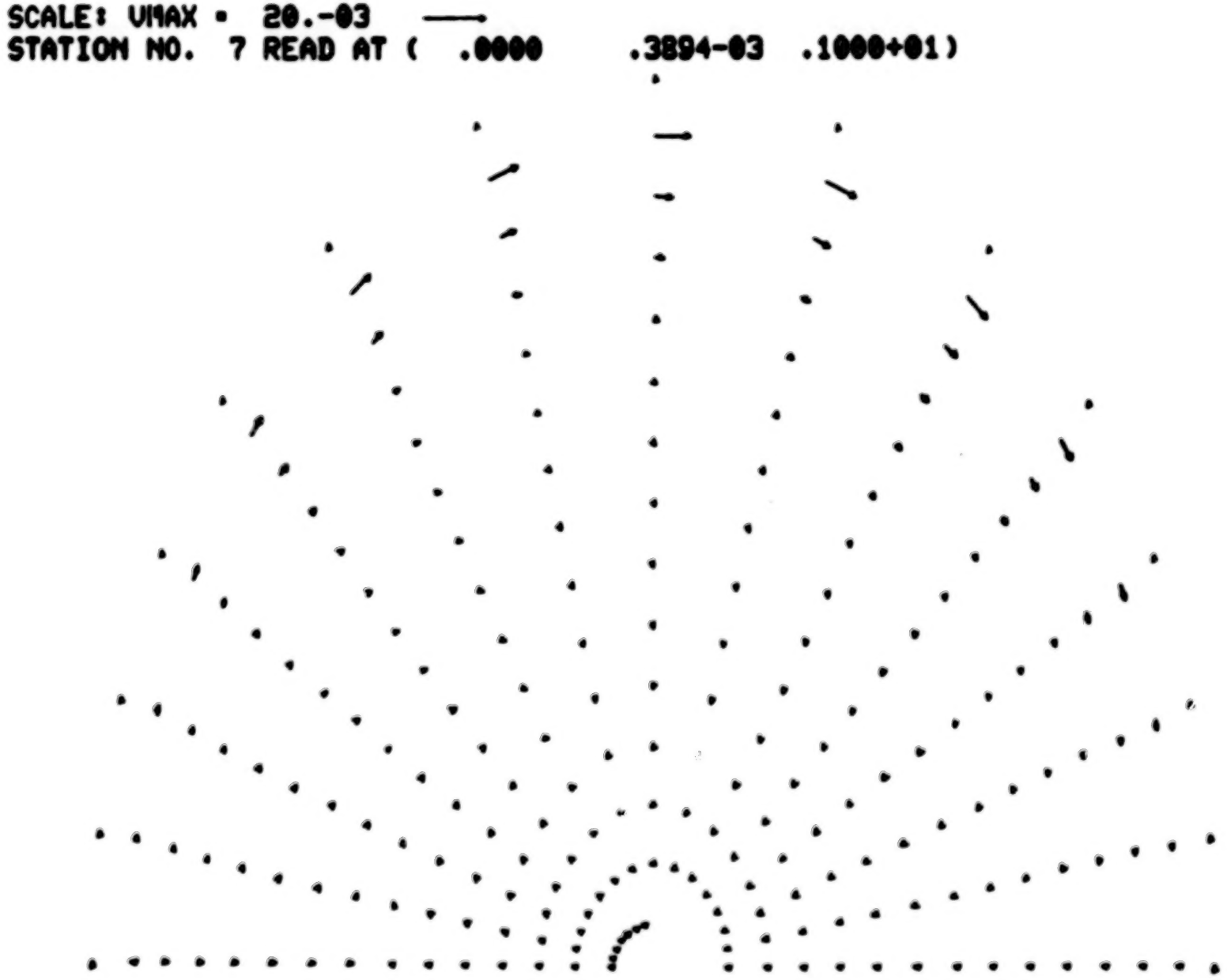

78-01-128-23

Figure 11c. – Cross Flow Velocity in a Curved Elliptic Duct, Shape = 0.667
, Sta. No. 7

Microfilmed From
Best Available Copy

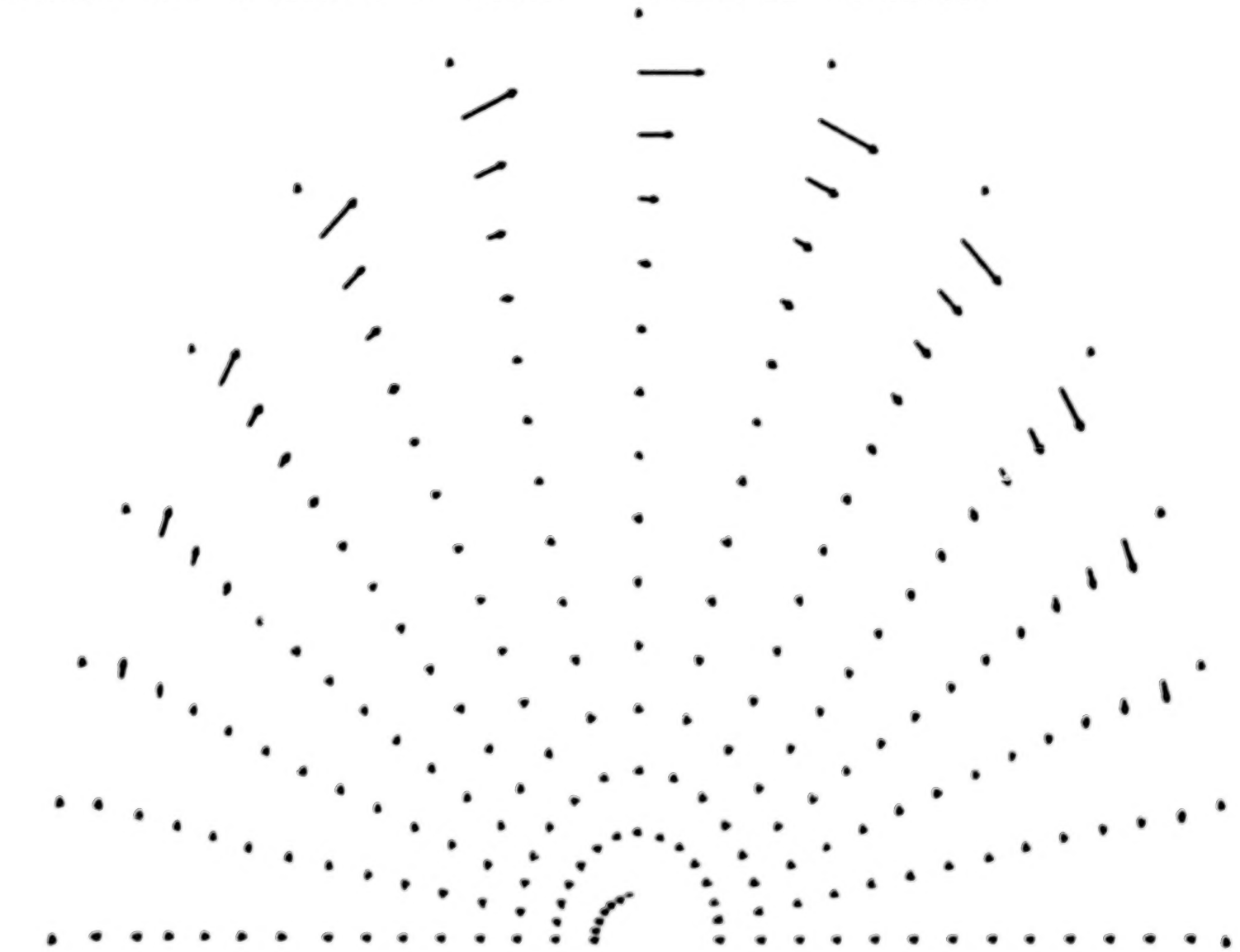

78-01-128-24

Figure 11d. – Cross Flow Velocity in a Curved Elliptic Duct, Shape = 0.667
, Sta. No. 8

Microfilmed From
Best Available Copy

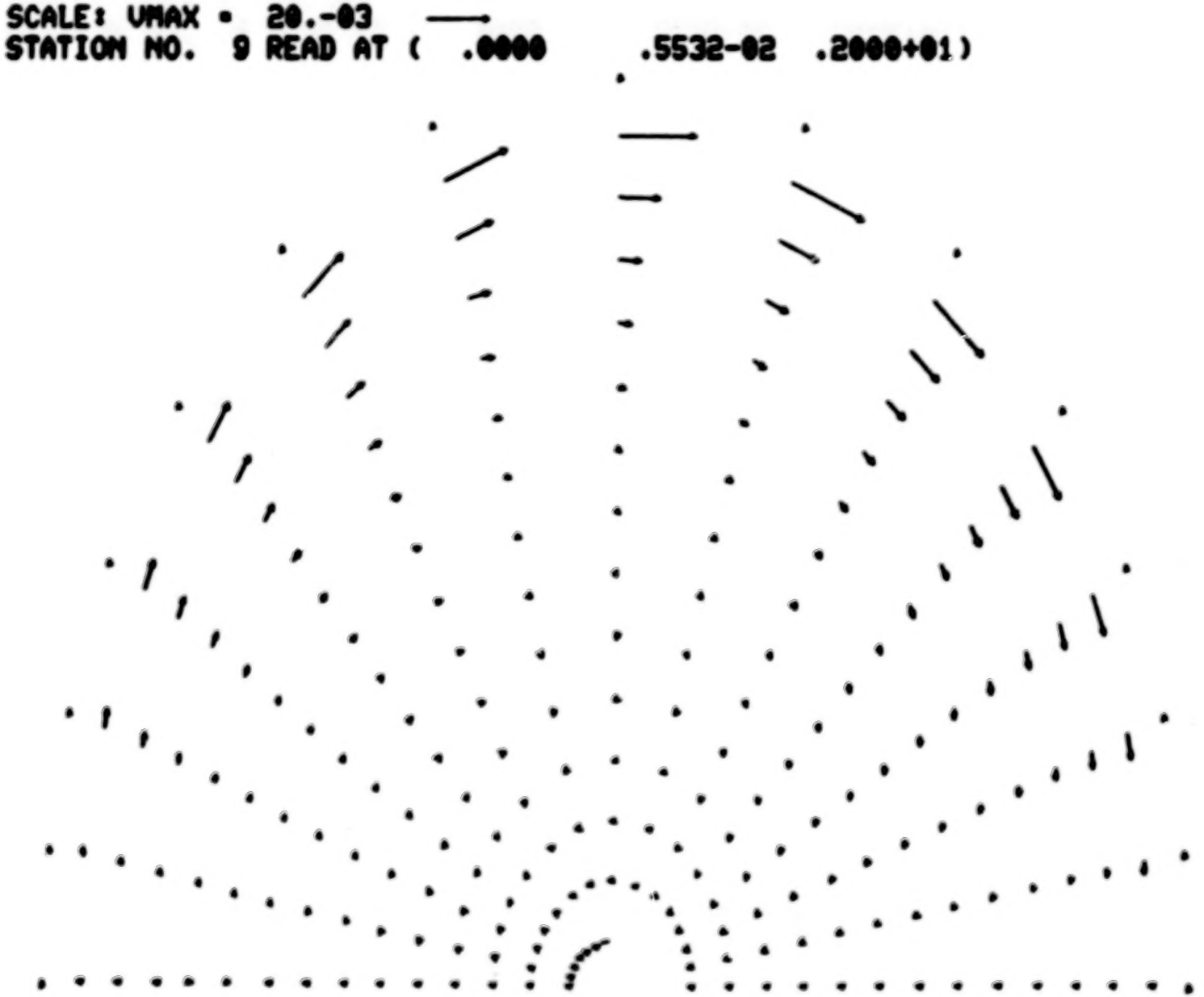

Figure 11e. – Cross Flow Velocity in a Curved Elliptic Duct, Shape = 0.667
, Sta. No. 9

78-01-128-26

Microfilmed From
Best Available Copy

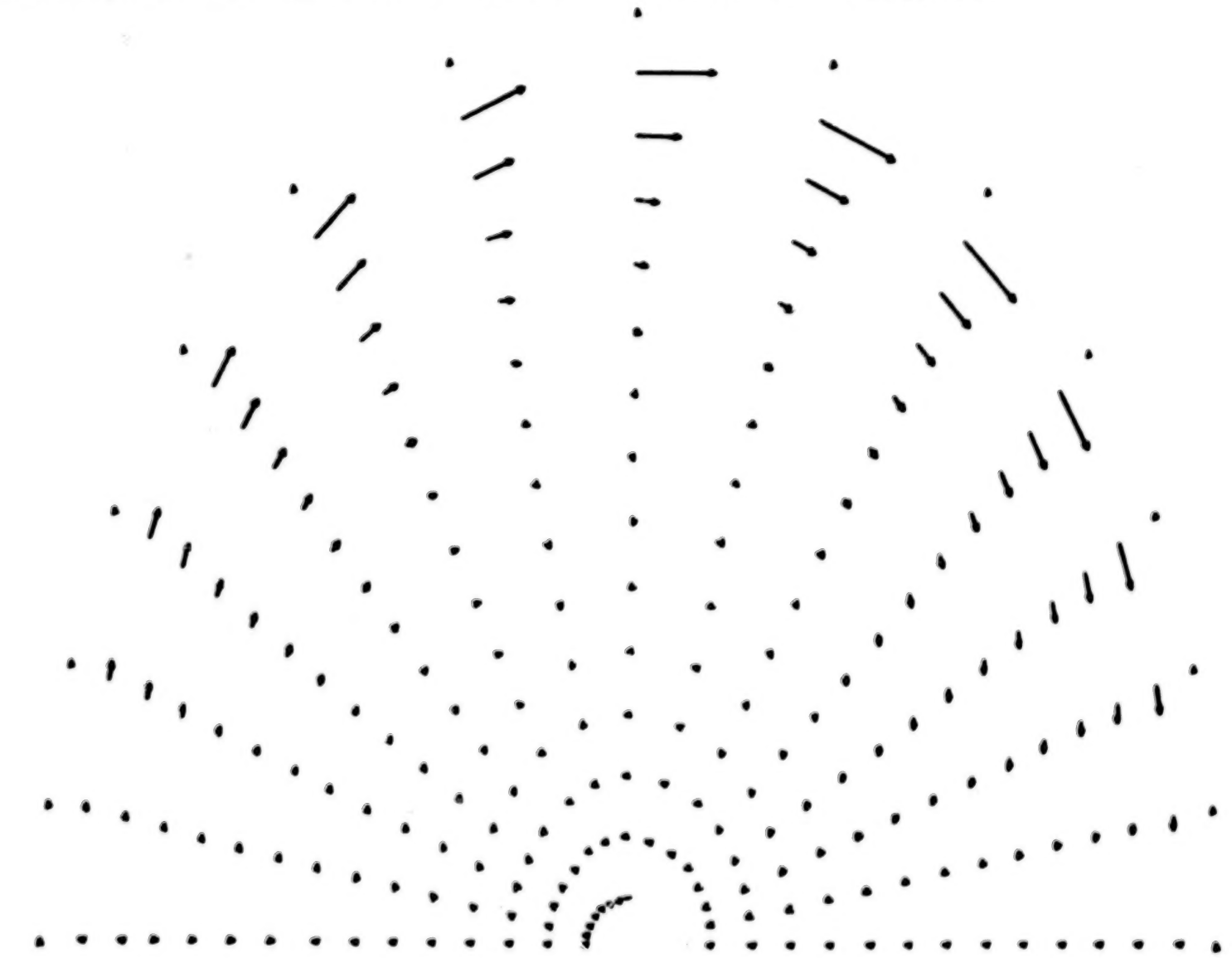

78-01-128-26

Figure 11f. – Cross Flow Velocity in a Curved Elliptic Duct, Shape = 0.667
, Sta. No. 10

Microfilmed From
Best Available Copy

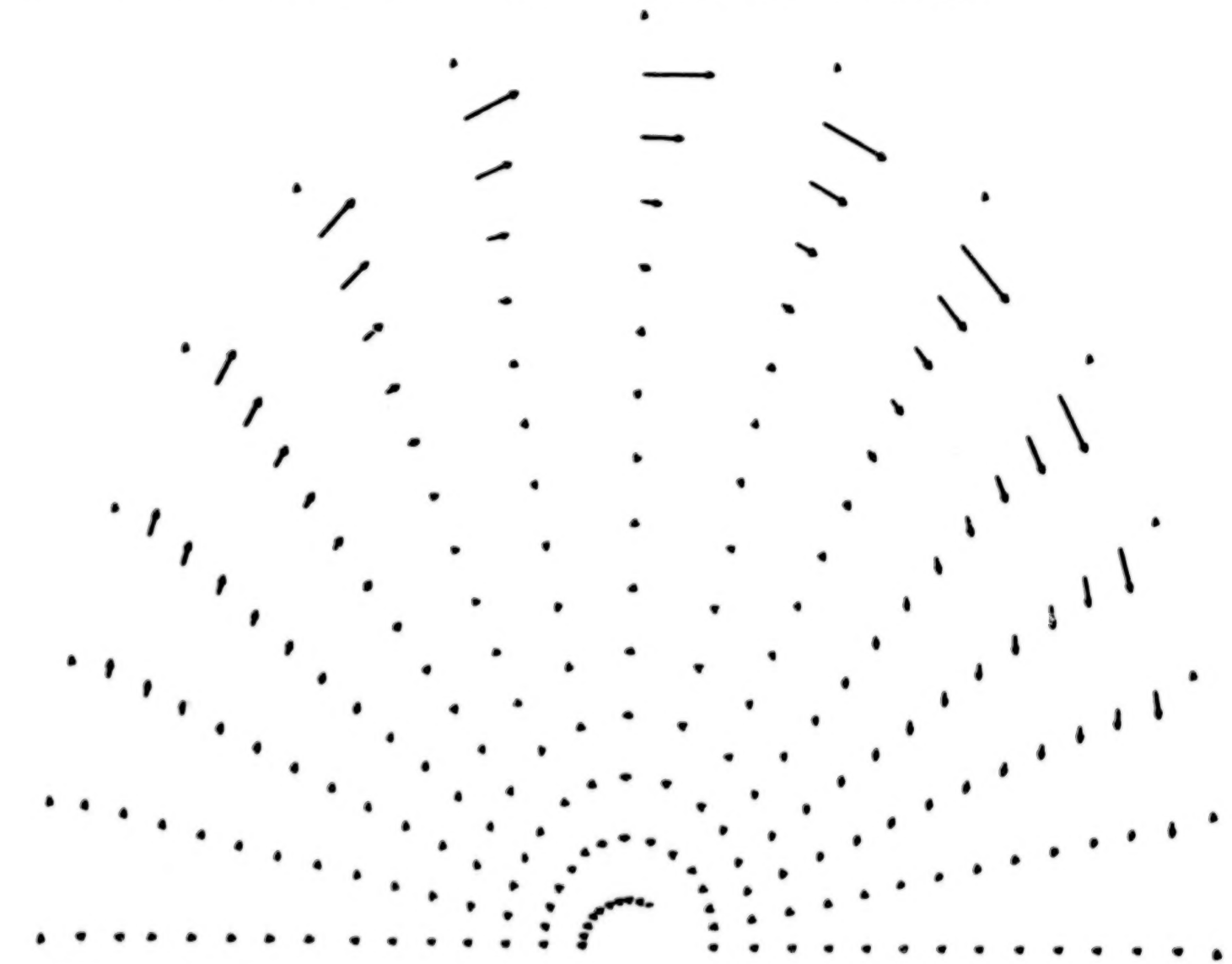

78-01-128-27

Figure 11g. – Cross Flow Velocity in a Curved Elliptic Duct, Shape = 0.667
, Sta. No. 11

Microfilmed From
Best Available Copy

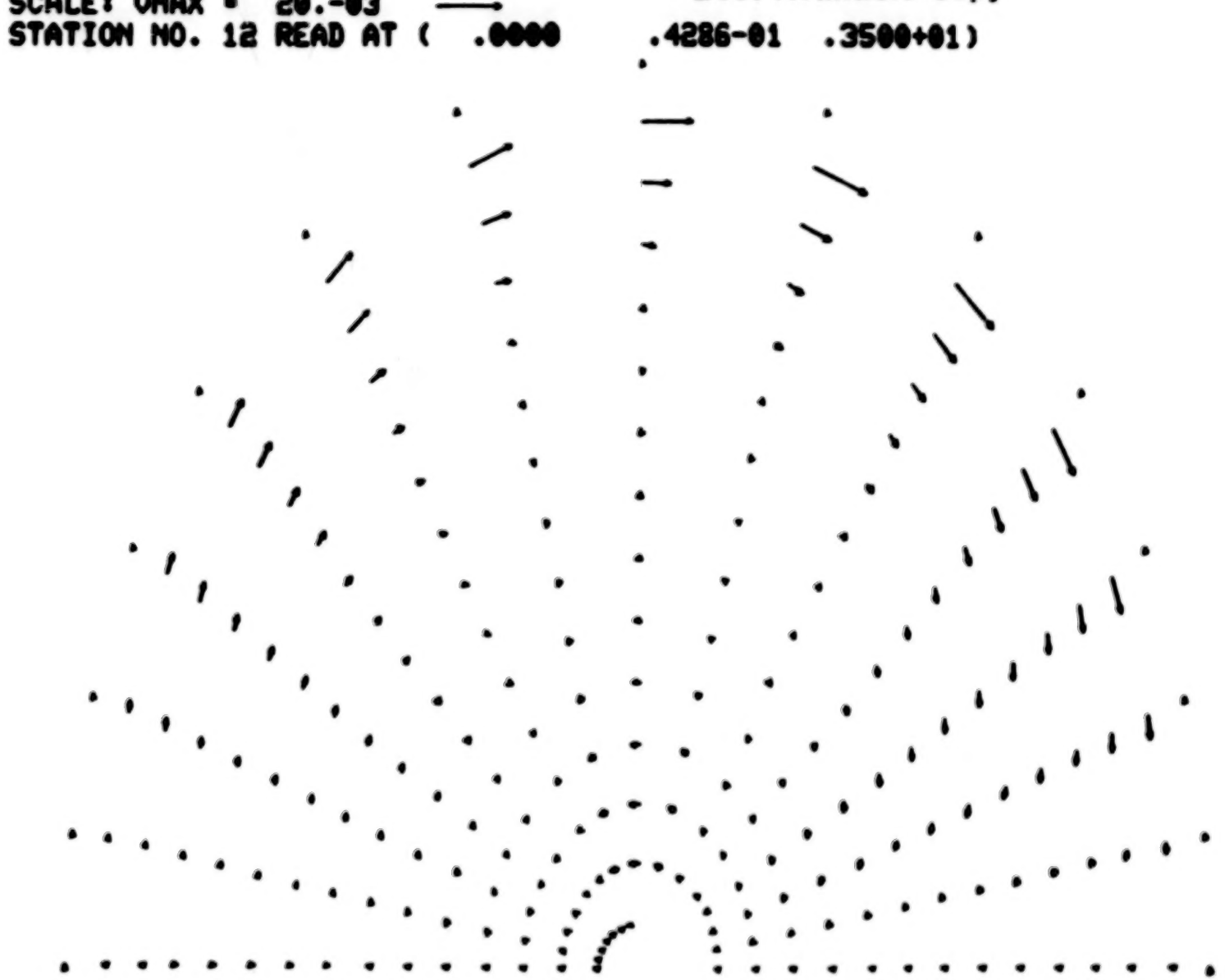

78-01-128-29

Figure 11h. – Cross Flow Velocity in a Curved Elliptic Duct, Shape = 0.667
, Sta. No. 12

Microfilmed From
Best Available Copy

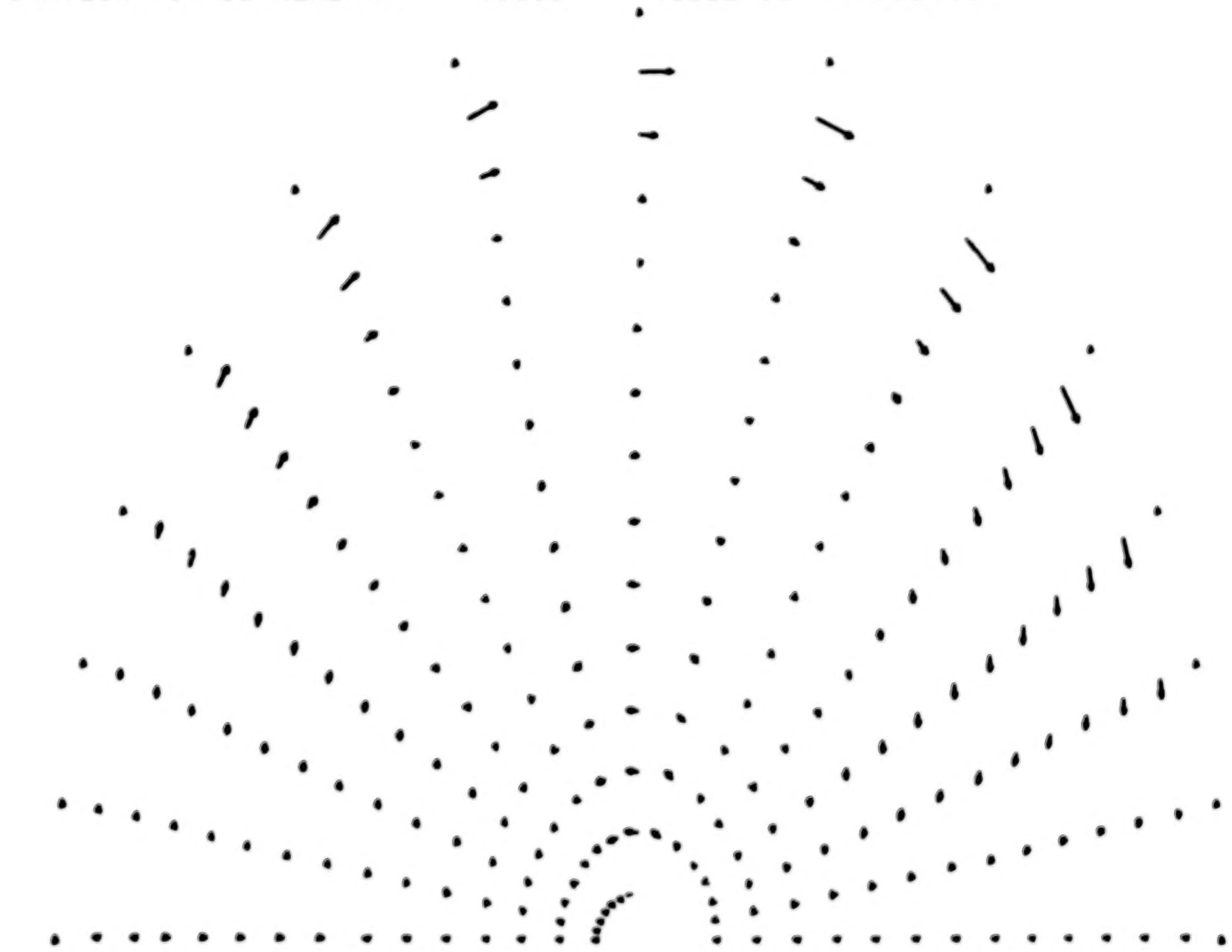

78-01-128-35

Figure 11i. — Cross Flow Velocity in a Curved Elliptic Duct, Shape = 0.667
, Sta. No. 13

Microfilmed From
Best Available Copy

SCALE: VMAX = 20.-03 ——→
STATION NO. 5 READ AT (.0000 .0000 .2475+01)

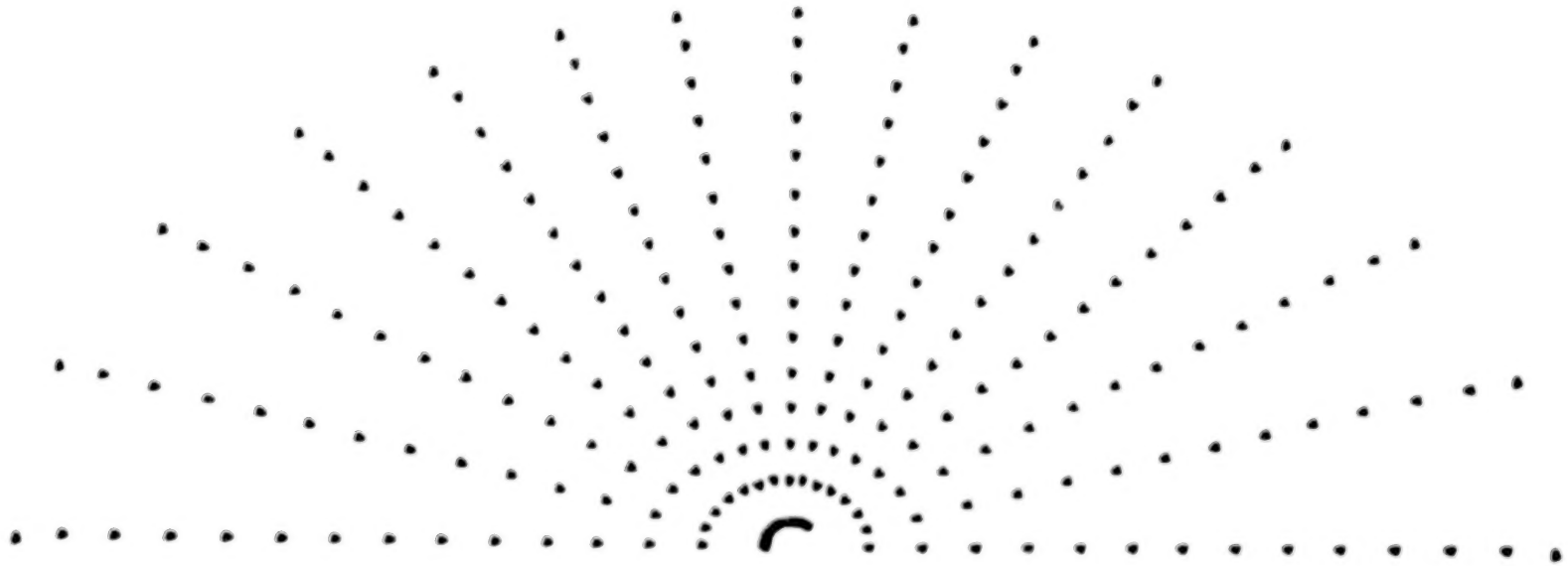

78-01-128-34

Figure 12a. – Cross Flow Velocity in a Curved Elliptic Duct, Shape = 1.5 , Sta. No. 5

Microfilmed From
Best Available Copy

SCALE: VMAX = 20.-03 ——→
STATION NO. 6 READ AT (.0000 .2577-04 .5000+00)

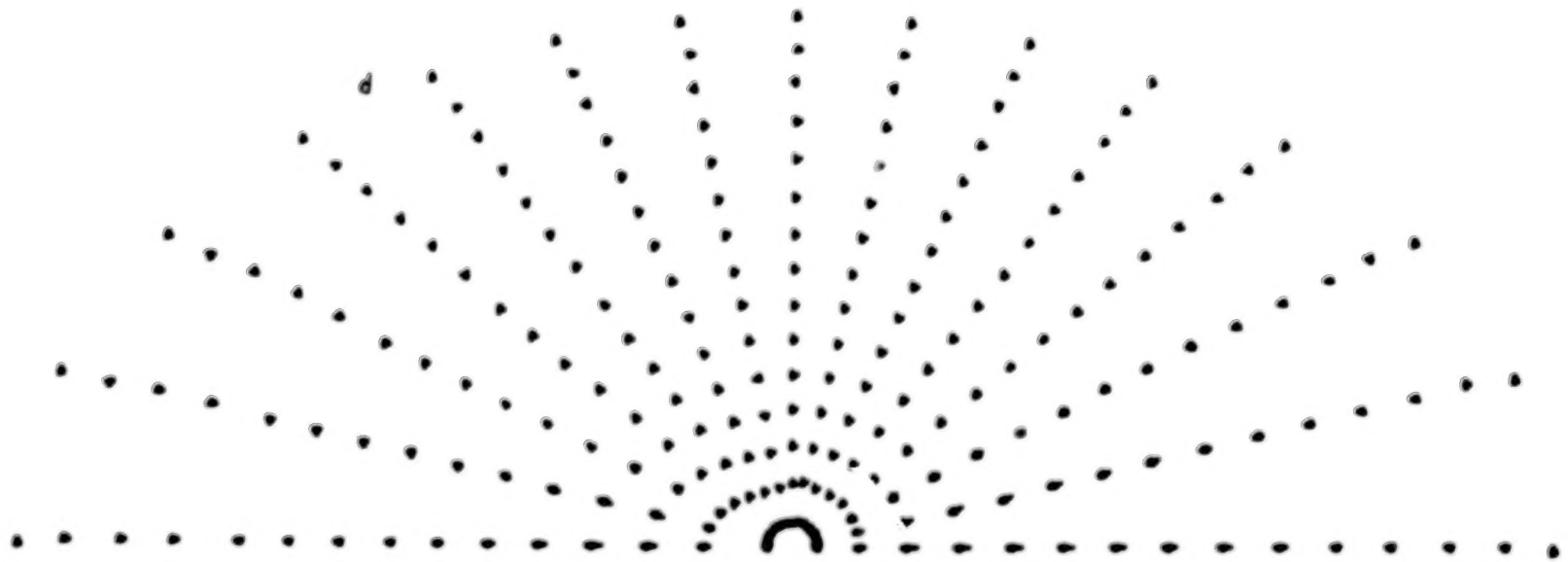

Figure 12b. – Cross Flow Velocity in a Curved Elliptic Duct, Shape = 1.5
, Sta. No. 6

Microfilmed From
Best Available Copy

SCALE: VMAX = 20.-03 ——→
STATION NO. 7 READ AT (.0000 .3894-03 .1000+01)

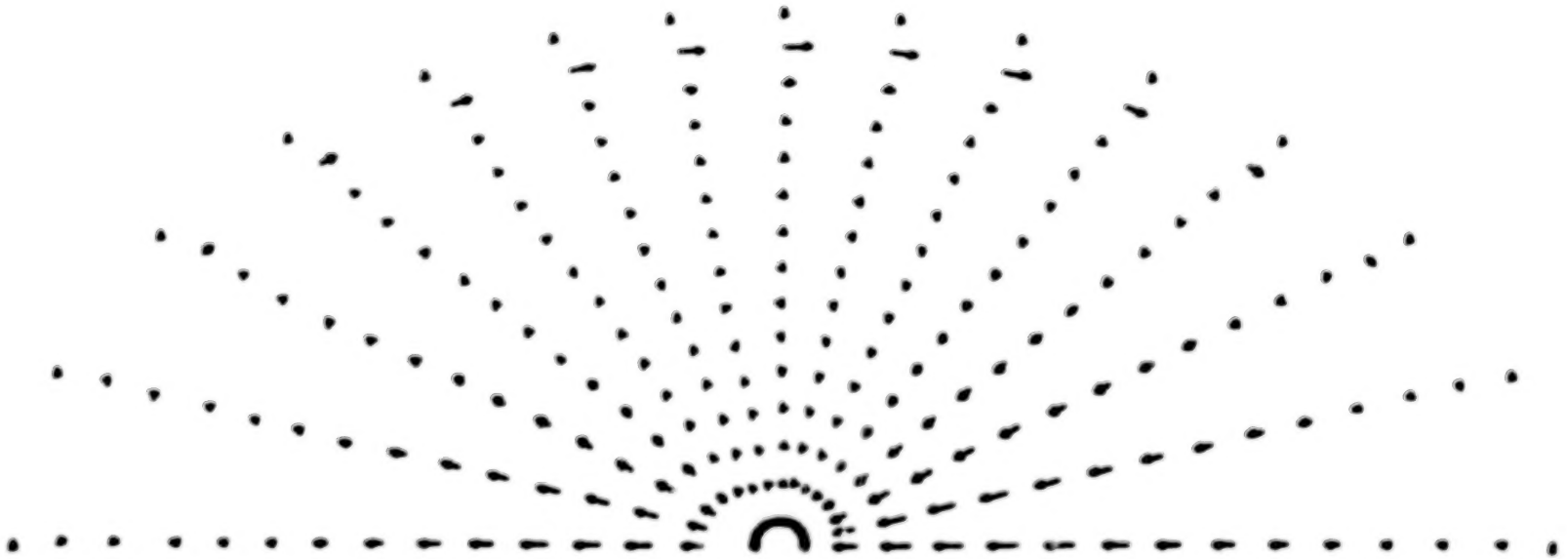

76-01-128-32

Figure 12c. Cross Flow Velocity in a Curved Elliptic Duct, Shape = 1.5
, Sta. No. 7

Microfilmed From
Best Available Copy

SCALE: VMAX = 20.-03 ——→
STATION NO. 8 READ AT (.6900 .1859-02 .1500+01)

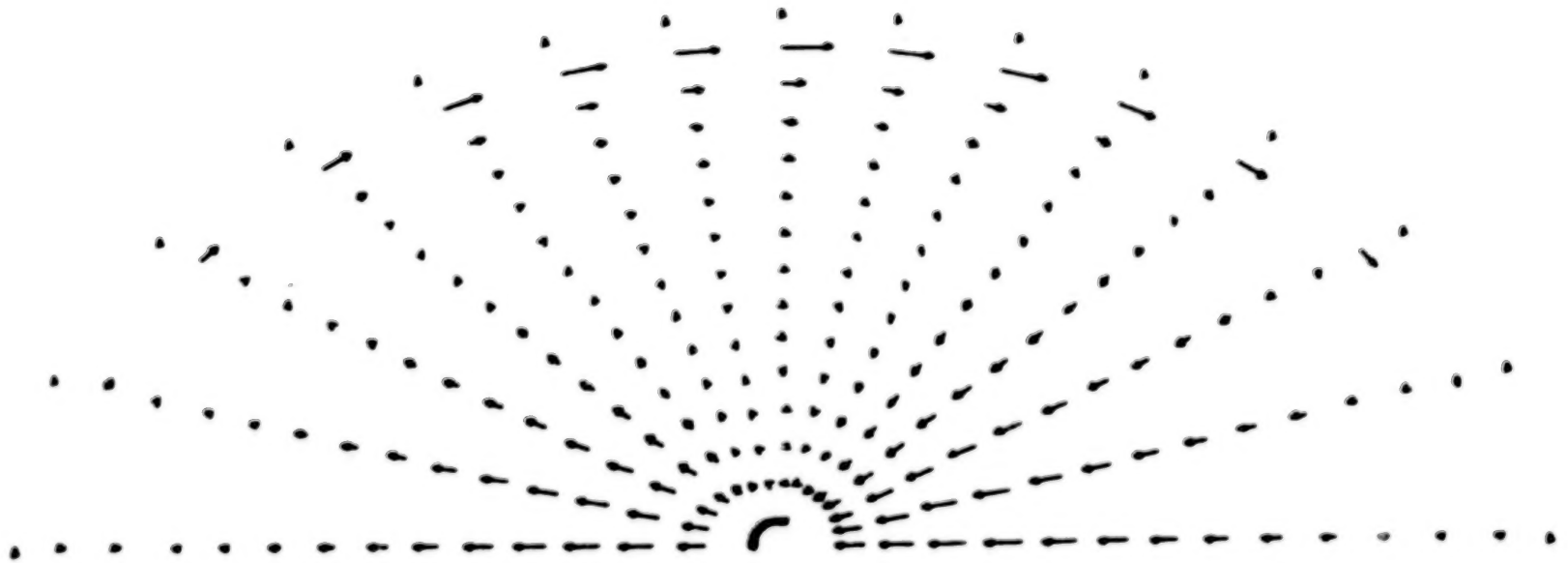

Figure 12d. – Cross Flow Velocity in a Curved Elliptic Duct, Shape = 1.5
, Sta. No. 8

Microfilmed From
Best Available Copy

SCALE: VMAX = 20.-03 ——→
STATION NO. 9 READ AT (.0000 .5532-02 .2000+01)

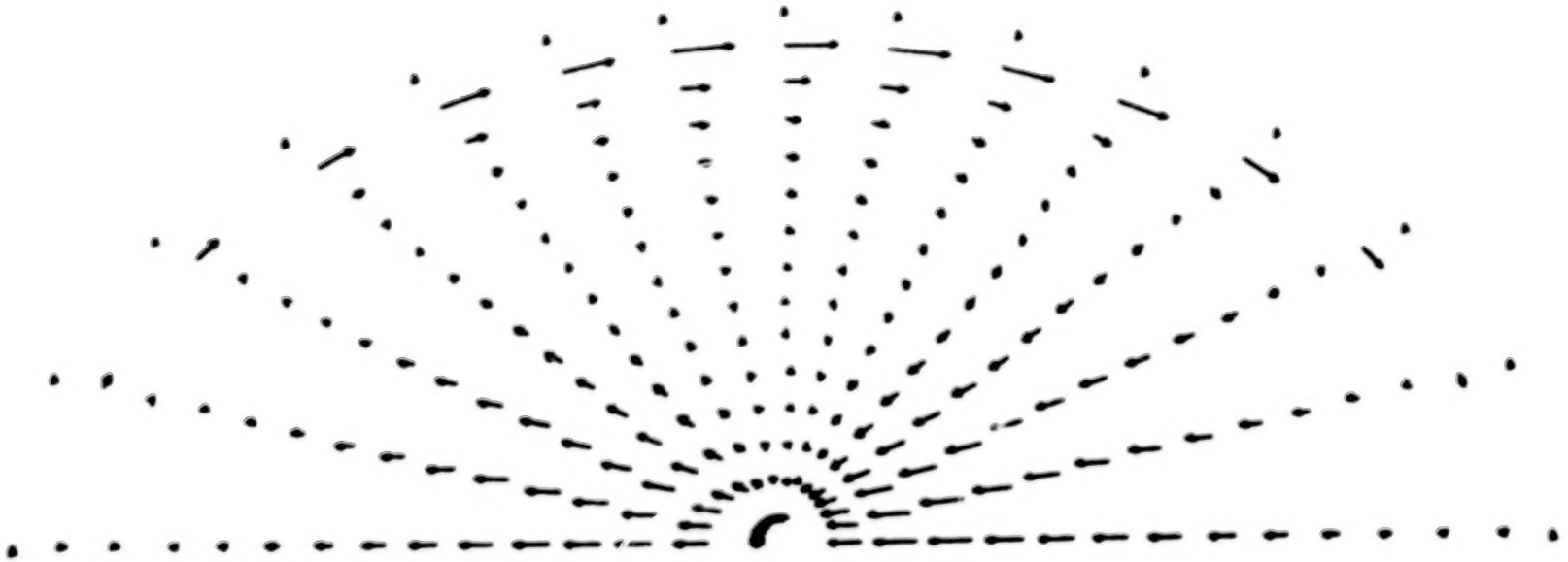

78-01-128-35

Figure 12e. — Cross Flow Velocity in a Curved Elliptic Duct, Shape = 1.5
, Sta. No. 9

Microfilmed From
Best Available Copy

SCALE: VMAX = 20.-03 ——→
STATION NO. 10 READ AT (.0000 .1270-01 .2500+01)

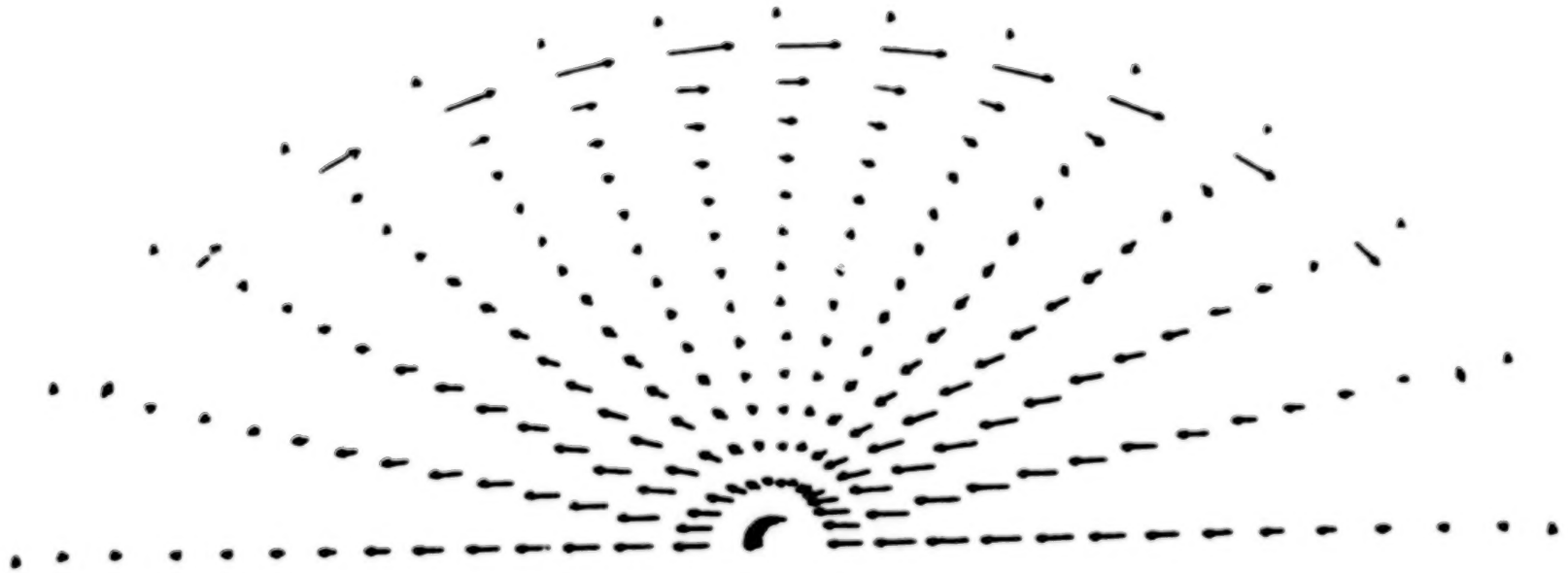

Figure 12f. – Cross Flow Velocity in a Curved Elliptic Duct, Shape = 1.5
, Sta. No. 10

Microfilmed From
Best Available Copy

SCALE: VMAX = 20.-03 ——→
STATION NO. 11 READ AT (.0000 .2470-01 .3000+01)

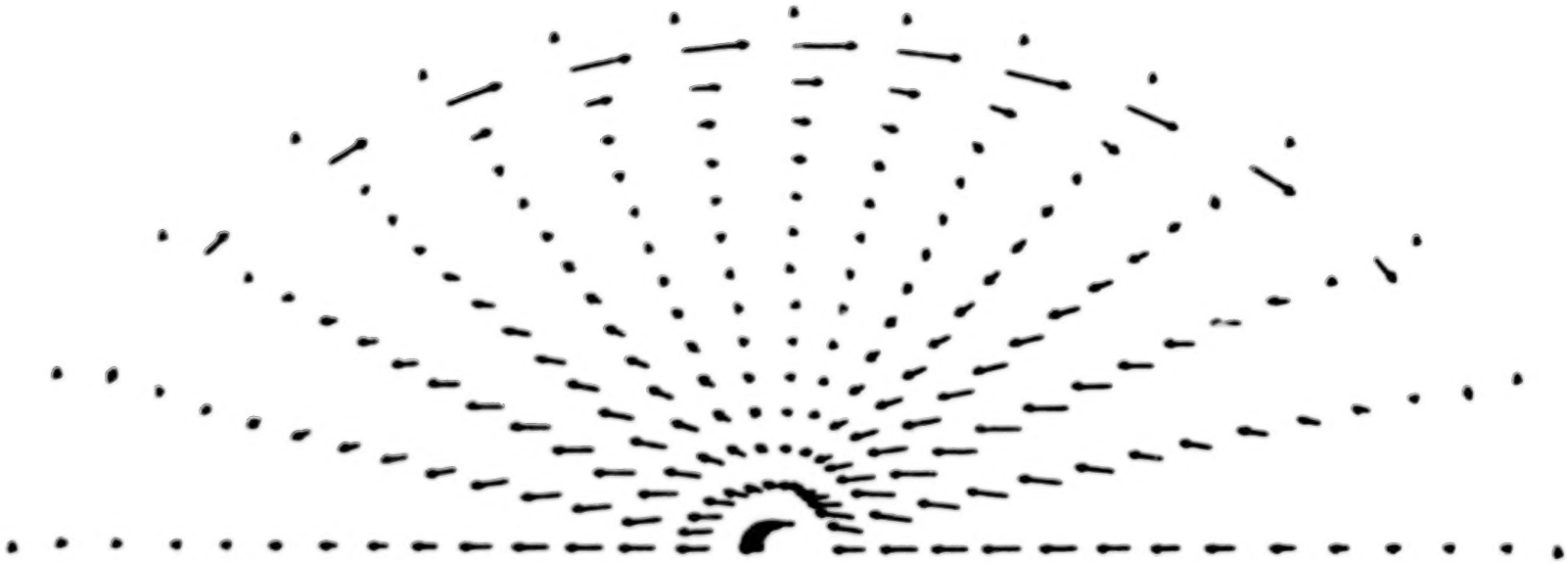

78-01-128-37

Figure 12g. – Cross Flow Velocity in a Curved Elliptic Duct, Shape = 1.5
, Sta. No. 11

Microfilmed From
Best Available Copy

SCALE: VMAX = 20.-03 ——→
STATION NO. 12 READ AT (.0000 .4286-01 .3500+01)

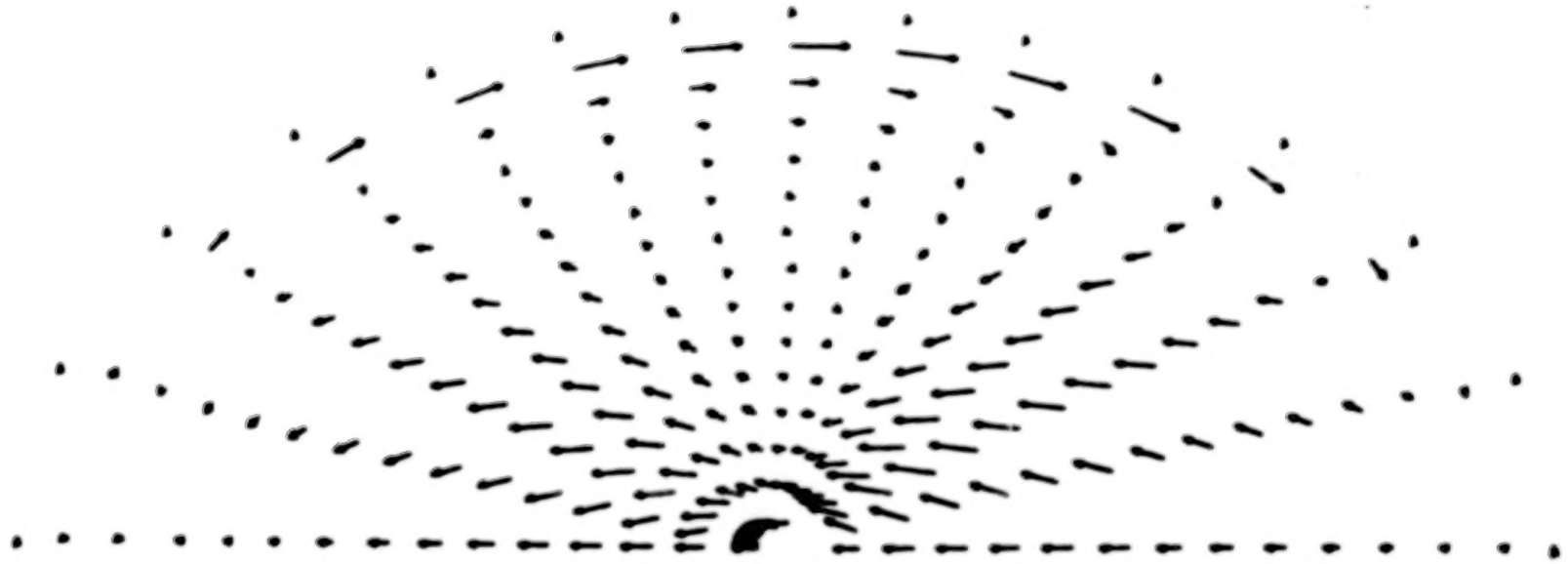

78-01-128-38

Figure 12h. – Cross Flow Velocity in a Curved Elliptic Duct, Shape = 1.5
, Sta. No. 12

Best Available Copy

SCALE: UMAX = 20.-03 ——
STATION NO. 13 READ AT (.0000 .5036-01 .4000+01)

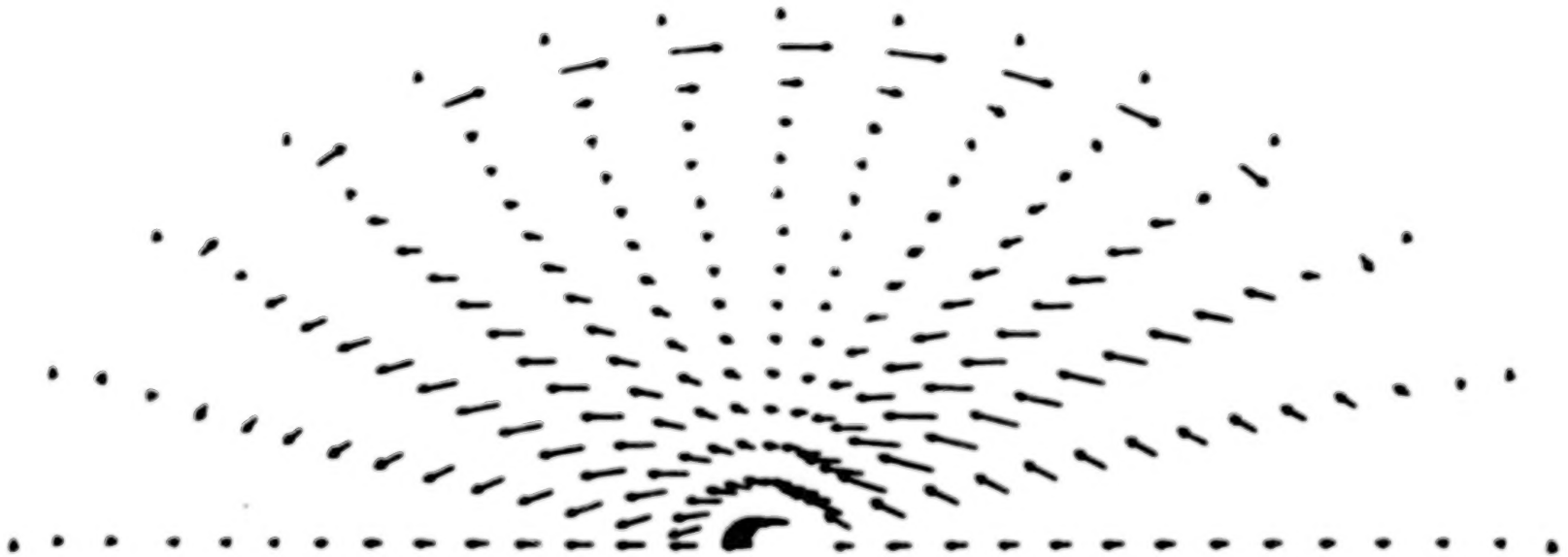

Figure 12i. – Cross Flow Velocity in a Curved Elliptic Duct, Shape = 1.5 , Sta. No. 13

Microfilmed From
Best Available Copy

SCALE: VMAX = 30.-03 ——→
STATION NO. 5 READ AT (.0000 .0000 .2475+01)

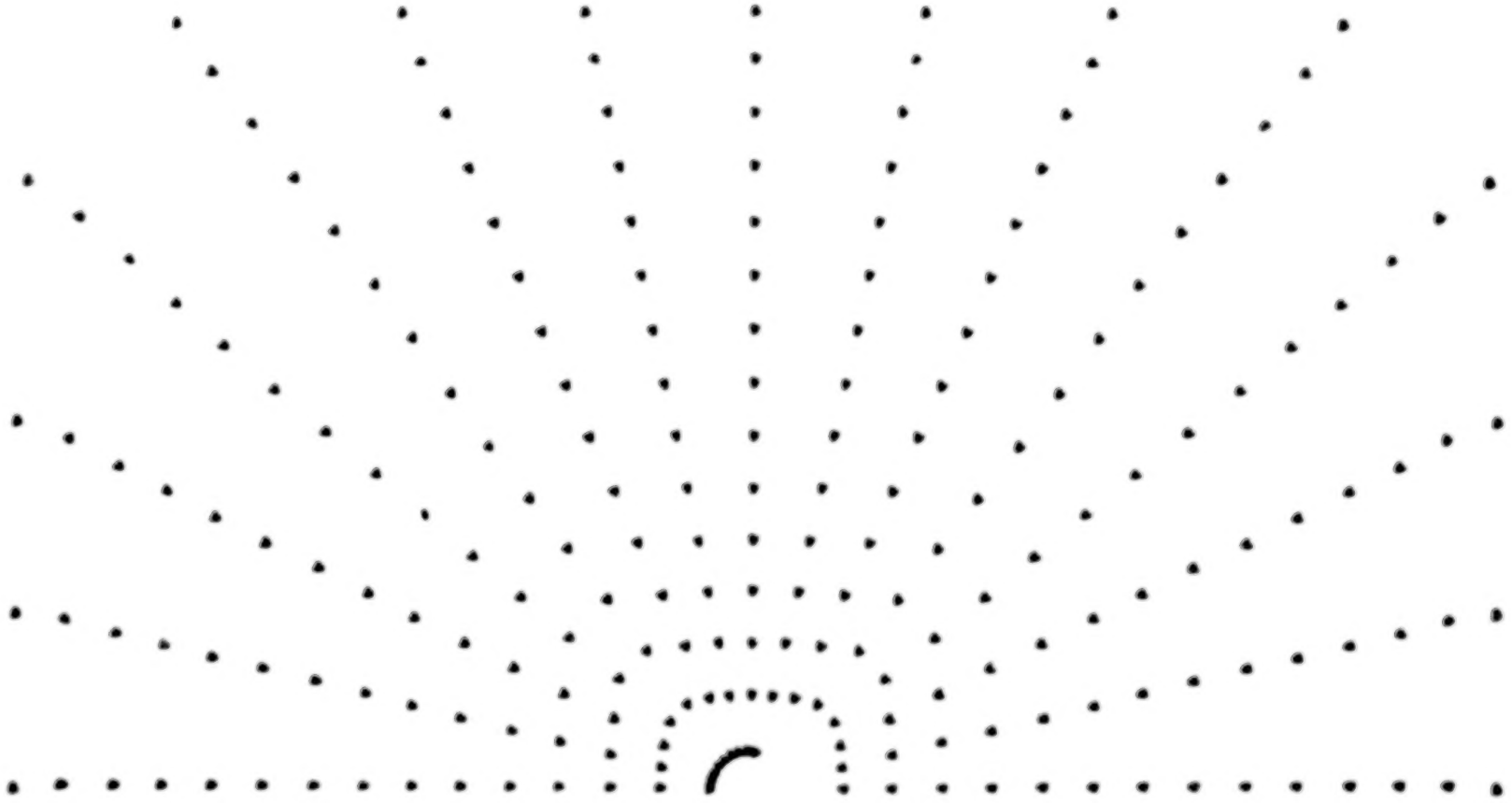

78-01-138-40

Figure 13a. – Cross Flow Velocity Vector in a Curved Superelliptic Duct, Exponent = 10 , Sta. No. 5

Microfilmed From
Best Available Copy

SCALE: VMAX = 30.-03 ⟶
STATION NO. 6 READ AT (.0000 .2577-04 .5000+00)

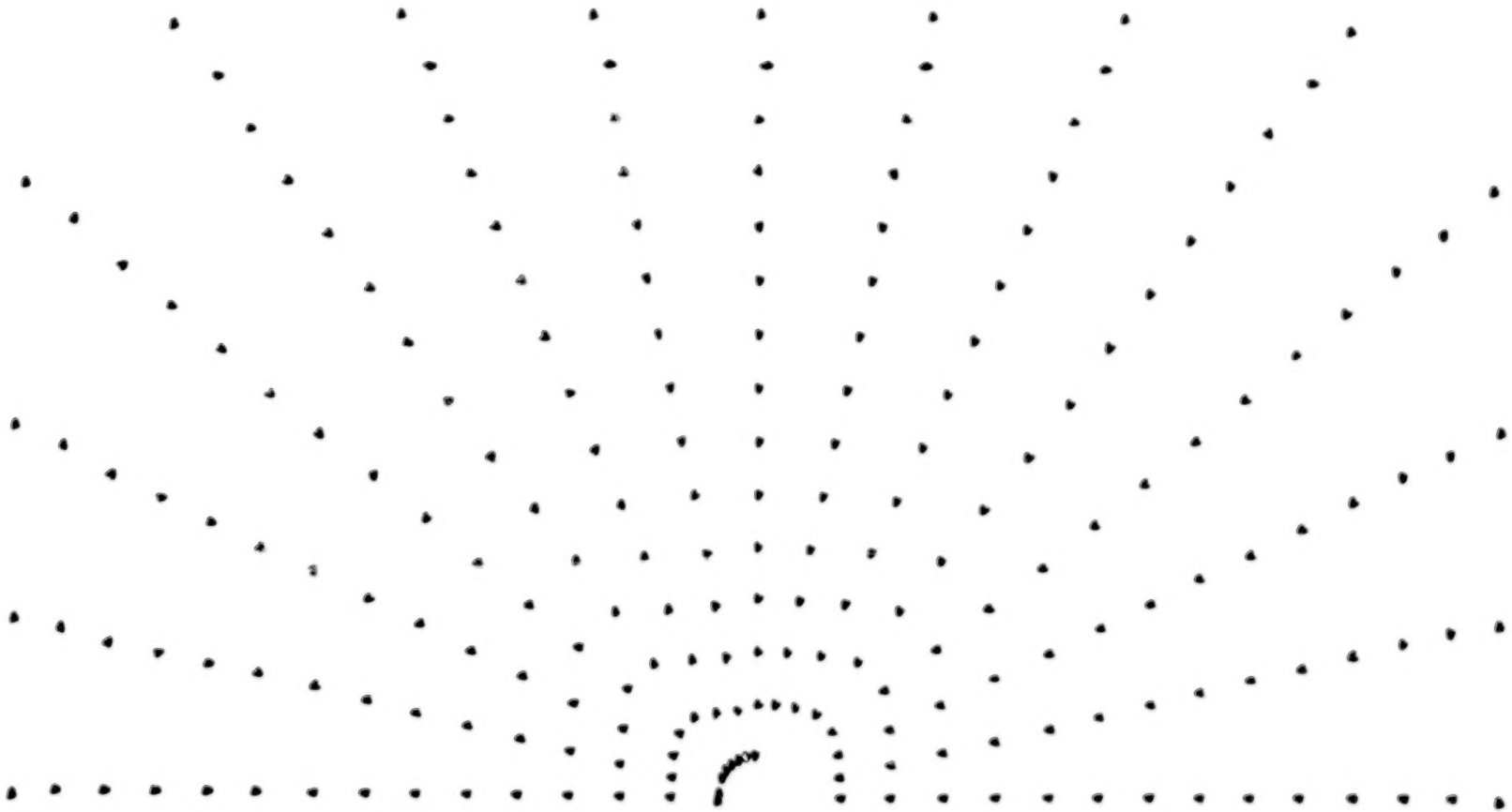

78-01-128-41

Figure 13b. – Cross Flow Velocity Vector in a Curved Superel iptic Duct, Exponent = 10
, Sta. No. 6

Microfilmed From
Best Available Copy

SCALE: VMAX = 30.-03 ——→
STATION NO. 7 READ AT (.0000 .3894-03 .1000+01)

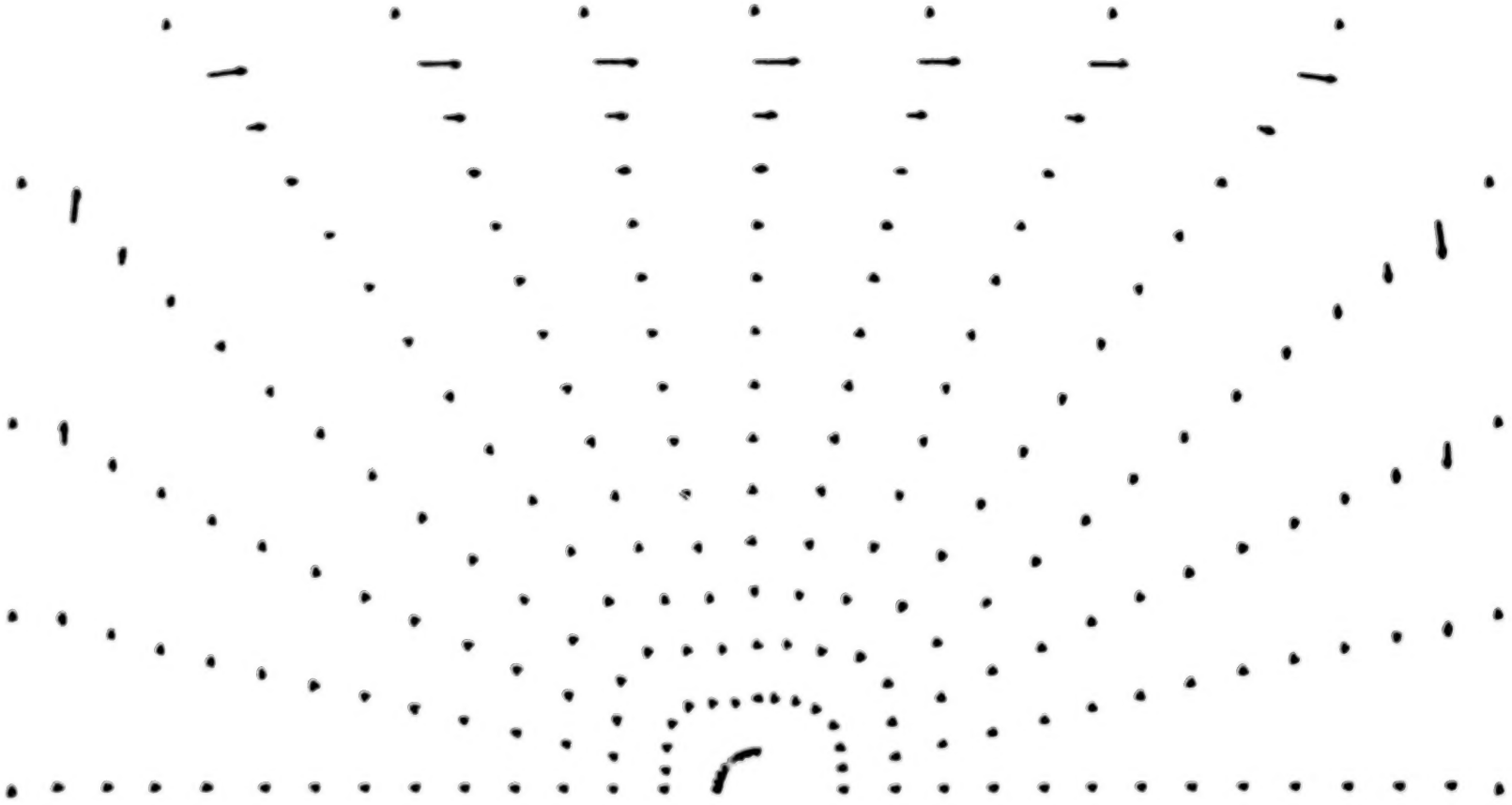

78-01-128-42

Figure 13c. – Cross Flow Velocity Vector in a Curved Superelliptic Duct, Exponent = 10
, Sta. No. 7

Microfilmed From
Best Available Copy

SCALE: VMAX = 30.-03 ⟶
STATION NO. 8 READ AT (.0000 .1859-02 .1500+01)

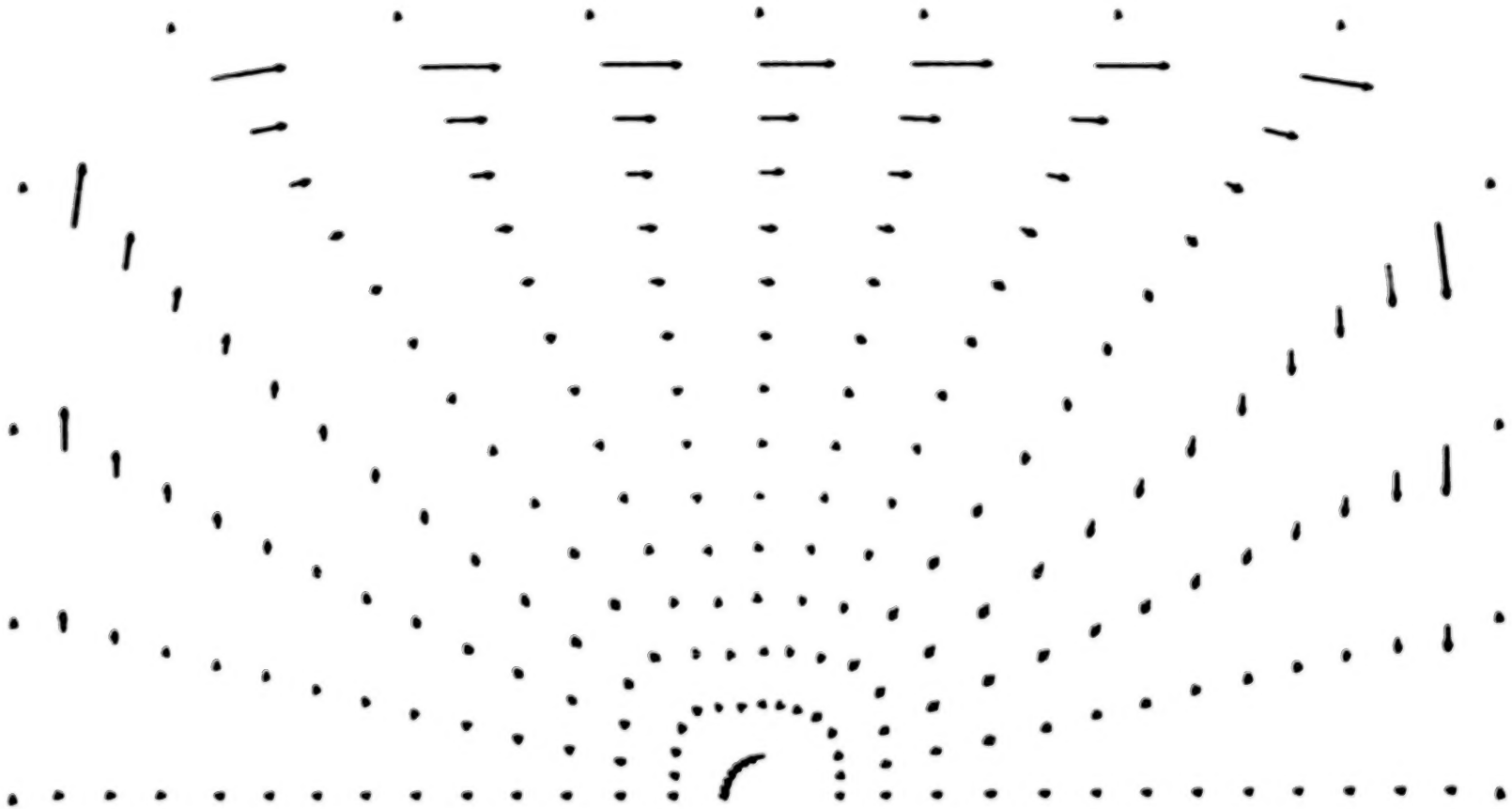

78-01-128-43

Figure 13d. – Cross Flow Velocity Vector in a Curved Superelliptic Duct, Exponent = 10
, Sta. No. 8

Microfilmed From
Best Available Copy

SCALE: VMAX = 30.-03 ——→
STATION NO. 9 READ AT (.0000 .5532-02 .2000+01)

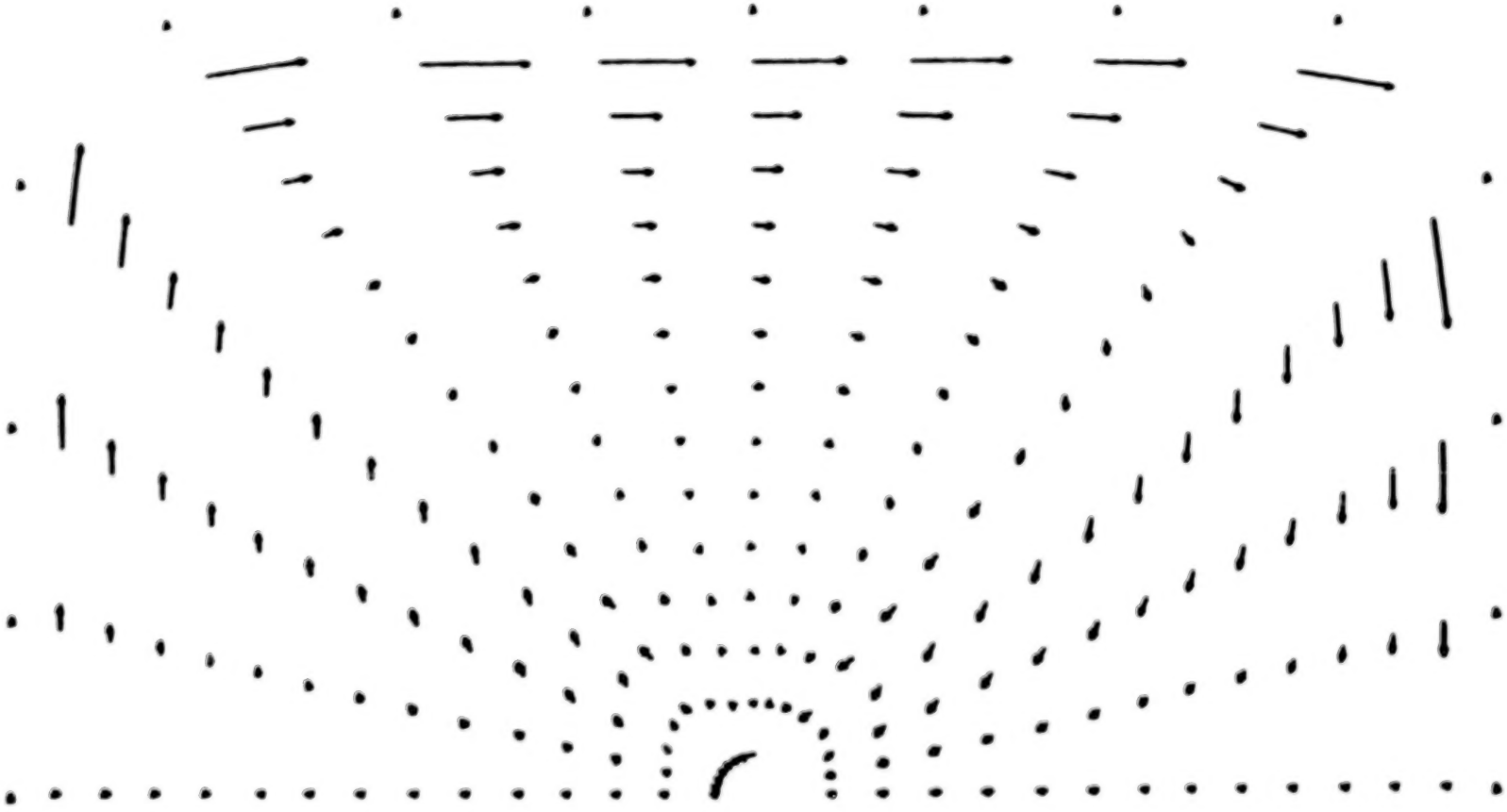

78-01-128-44

Figure 13e. — Cross Flow Velocity Vector in a Curved Superelliptic Duct, Exponent = 10
, Sta. No. 9

Microfilmed From
Best Available Copy

SCALE: VMAX = 30.-03
STATION NO. 10 READ AT (.0000 .1270-01 .2500+01)

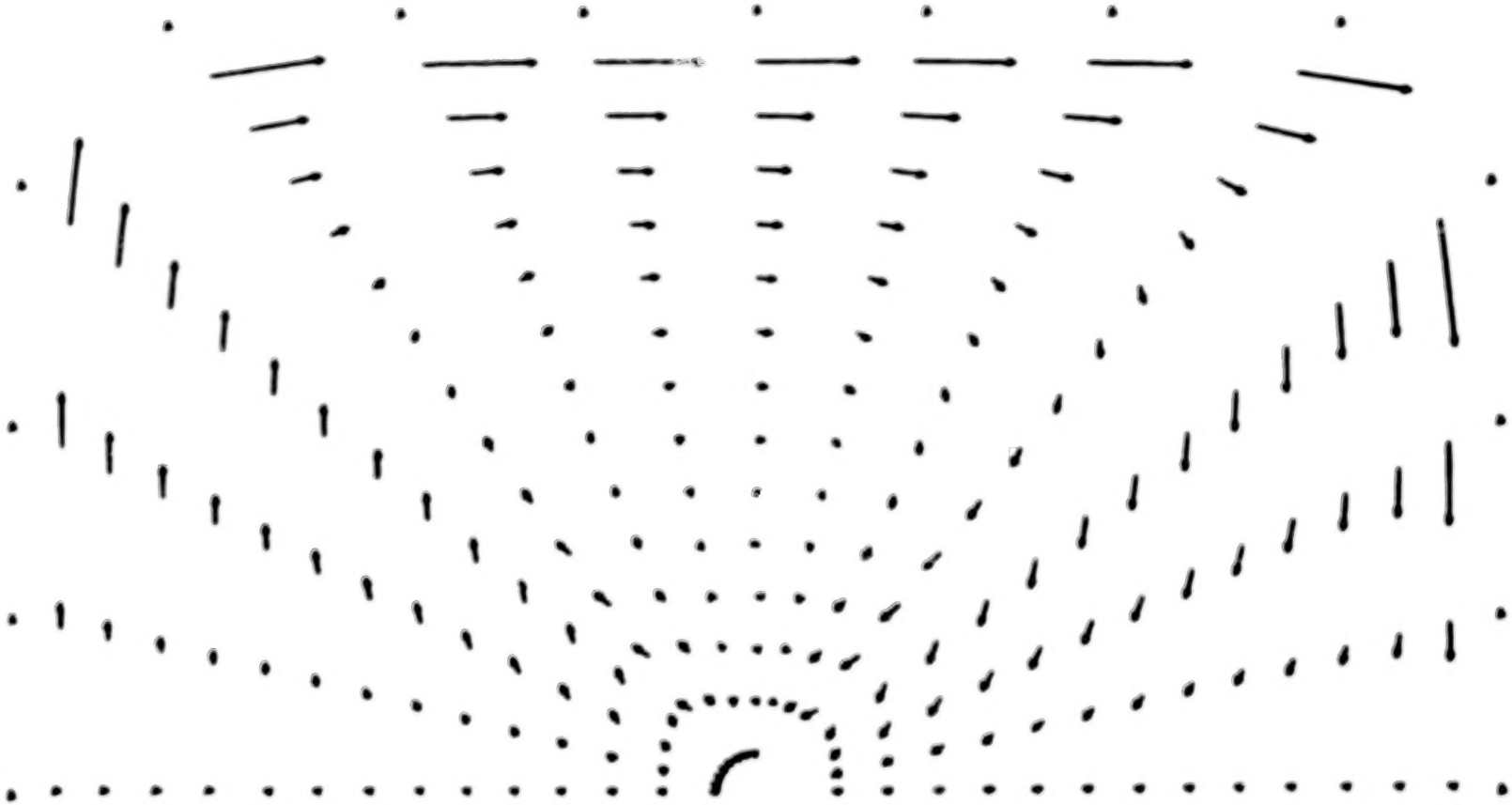

78-01-128-45

Figure 13f. – Cross Flow Velocity Vector in a Curved Superelliptic Duct, Exponent = 10 , Sta. No. 10

Microfilmed From
Best Available Copy

SCALE: VMAX = 30.-03 ——→
STATION NO. 11 READ AT (.0000 .2470-01 .3000+01)

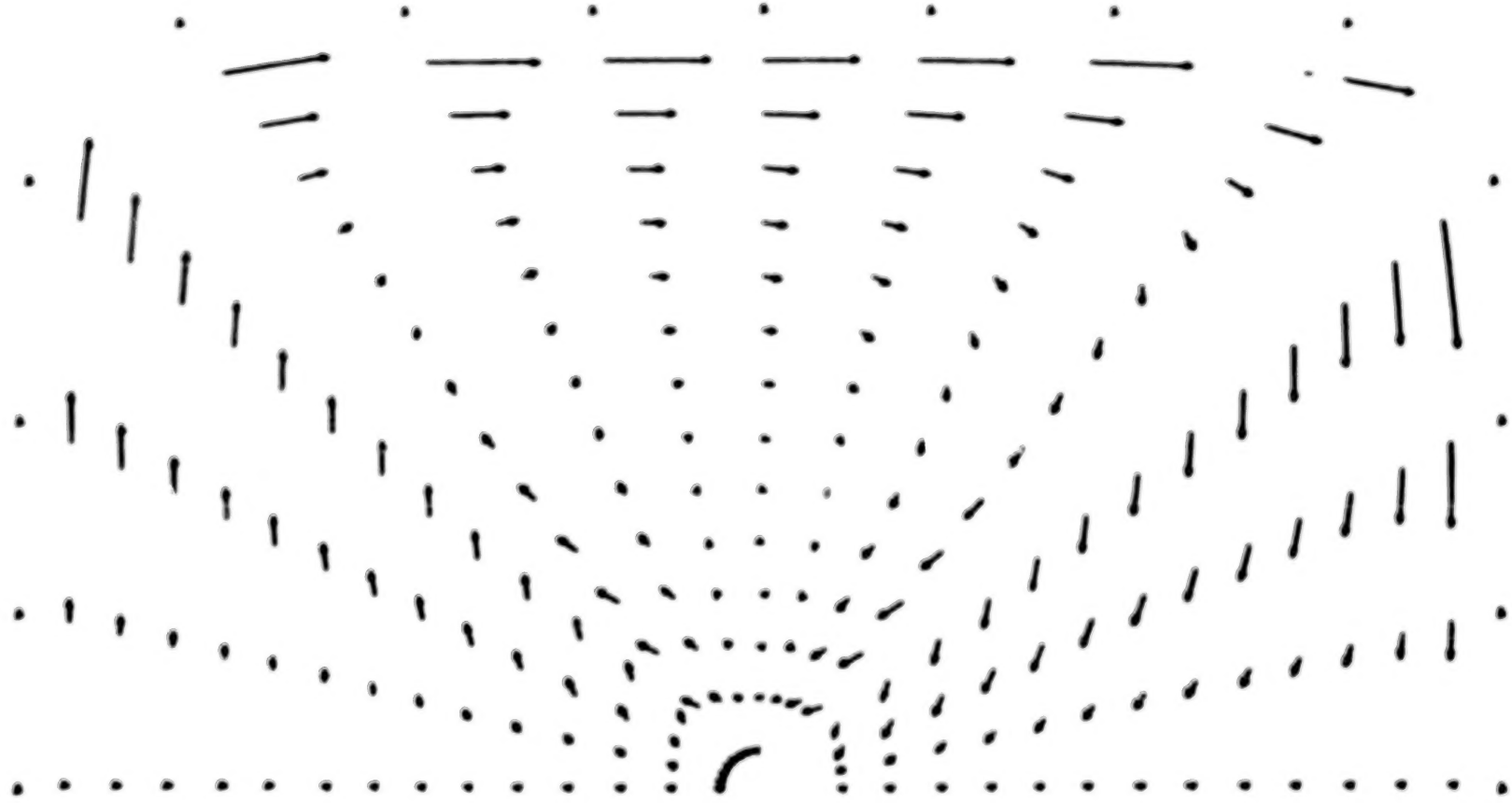

78-01-128-46

Figure 13g. – Cross Flow Velocity Vector in a Curved Superelliptic Duct, Exponent = 10 , Sta. No. 11

Microfilmed From
Best Available Copy

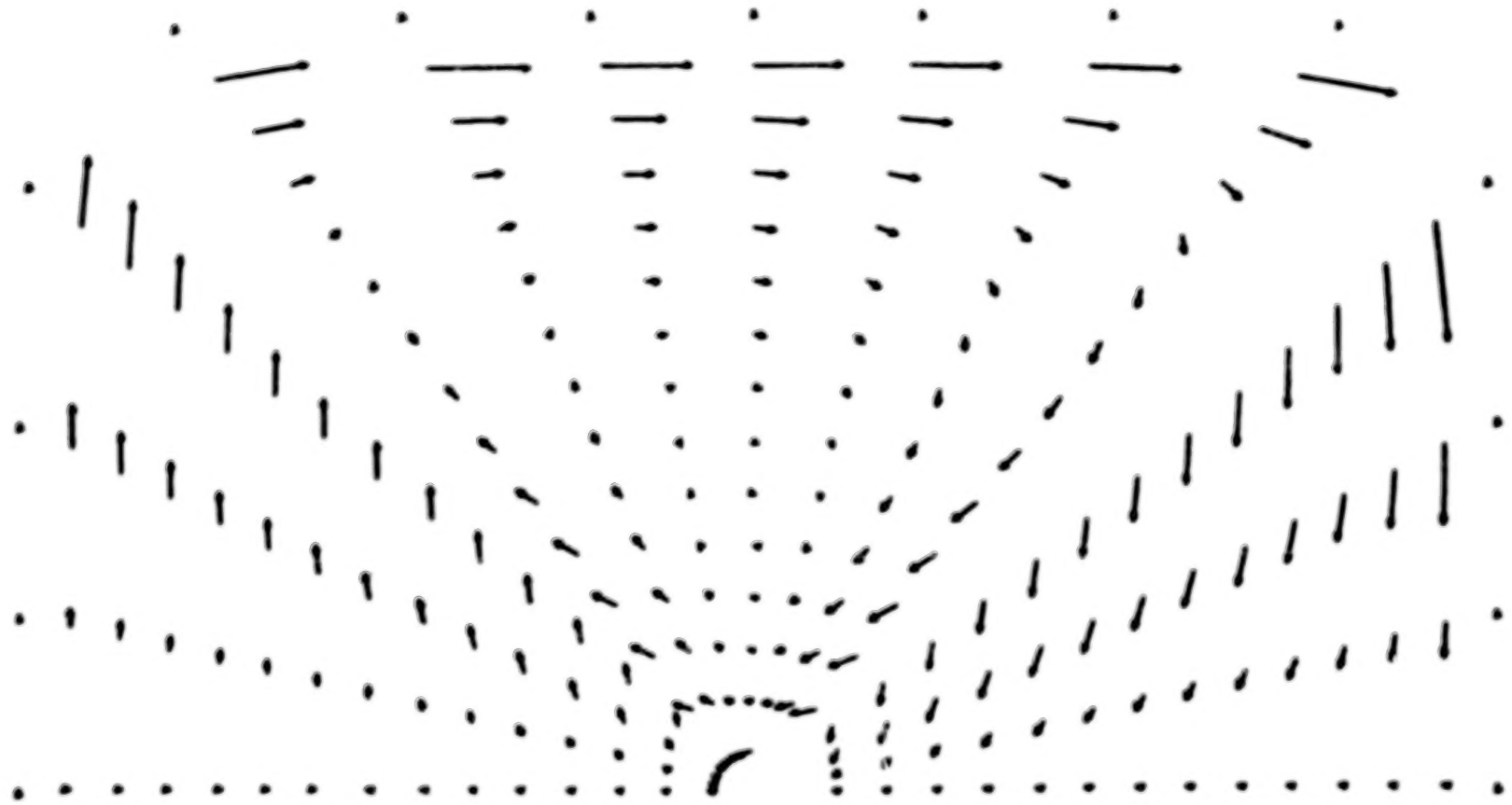

78-01-128-48

Figure 13h. -- Cross Flow Velocity Vector in a Curved Superelliptic Duct, Exponent = 10
, Sta. No. 12

Microfilmed From
Best Available Copy

SCALE: VMAX = 30.-03 ⟶
STATION NO. 13 READ AT (.0000 .6836-01 .4000+01)

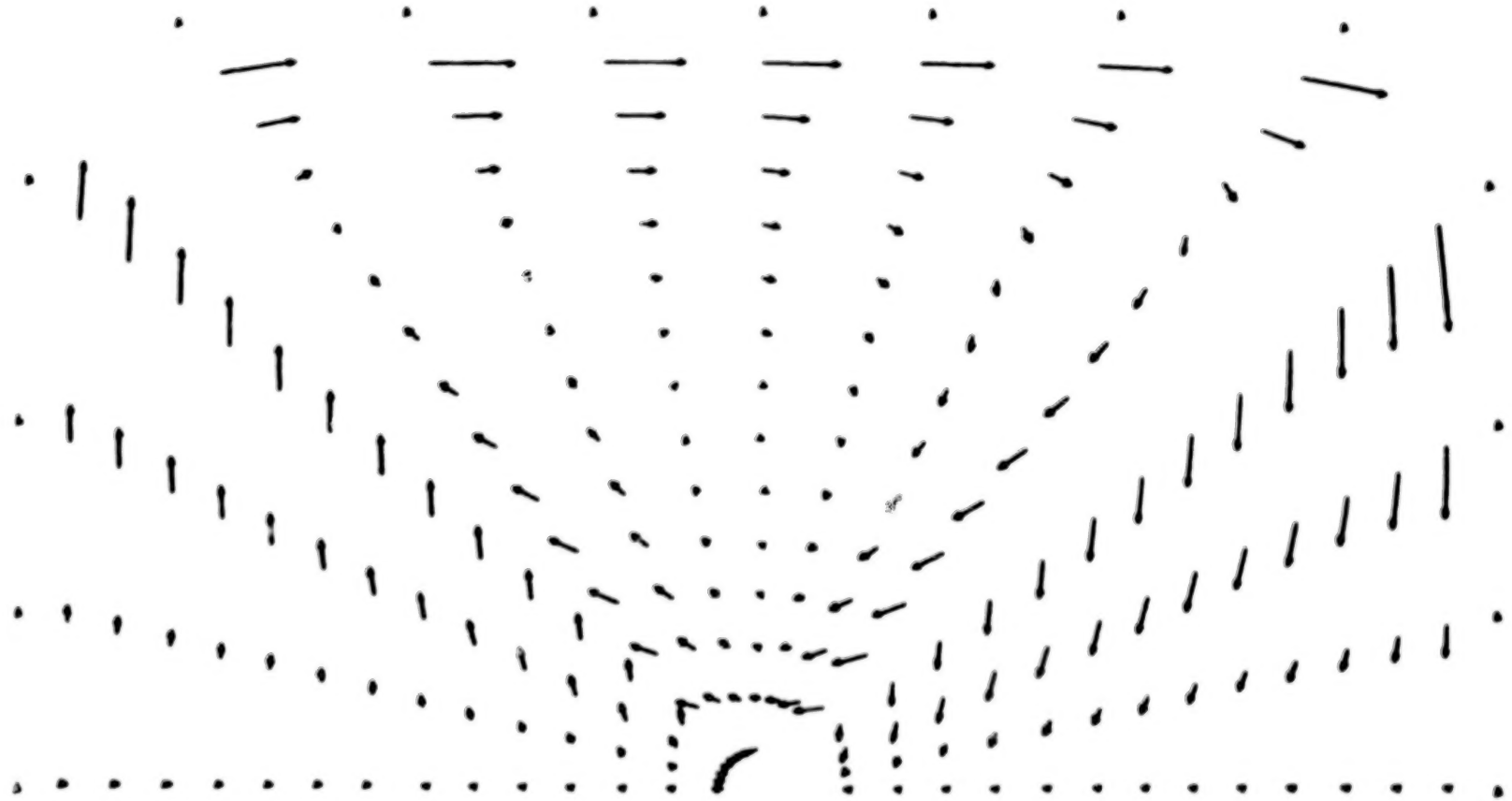

78-01-128-47

Figure 13i. – Cross Flow Velocity Vector in a Curved Superelliptic Duct, Exponent = 10 , Sta. No. 13

Microfilmed From
Best Available Copy

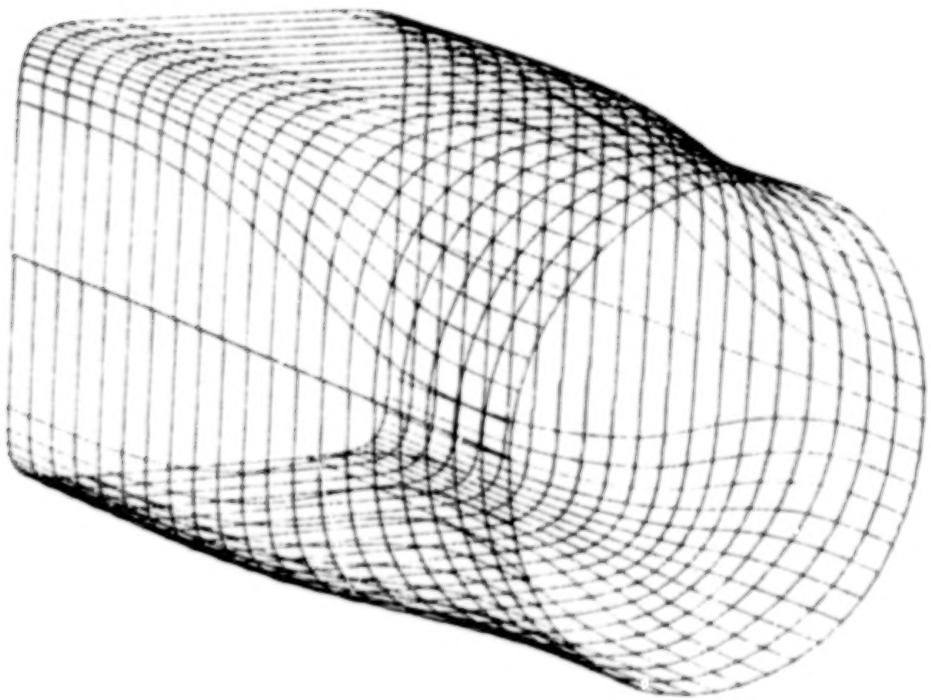

Figure 14. Transition Duct Superellipse Exponent = 10 to Circular

Microfilmed From
Best Available Copy

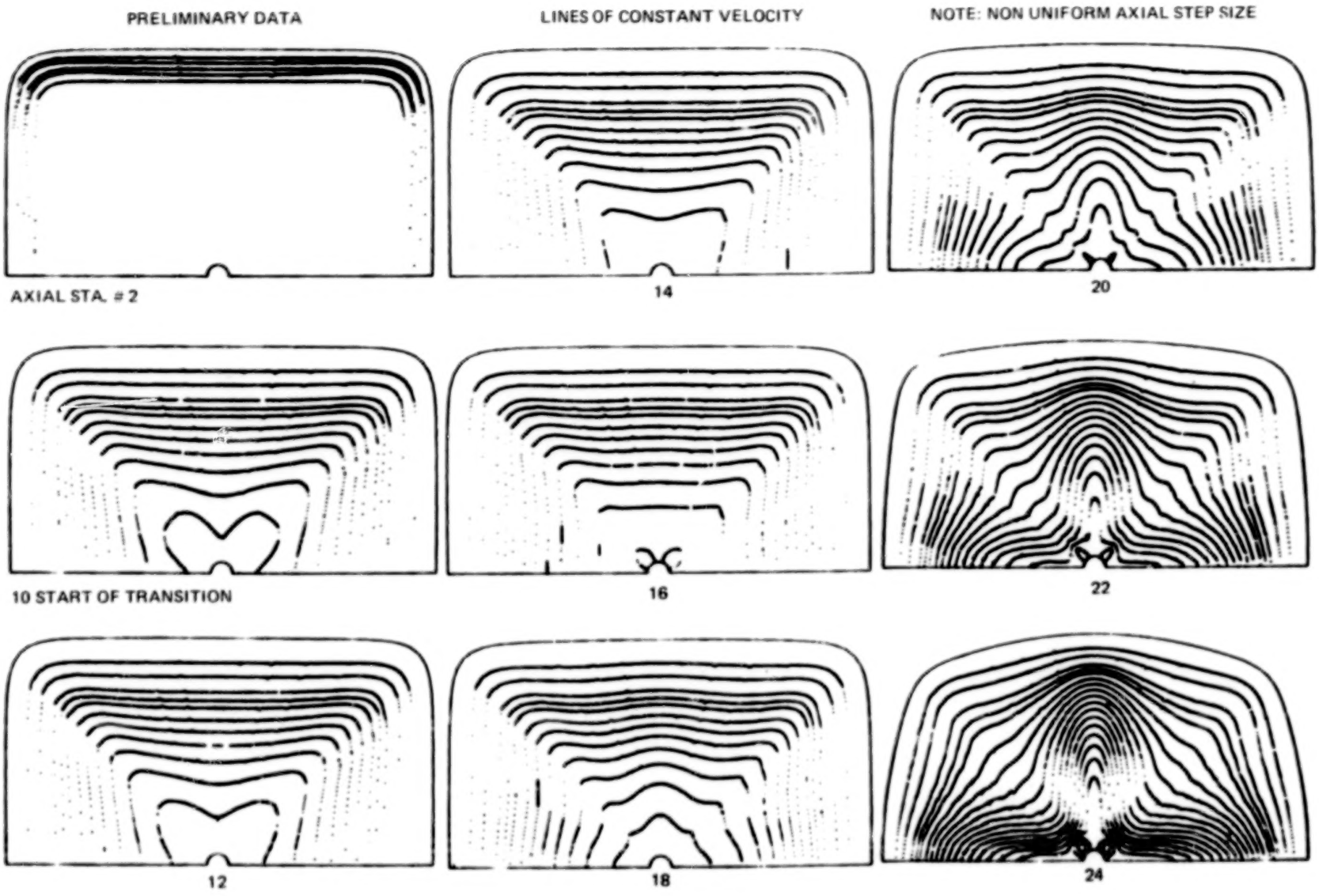

78-01-128-10

Figure 15. Transition from Superelliptic Pipe (C = 10) to Circular Pipe

Microfilmed From
Best Available Copy

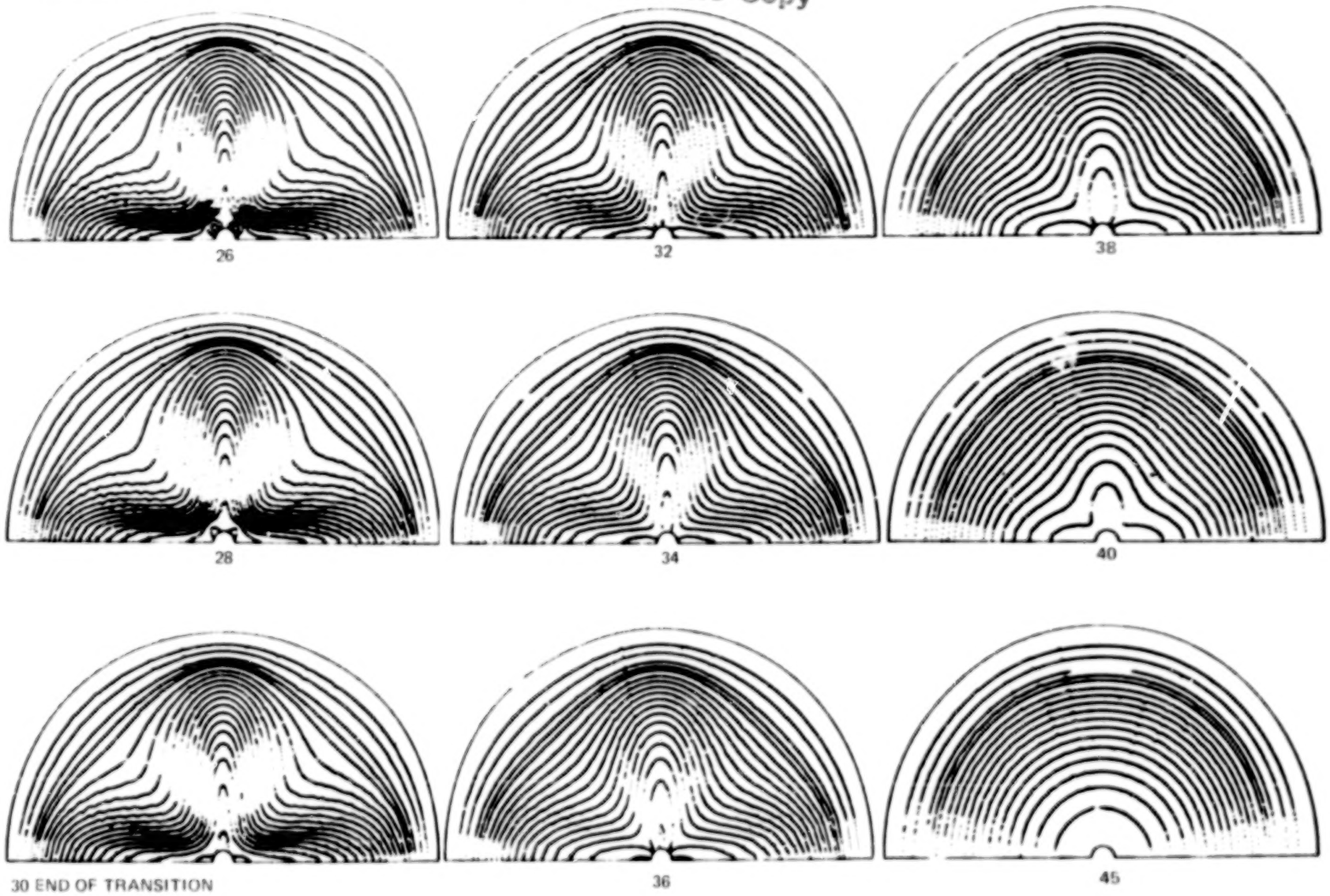

78-01-128-11

Figure 15. (Cont'd) Transition from Superelliptic Pipe (C = 10) to Circular Pipe

1. Report No.	2. Government Accession No.	3. Recipient's Catalog No.
NASA CR-3029		

4. Title and Subtitle	5. Report Date
DEVELOPMENT OF A THREE-DIMENSIONAL TURBULENT DUCT FLOW ANALYSIS	November 1978
	6. Performing Organization Code

7. Author(s)	8. Performing Organization Report No.
P. R. Eiseman, R. Levy, H. McDonald, and W. R. Briley	
	10. Work Unit No.

9. Performing Organization Name and Address	11. Contract or Grant No.
United Technologies Research Center East Hartford, Connecticut 06108	NAS3-19856
	13. Type of Report and Period Covered
12. Sponsoring Agency Name and Address	Contractor Report
National Aeronautics and Space Administration Washington, D.C. 20546	14. Sponsoring Agency Code

15. Supplementary Notes

Final report. Project manager, B. H. Anderson, Wind Tunnel and Flight Division, NASA Lewis Research Center, Cleveland, Ohio 44135.

16. Abstract

A method for computing three-dimensional turbulent subsonic flow in curved ducts is described. An approximate set of governing equations is given for viscous flows which have a primary flow direction. The derivation is coordinate invariant, and the resulting equations are expressed in terms of tensors. General tube-like coordinates were developed for a general class of geometries applicable to many internal flow problems. The coordinates are then particularized to pipes having superelliptic cross sections whose shape can vary continuously between a circle and a near rectangle. The analysis is applied to a series of relevant aerodynamics problems including transition from nearly square to round pipes and flow through a pipe with an S-shaped bend.

17. Key Words (Suggested by Author(s))	18. Distribution Statement
Three-dimensional flow; Turbulent duct flow; Parabolized Navier-Stokes; Transition duct; S-bend. Offset bend; Three-dimensional viscous flow	Unclassified - unlimited STAR Category 34

19. Security Classif. (of this report)	20. Security Classif. (of this page)	21. No. of Pages	22. Price*
Unclassified	Unclassified	115	A06

* For sale by the National Technical Information Service, Springfield, Virginia 22161

NASA-Langley, 1978

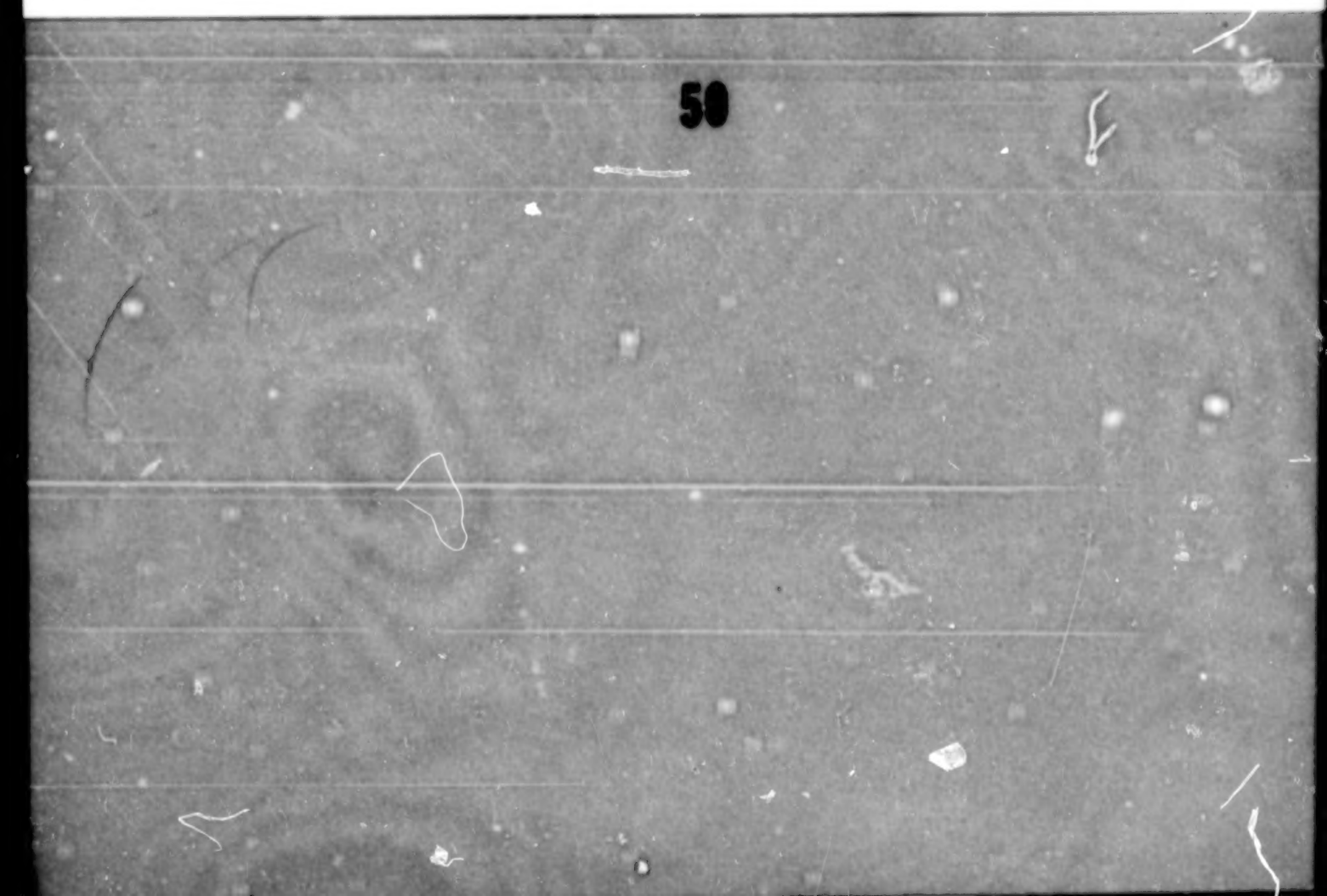
50

END

MAR 2 1979